

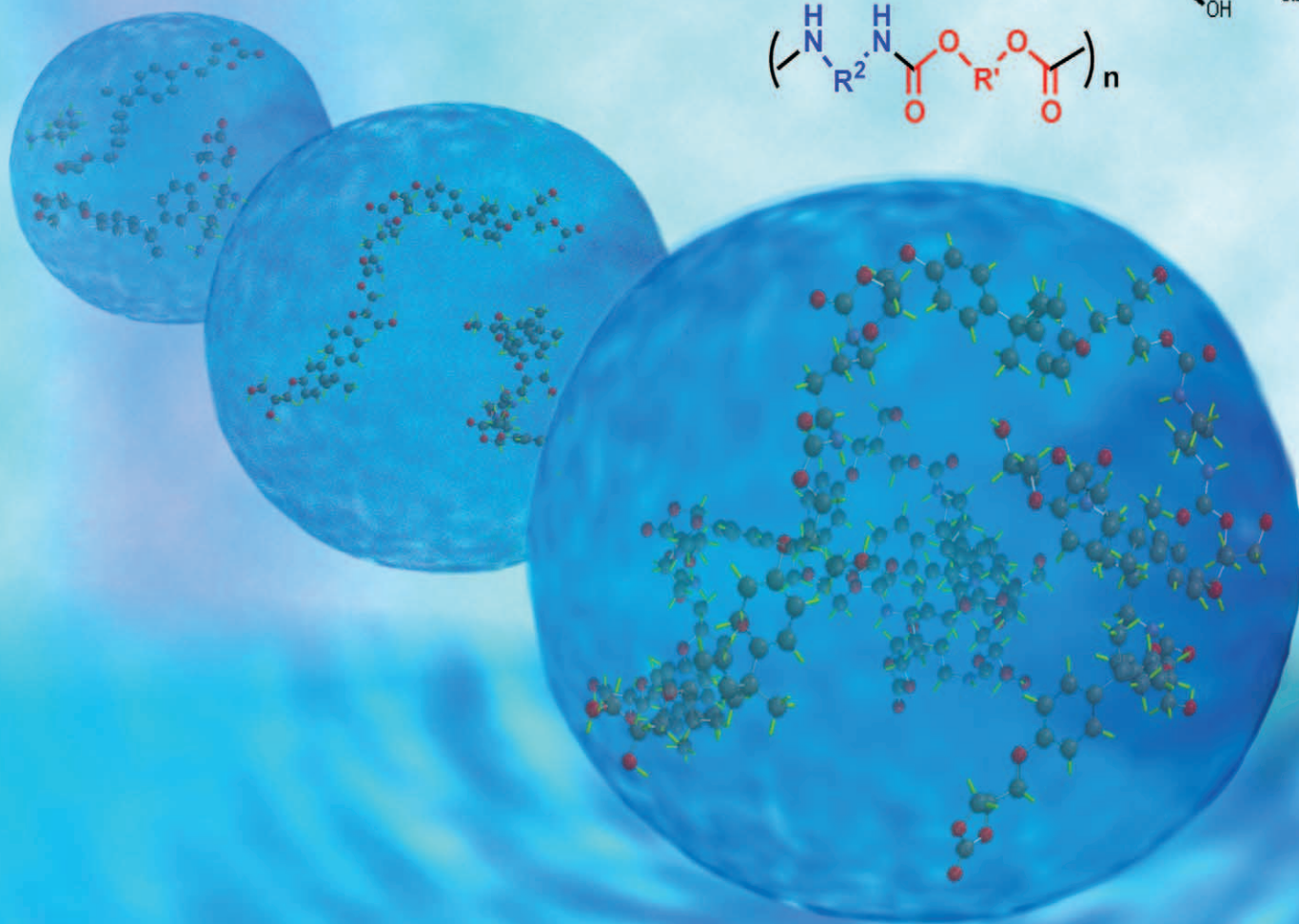
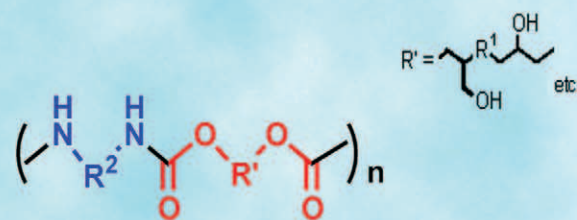
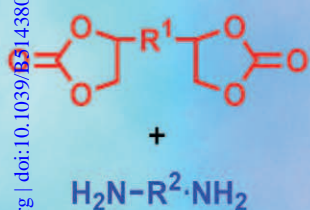
Green Chemistry

Cutting-edge research for a greener sustainable future

www.rsc.org/greenchem

Volume 7 | Number 11 | November 2005 | Pages 753–808

Downloaded on 06 November 2010
Published on 21 October 2005 on http://pubs.rsc.org | doi:10.1039/B514380M



ISSN 1463-9262

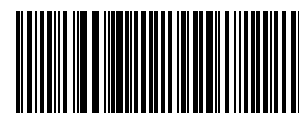
RSC Publishing

Choudhary *et al.*
Selective molecular oxidation of
benzaldehyde

Celzard *et al.*
Preparation and catalytic activity of
Mo₂C nanoparticles

Ochiai *et al.*
Nucleophilic polyaddition in
water

Litvić *et al.*
Preparation of β-amino-α, β-
unsaturated esters



1463-9262 (2005) 7:11;1-3

Looking for a stimulating read?

Try Critical Reviews in Chem Soc Rev - they provide:

- accessibility to the general reader via a specially written introduction
- a critical discussion of the existing state of knowledge
- a balanced assessment of the current primary literature
- emphasis on implications for the wider scientific community

See below for recent examples of Critical Reviews:



Cyclam complexes and their applications in medicine
Xiangyang Liang and Peter J Sadler

The syntheses and catalytic applications of unsymmetrical ferrocene ligands
Robert C J Atkinson, Vernon C Gibson and Nicholas J Long

Recent developments in the supramolecular chemistry of terpyridine-metal complexes
Harold Hofmeier and Ulrich S Schubert

Chiral N-heterocyclic carbenes as stereodirecting ligands in asymmetric catalysis
Vincent César, Stéphane Bellemin-Laponnaz and Lutz H Gade

Microwaves in organic synthesis. Thermal and non-thermal microwave effects
Antonio de la Hoz, Ángel Diaz-Hortiz and Andrés Moreno

Stimuli responsive polymers for biomedical applications
Carolina de las Heras Alarcón, Sivanand Pennadam and Cameron Alexander

Anti-inflammatory metabolites from marine sponges
Robert A Keyzers and Michael T Davies-Coleman

Activity of water in aqueous systems: a frequently neglected property
Mike J Blandamer, Jan B F N Engberts, Peter T Gleeson and João Carlos R Reis

Role of sulfur chirality in the chemical processes of biology
Ronald Bentley

The cyclopropene pyrolysis story
Robin Walsh

Dinitroso and polynitroso compounds
Brian G. Gowenlock and George B. Richter-Addo

IN THIS ISSUE

ISSN 1463-9262 CODEN GRCHFJ 7(11) 753-808 (2005)

In this issue...

Samantha Tang *et al.* discuss the condensed principles of green chemistry: PRODUCTIVELY



Chemical biology articles published in this journal also appear in the *Chemical Biology Virtual Journal*: www.rsc.org/chembiol



Cover

The cover image depicts nucleophilic polyaddition proceeding in water that is free from surfactants and organic solvents.

Image reproduced by permission of Takeshi Endo from *Green Chem.*, 2005, 7(11), 765.

CHEMICAL TECHNOLOGY

T41

Chemical Technology highlights the latest applications and technological aspects of research across the chemical sciences.

Chemical Technology

November 2005/Volume 2/Issue 11

www.rsc.org/chemicaltechnology

NEWS

761

Principles of green chemistry: PRODUCTIVELY

Samantha L. Y. Tang,* Richard L. Smith and Martyn Poliakoff

The acronym 'PRODUCTIVELY' is used to try to capture the spirit of each of the twelve principles of green chemistry in just two or three words.

Condensed Principles of Green Chemistry

- P - Prevent wastes
- R - Renewable materials
- O - Omit derivatization steps
- D - Degradable chemical products
- U - Use safe synthetic methods
- C - Catalytic reagents
- T - Temperature, Pressure ambient
- I - In-Process Monitoring
- V - Very few auxiliary substances
- E - E-factor, maximise feed in product
- L - Low toxicity of chemical products
- Y - Yes, it is safe

EDITORIAL STAFF

Editor

Harpal Minhas

Assistant editors

Nina Athey-Pollard, Merlin Fox, Katie Gibb

News writer

Markus Hölscher

Publishing assistant

Jackie Cockrill

Team leader, serials production

Stephen Wilkes

Technical editors

Katherine Davies, Christopher Ingle, Kathryn Lees

Administration coordinator

Sonya Spring

Editorial secretaries

Lynne Braybrook, Rebecca Gotobed, Julie Thompson

Publisher

Adrian Kybett

Green Chemistry (print: ISSN 1463-9262; electronic: ISSN 1463-9270) is published 12 times a year by the Royal Society of Chemistry, Thomas Graham House, Science Park, Milton Road, Cambridge, UK CB4 0WF.

All orders, with cheques made payable to the Royal Society of Chemistry, should be sent to RSC Distribution Services, c/o Portland Customer Services, Commerce Way, Colchester, Essex, UK CO2 8HP. Tel +44 (0) 1206 226050; E-mail sales@rscdistribution.org

2005 Annual (print + electronic) subscription price: £795; US\$1310. 2005 Annual (electronic) subscription price: £715; US\$1180. Customers in Canada will be subject to a surcharge to cover GST. Customers in the EU subscribing to the electronic version only will be charged VAT.

If you take an institutional subscription to any RSC journal you are entitled to free, site-wide web access to that journal. You can arrange access via Internet Protocol (IP) address at www.rsc.org/ip. Customers should make payments by cheque in sterling payable on a UK clearing bank or in US dollars payable on a US clearing bank. Periodicals postage paid at Rahway, NJ, USA and at additional mailing offices. Airfreight and mailing in the USA by Mercury Airfreight International Ltd., 365 Blair Road, Avenel, NJ 07001, USA.

US Postmaster: send address changes to Green Chemistry, c/o Mercury Airfreight International Ltd., 365 Blair Road, Avenel, NJ 07001. All despatches outside the UK by Consolidated Airfreight.

PRINTED IN THE UK

Advertisement sales: Tel +44 (0) 1223 432243; Fax +44 (0) 1223 426017; E-mail advertising@rsc.org

Green Chemistry

Cutting-edge research for a greener sustainable future

www.rsc.org/greenchem

Green Chemistry focuses on cutting-edge research that attempts to reduce the environmental impact of the chemical enterprise by developing a technology base that is inherently non-toxic to living things and the environment.

EDITORIAL BOARD

Chair

Professor Colin Raston,
Department of Chemistry
University of Western Australia
Perth, Australia
E-mail clraston@chem.uwa.edu.au

Scientific editor

Professor Walter Leitner,
RWTH-Aachen, Germany
E-mail leitner@itmc.rwth-aachen.de
Professor Joan Brennecke,
University of Notre Dame, USA
Professor Steve Howdle, University
of Nottingham, UK
Dr Janet Scott, Centre for Green
Chemistry, Monash University,
Australia

Dr A Michael Warhurst,
WWF, Brussels, Belgium
Professor Tom Welton,
Imperial College, UK
E-mail t.welton@ic.ac.uk
Professor Roshan Jachuck,
Clarkson University, USA
E-mail rjachuck@clarkson.edu
Dr Paul Anastas, Green Chemistry
Institute, USA
Email p_anastas@acs.org
Professor Buxing Han, Chinese
Academy of Sciences
Email hanbx@iccas.ac.cn

Associate editor for the Americas

Professor C. J. Li, McGill
University, Canada
E-mail cj.li@mcgill.ca

INTERNATIONAL ADVISORY EDITORIAL BOARD

James Clark, York, UK
Avelino Corma, Universidad
Politécnica de Valencia, Spain
Mark Harmer, DuPont Central
R&D, USA
Herbert Hugl, Lanxess Fine
Chemicals, Germany
Makato Misono, Kogakuin
University, Japan
Robin D. Rogers, Centre for Green
Manufacturing, USA

Kenneth Seddon, Queen's
University, Belfast, UK
Roger Sheldon, Delft University of
Technology, The Netherlands
Gary Sheldrake, Queen's
University, Belfast, UK
Pietro Tundo, Università ca
Foscari di Venezia, Italy
Tracy Williamson, Environmental
Protection Agency, USA

INFORMATION FOR AUTHORS

Full details of how to submit material for publication in Green Chemistry are given in the Instructions for Authors (available from <http://www.rsc.org/authors>). Submissions should be sent via ReSource: <http://www.rsc.org/resource>.

Authors may reproduce/republish portions of their published contribution without seeking permission from the RSC, provided that any such republication is accompanied by an acknowledgement in the form: (Original citation) – Reproduced by permission of the Royal Society of Chemistry.

© The Royal Society of Chemistry 2005. Apart from fair dealing for the purposes of research or private study for non-commercial purposes, or criticism or review, as permitted under the Copyright, Designs and Patents Act 1988 and the Copyright and Related Rights Regulations 2003, this publication may only be reproduced, stored or transmitted, in any form or by any means, with the prior permission in writing of the Publishers or in the case of reprographic reproduction in accordance with the terms of

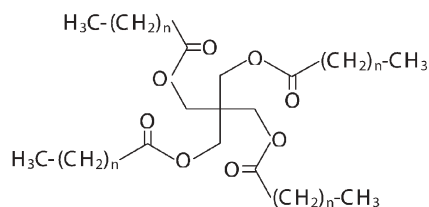
licences issued by the Copyright Licensing Agency in the UK. US copyright law is applicable to users in the USA.

The Royal Society of Chemistry takes reasonable care in the preparation of this publication but does not accept liability for the consequences of any errors or omissions.

Ⓢ The paper used in this publication meets the requirements of ANSI/NISO Z39.48-1992 (Permanence of Paper).

Royal Society of Chemistry: Registered Charity No. 207890

775

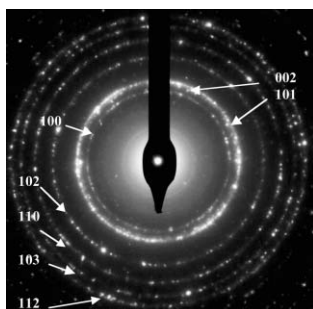


Volumetric behaviour of the environmentally compatible lubricants pentaerythritol tetraheptanoate and pentaerythritol tetranonanoate at high pressures

Olivia Fandiño, Alfonso S. Pensado, Luis Lugo, Enriqueta R. López* and Josefa Fernández

Polyol ester oils have been proposed as lubricant candidates for refrigeration systems. We have studied the density, thermal expansion coefficient, isothermal compressibility coefficient and internal pressure of two polyol esters.

784

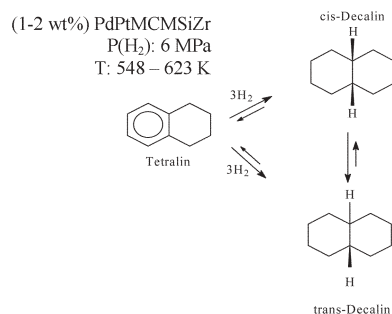


Preparation and catalytic activity of active carbon-supported Mo₂C nanoparticles

A. Celzard,* J. F. Maréché, G. Furdin, V. Fierro, C. Sayag and J. Pielaszek

Mo₂C nanoparticles dispersed on two kinds of active carbon and their catalytic properties in both HDS and HDN reactions were tested. Such catalysts favour the HDN and HDS routes which consume the lowest amounts of hydrogen.

793

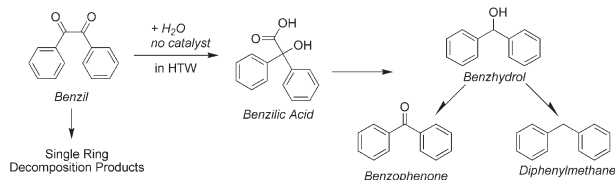


Influence of the metallic precursor in the hydrogenation of tetralin over Pd–Pt supported zirconium doped mesoporous silica

M. C. Carrión, B. R. Manzano, F. A. Jalón, D. Eliche-Quesada, P. Maireles-Torres, E. Rodríguez-Castellón and A. Jiménez-López*

(1–2 wt%) PdPt supported on zirconium doped mesoporous silica catalysts, prepared from bimetallic and monometallic precursors, are active in the tetralin hydrogenation at 6 MPa of P(H₂), producing selectively *trans*- and *cis*-decalins, even in the presence of dibenzothiophene in the feed.

800



The benzil–benzilic acid rearrangement in high-temperature water

Craig M. Comisar and Phillip E. Savage

The benzil rearrangement, base-catalyzed at conventional conditions, proceeds in high-temperature water without added base. Manipulating pH provides control of the rate and selectivity. Surprisingly, acid catalysis also occurred in HTW.

AUTHOR INDEX

Carrión, M. C., 793
 Celzard, A., 784
 Cepanec, Ivica, 771
 Choudhary, Vasant R., 768
 Comisar, Craig M., 800
 Dhar, Anirban, 768
 Eliche-Quesada, D., 793
 Endo, Takeshi, 765
 Fandiño, Olivia, 775

Fernández, Josefa, 775
 Fierro, V., 784
 Filipan, Mirela, 771
 Furdin, G., 784
 Jalón, F. A., 793
 Jana, Prabhas, 768
 Jha, Rani, 768
 Jiménez-López, A., 793
 Litvić, Mladen, 771


López, Enriqueta R., 775
 Lugo, Luis, 775
 Maireles-Torres, P., 793
 Manzano, B. R., 793
 Marêché, J. F., 784
 Ochiai, Bungo, 765
 Pensado, Alfonso S., 775
 Pielaszek, J., 784
 Pogorelič, Ivan, 771

Poliakoff, Martyn, 761
 Rodríguez-Castellón, E., 793
 Satoh, Yuriko, 765
 Savage, Phillip E., 800
 Sayag, C., 784
 Smith, Richard L., 761
 Tang, Samantha L. Y., 761
 Uphade, Balu S., 768

FREE E-MAIL ALERTS

Contents lists in advance of publication are available on the web *via* www.rsc.org/greenchem - or take advantage of our free e-mail alerting service (www.rsc.org/ej_alert) to receive notification each time a new list becomes available.

* Indicates the author for correspondence: see article for details.

 Electronic supplementary information (ESI) is available *via* the online article (see <http://www.rsc.org/esi> for general information about ESI).

ADVANCE ARTICLES AND ELECTRONIC JOURNAL

Free site-wide access to Advance Articles and the electronic form of this journal is provided with a full-rate institutional subscription. See www.rsc.org/ejs for more information.

ReSource

Lighting your way through the publication process

A website designed to provide user-friendly, rapid access to an extensive range of online services for authors and referees.

ReSource enables **authors** to:

- Submit manuscripts electronically
- Track their manuscript through the peer review and publication process
- Collect their free PDF reprints
- View the history of articles previously submitted

ReSource enables **referees** to:

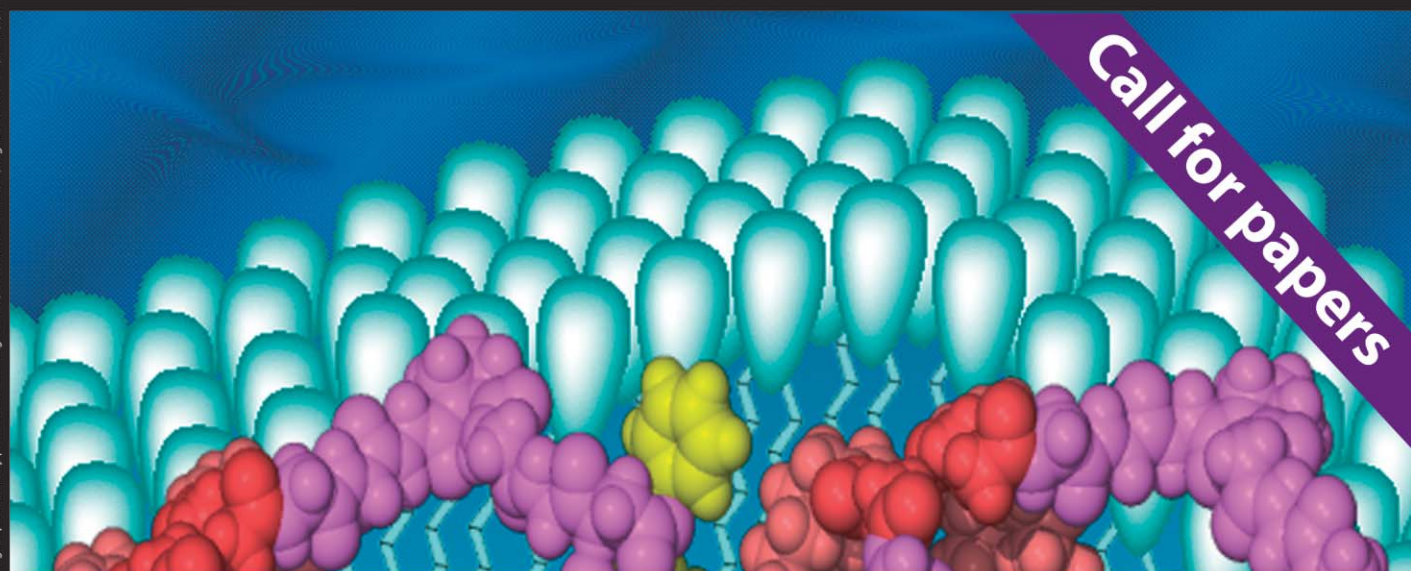
- Download and report on articles
- Monitor outcome of articles previously reviewed
- Check and update their research profile

Register today!

RSC Publishing

www.rsc.org/resource

02030508

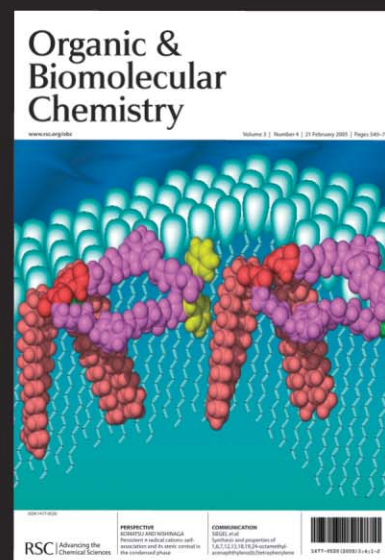


Organic & Biomolecular Chemistry

A major peer-reviewed international, high quality journal covering the full breadth of synthetic, physical and biomolecular organic chemistry.

Publish your review, article, or communication in OBC and benefit from:

- The fastest times to publication (80 days for full papers, 40 days for communications)
- High visibility (OBC is indexed in MEDLINE)
- Free colour (where scientifically justified)
- Electronic submission and manuscript tracking via ReSource (www.rsc.org/ReSource)
- A first class professional service
- No page charges



Submit today!

RSC Publishing

www.rsc.org/obc

Principles of green chemistry: PRODUCTIVELY

Samantha L. Y. Tang,^{*a} Richard L. Smith^b and Martyn Poliakoff^a

DOI: 10.1039/b513020b

The twelve principles of green chemistry (see Fig. 1) have played a major role in promoting the subject and in explaining its aims, ever since they were first propounded by Paul Anastas and John Warner.¹ Indeed, they have inspired others to devise their own principles

including Neil Winterton² and his twelve additional green chemistry principles, and Paul Anastas and Julie Zimmerman's³ principles of green engineering. Despite their inherent value, all of these principles are very cumbersome to present to a lecture audience; one needs one or even two whole lectures to explain them depending on the background of the listeners. Mnemonics, on the other hand, can provide a very pleasant way to communicate and learn the principles.

As part of an ongoing Anglo–Japanese collaboration (JUICE — Japan UK Innovation in Chemistry and Engineering), we have felt the need to produce a simpler statement of the principles that can be presented as a single slide, which is understandable to a wide range of audiences including non-native English speakers. After some consideration, we have devised the acronym, 'PRODUCTIVELY', in which we have tried to capture the spirit of each of the twelve principles of green chemistry in just two or three words, see Fig. 2.

^aSchool of Chemistry, The University of Nottingham, University Park, Nottingham, UK, NG7 2RD

E-mail: samantha.tang@nottingham.co.uk

^bTohoku University, Research Center of Supercritical Fluid Technology, Aramaki Aza Aoba-6-6-11, Aoba-ku, Sendai 980-8579, Japan

1. It is better to prevent waste than to treat or clean up waste after it is formed.
2. Synthetic methods should be designed to maximize the incorporation of all materials used in the process into the final product.
3. Wherever practicable, synthetic methodologies should be designed to use and generate substances that possess little or no toxicity to human health and the environment.
4. Chemical products should be designed to preserve efficacy of function while reducing toxicity.
5. The use of auxiliary substances (e.g. solvents, separation agents, etc.) should be made unnecessary wherever possible and, innocuous when used.
6. Energy requirements should be recognized for their environmental and economic impacts and should be minimized. Synthetic methods should be conducted at ambient temperature and pressure.
7. A raw material or feedstock should be renewable rather than depleting wherever technically and economically practicable.
8. Unnecessary derivatization (blocking group, protection/deprotection, temporary modification of physical/chemical processes) should be avoided whenever possible.
9. Catalytic reagents (as selective as possible) are superior to stoichiometric reagents.
10. Chemical products should be designed so that at the end of their function they do not persist in the environment and break down into innocuous degradation products.
11. Analytical methodologies need to be developed further to allow for real-time in-process monitoring and control prior to the formation of hazardous substances.
12. Substances and the form of a substance used in a chemical process should be chosen so as to minimize the potential for chemical accidents, including releases, explosions, and fires.

Fig. 1 The twelve principles of green chemistry.¹

Condensed Principles of Green Chemistry

- P** - Prevent wastes
- R** - Renewable materials
- O** - Omit derivatization steps
- D** - Degradable chemical products
- U** - Use safe synthetic methods
- C** - Catalytic reagents
- T** - Temperature, Pressure ambient
- I** - In-Process Monitoring
- V** - Very few auxiliary substances
- E** - E-factor, maximise feed in product
- L** - Low toxicity of chemical products
- Y** - Yes, it is safe

Fig. 2 Twelve principles of green chemistry written in the form of a mnemonic: PRODUCTIVELY.

A first glance at Fig. 2 shows that the order of some of the principles has been changed or other principles have been combined or simplified. However, in the course of our lectures, we are finding that

this approach allows the listener to rapidly grasp the concepts.

Much to our pleasure, the PRODUCTIVELY principles have been well received by all of those who have

seen them. We believe that having such an instant set of principles is important for the development of green chemistry and we invite others to build on our idea, and perhaps to devise an even simpler and more striking set of principles.

Acknowledgements

We thank Mr Andy Rigione, Dr Ed Wright and Ms Tomoko Watanabe; the British Embassy and the British Council in Tokyo for their support for Japan–UK research collaboration in green chemistry.

References

- 1 P. T. Anastas and J. C. Warner, *Green Chemistry: Theory and Practice*, Oxford University Press, 1998, p. 30.
- 2 N. Winterton, *Green Chem.*, 2001, **3**, G73.
- 3 P. T. Anastas and J. B. Zimmerman, *Environ. Sci. Technol.*, 2003, **37**, 94A.

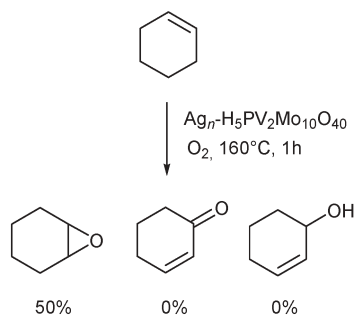
Highlights

DOI: 10.1039/b513789f

Markus Hölscher reviews some of the recent literature in green chemistry

Aerobic epoxidation of alkenes by supported polyoxometalate stabilized metal nanoparticles

A commercially very interesting oxidation reaction is the transformation of alkenes by molecular oxygen to epoxides. Though practicable for ethylene this approach has largely been unsuccessful for the many other interesting alkenes that could potentially be epoxidized. The main problem for many cases is associated with the formation of allylic C–H moieties, which easily undergo C–H bond cleavage and are oxidized to other products. Maayan and Neumann from the Weizmann institute, Rehovot, reasoned that nanoparticles stabilized by polyoxometalates should be promising catalyst candidates for aerobic oxidation of alkenes as some of them were shown to inhibit free radical autooxidation reactions and homolytic C–H bond cleavage in some cases.¹ The authors prepared novel Ag- and Ru/POM (POM = polyoxometalate) nanoparticle combinations and applied them to suitable carriers like α -Al₂O₃. In alkene epoxidation reactions they obtained promising results for the alkenes cyclohexene and 1-methylcyclohexene, which usually are highly sensitive to autooxidation.

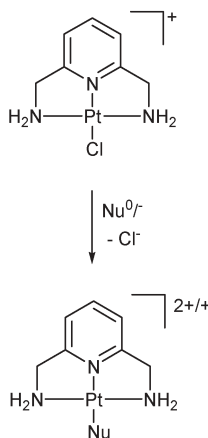


For cyclohexene epoxidation selectivities reached 50% using a Ag-POM catalyst, while a Ru-POM catalyst yielded up to 90% epoxidation selectivity for 1-methylcyclohexene. Unfortunately a fairly large amount of undetected by-products were also produced, which the

authors claim to be oligomeric or polymeric compounds.

Ionic liquids behave like normal solvents in substitution reactions at metal complexes

As the academic and industrial interest in ionic liquids (ILs) has been growing steadily over the past few years, scientific studies that turn to the investigation of the characteristic properties of these interesting solvents have started to emerge more frequently. Especially interesting are mechanistic studies that reveal the true nature and solvation properties of ILs, which is important *e.g.* for rational catalyst design. Van Eldik *et al.* studied the kinetics of ligand substitution reactions at platinum(II) complexes in water, methanol and IL 1-butyl-3-methylimidazolium bis(trifluoromethylsulfonyl)amide ([BMIM]BTA) employing thiourea and iodide as nucleophiles.²

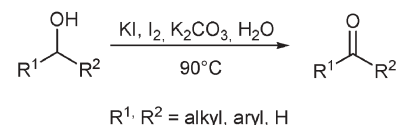


Thiourea being a stronger nucleophile than iodide reacts much faster with the complexes, and the polarity of the solvent influences the reaction rate significantly, with k_2 values for water being much larger than for methanol and the IL (k_2 values for methanol and [BMIM]BTA are similar). This indicates the IL behaves like methanol *i.e.* as a

“normal” solvent with no drastic acceleration or deceleration of the substitution of chloride. With regard to the activation parameters ΔH^\ddagger , ΔS^\ddagger and ΔV^\ddagger the authors reasoned that volume changes do not respond to changes in the overall charge of the reaction’s transition state in the ionic liquid, possibly due to strong hydrogen bonds. DFT calculations supported an associative ligand-substitution mechanism.

Anaerobic oxidation of alcohols to aldehydes and ketones in water

The selective oxidation of alcohols is an important reaction in organic chemistry and especially desirable is the suppression of over-oxidation. A number of approaches have been developed including transition metal catalyzed reactions, however these are associated with waste disposal problems and other drawbacks. A metal free approach would be an interesting and possibly environmentally friendly alternative, which was recently pursued by Gogoi and Konwar from the Regional Research Laboratory (Organic Chemistry Division), Jorhat, India.³ The authors focused on the use of iodine which has been used increasingly in recent years as it shows low toxicity and is easy to handle. They developed a metal free version of the oxidation of alcohols to aldehydes and ketones that can be performed in water with no additional organic solvent.



The optimum oxidation system consists of I₂, KI (25 mol%), K₂CO₃, and water, as was elucidated by test oxidations of 4-methoxybenzyl alcohol, for which the yield of the product *p*-anisaldehyde amounted to 96%. A variety of

primary and secondary alcohols was screened yielding high yields in many cases with no observation of over-oxidized products.

References

- 1 G. Maayan and R. Neumann, *Chem. Commun.*, 2005, 4595–4597.
- 2 C. C. Weber, R. Puchta, N. van Eikema Hommes, P. Wasserscheid and R. van Eldik, *Angew. Chem.*, 2005, **117**, 6187–6192.
- 3 P. Gogoi and D. Konwar, *Org. Biomol. Chem.*, 2005, **3**, 3473–3475.

Nucleophilic polyaddition in water based on chemo-selective reaction of cyclic carbonate with amine†

Bungo Ochiai, Yuriko Satoh and Takeshi Endo*

Received 2nd August 2005, Accepted 9th September 2005

First published as an Advance Article on the web 26th September 2005

DOI: 10.1039/b511019j

The appropriate choice of the monomers and the polymerization temperatures enabled polyaddition of bifunctional cyclic carbonates and diamines in water completely free from surfactants and organic solvents, although the primary reaction is a nucleophilic addition.

The recent requirements for saving use of petroleum resources have been encouraging the development of reactions using water as a solvent instead of organic liquids.^{1–4} On applying water as a solvent for a reaction, one must consider side reactions such as hydrolysis that decrease yields of products compared to those in organic solvents. That is, reactions in aqueous media require appropriate choices of reactions or reaction conditions to attain results competitive with reactions in organic solvents. For polymer synthesis, some chain polymerizations successfully proceed in aqueous emulsion or suspension to attain easy purification, diffusion of heat of polymerization, and so forth.^{5–7} In the case of step polymerizations, polymerizations in aqueous media usually requires the presence of organic solvents.^{8–11} For example, synthesis of polyurethanes, which are usually prepared from diols and water-sensitive diisocyanates, was achieved in aqueous media to obtain a convenient aqueous dispersion in spite of employing a trace amount of organic solvents.^{10,11} Step polymerizations, especially those based on nucleophilic addition, in aqueous media without containing organic solvent will need polymerizations based on more chemo-selective primary reactions.

As an example of chemo-selective polyadditions, it has been reported that the polyaddition of bifunctional carbonates and diamines efficiently gives polyurethanes with hydroxyl groups (*i.e.*, polyhydroxyurethanes) without employing toxic and unstable diisocyanates.^{12–17} The chemo-selectivity allowed the polyaddition to employ monomers with various functional groups (*e.g.* lysine,¹⁶ triethylenetetramine¹³ or diethylenetriamine¹⁷) and to be conducted in the presence of impurities including water and alcohol. It is also noteworthy that the bifunctional cyclic carbonates can be quantitatively prepared from diepoxides and carbon dioxide. Accordingly, we attempted to explore polyaddition of bifunctional carbonates and diamines in water instead of organic solvents.

The polymerization was conducted using 1.0 mL of water for 500 μmol amounts of bifunctional carbonates (BisAC and C4C) and diamines (HDA and HMDA) at various temperatures for 24 h

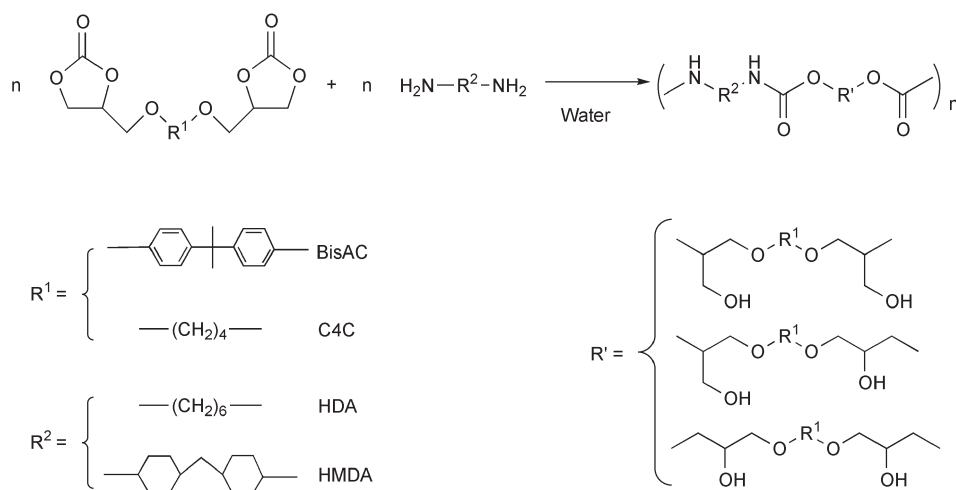
(Scheme 1, Table 1 runs 1–5 and 8–11). All the initial polymerization mixtures were heterogeneous, because both of the carbonates are insoluble in water at the reaction temperatures. Whereas the reaction mixtures in the polymerizations using BisAC stayed heterogeneous, those in the polymerizations using C4C became homogeneous solutions. The higher reaction temperature resulted in higher conversions of the carbonate monomers, determined from ¹H NMR spectroscopic analysis. Polymerizations of BisAC and HDA conducted below 70 °C gave polymers with yields that agree with the conversions of BisAC, while those above 80 °C resulted in oligomers in low yields. On the other hand, polymerizations employing HMDA, which is insoluble in water, were less influenced by reaction temperature. This may be ascribed to the high hydrophobicity and the weak nucleophilicity of HMDA. That is, although the hydrophobicity may have slowed the hydrolysis, weakly nucleophilic HMDA could not have attacked the carbonate moieties predominantly over the hydrolysis regardless of the temperature. In contrast to the polyadditions employing BisAC, the attempts to polymerize C4C in water failed (discussed later). These results suggest that heterogeneity to protect the carbonates from hydrolysis and sufficient nucleophilicity of the diamine are the important factors to acquire the selectivity in this polyaddition in aqueous media.

Additionally, we polymerized BisAC and HDA at 50 and 60 °C for 48 h (runs 6 and 7). The longer reaction time increased the molecular weights of the polyhydroxyurethane a little, which would have originated from the further polyaddition of the few remaining terminal groups. These increased molecular weights support the observation that the polyhydroxyurethanes produced are stable under these polymerization conditions. However, the molecular weights of the polymers were lower than the polymerizations in dimethyl sulfoxide containing water (2 molar-equivalent to BisAC),¹⁵ probably because the excess amounts of water resulted in the slight hydrolysis of the cyclic carbonate under the basic conditions. The ratios of the primary and secondary alcohols in the polymers are almost identical to the polymerizations in organic solvents.

To elucidate the hydrolysis behavior in the aminolysis of the cyclic carbonates in water, we reacted the cyclic carbonates (500 μmol) with *n*-butylamine (1.0 equiv. to carbonate moieties) in water (500 μL) for 24 h at 70 °C (Scheme 2). Whereas the aminolysis of BisAC predominantly afforded the objective hydroxyurethanes over the hydrolyzed diol (hydroxyurethane : diol = 84 : 16),¹⁸ that of C4C gave the corresponding hydrolyzed diol quantitatively instead of the hydroxyurethane derivative. The differing hydrophobicity of the carbonate monomers is a probable reason for this clear difference, *i.e.*, BisAC that contains a

Department of Polymer Science and Engineering, Faculty of Engineering, Yamagata University, Jonan 4-3-16, Yonezawa, Yamagata, 992-8510, Japan. E-mail: tendo@yz.yamagata-u.ac.jp; Fax: +81-238-26-3090; Tel: +81-238-26-3090

† Electronic supplementary information (ESI) available: materials and measurement conditions. See <http://dx.doi.org/10.1039/b511019j>

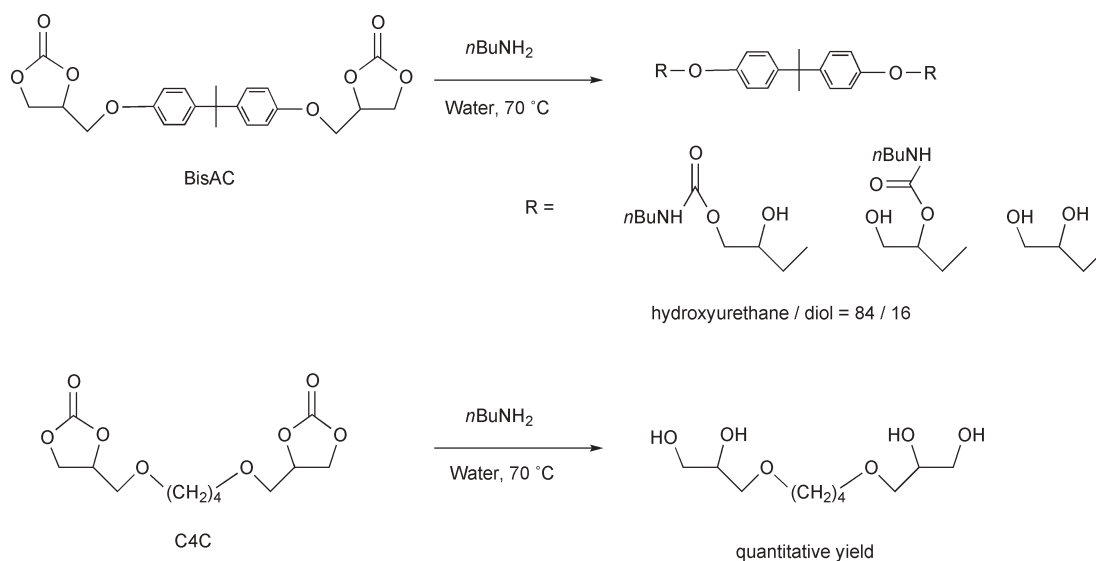


Scheme 1 Polyaddition of bifunctional cyclic carbonate and diamine in water.

Table 1 Polyaddition of bifunctional cyclic carbonate and diamine in water^a

Run	Carbonate	Diamine	Time/h	Temp./°C	Conversion of carbonate (%) ^b	Yield (%) ^c	M_n (M_w/M_n) ^d	Primary OH : secondary OH ^e
1	BisAC	HDA	24	50	100	97	3600 (2.16)	28 : 72
2	BisAC	HDA	24	60	100	99	3900 (1.98)	31 : 69
3	BisAC	HDA	24	70	100	>99	4200 (1.86)	35 : 65
4	BisAC	HDA	24	90	100	70	1600 (1.22)	27 : 73
5	BisAC	HDA	24	100	100	37	500 (1.03)	n.d. ^f
6	BisAC	HDA	48	50	100	99	3900 (1.92)	24 : 76
7	BisAC	HDA	48	60	100	90	4400 (1.90)	23 : 77
8	BisAC	HMDA	24	70	100	70	2100 (1.88)	24 : 76
9	BisAC	HMDA	24	100	100	69	2000 (1.14)	32 : 68
10	C4C	HDA	24	70	100	<5	n.d. ^f	n.d. ^f
11	C4C	HMDA	24	70	100	<5	n.d. ^f	n.d. ^f

^a Conditions: 24 h, degassed sealed tube, monomers; 500 μmol each, water 1.0 mL. ^b Determined by ¹H NMR spectra of reaction mixtures (270 MHz, *d*₆-DMSO). ^c Yields based on the calculated weights of the polymers, after the weights of the contaminants estimated by ¹H NMR spectroscopy were subtracted from those of the insoluble parts of saturated aqueous NaCl solutions. No contaminants were detectable in the polymers when the yields of the polymers were quantitative. ^d Estimated by SEC based on polystyrene standards eluted with DMF containing 50 mM phosphoric acid and 50 mM lithium bromide. ^e Determined by ¹H NMR spectroscopy (270 MHz, *d*₆-DMSO). ^f Not determined.



Scheme 2 Nucleophilic addition of *n*-butylamine to BisAC and C4C in water.

considerable degree of hydrophobic structure may have excluded water from the carbonate moieties to prevent the hydrolysis. In addition, the aminolysis of 4-phenoxyethyl-1,3-dioxolan-2-one¹⁹ having less hydrophobic character than BisAC gave the corresponding hydroxyurethanes (74%) accompanied by the hydrolyzed product (26%), supporting the aforementioned hypothesis.¹⁸

In conclusion, polyaddition of a hydrophobic bifunctional cyclic carbonate and hexamethylenediamine effectively gives polyurethane with hydroxyl groups in aqueous media free from any organic solvents and surfactants, although possibly accompanied by trace degrees of hydrolysis. This method is potentially applicable to the preparation of new polyurethane emulsions by an environmentally benign procedure.

References

- 1 K. Makabe and S. Kobayashi, *Chem.—Eur. J.*, 2002, **8**, 4095.
- 2 T. Okuhara, *Chem. Rev.*, 2002, **102**, 3641.
- 3 U. M. Lindstrom, *Chem. Rev.*, 2002, **102**, 2751.
- 4 R. Breslow, *Acc. Chem. Res.*, 1991, **24**, 159.
- 5 J. P. Claverie and R. Soula, *Prog. Polym. Sci.*, 2003, **28**, 619.
- 6 K. Satoh, M. Kamigaito and M. Sawamoto, *Macromolecules*, 2000, **33**, 5830.
- 7 K. Satoh, M. Kamigaito and M. Sawamoto, *Macromolecules*, 2000, **33**, 5836.
- 8 T. Nishikubo, A. Kameyama, A. Kaneko and Y. Yamada, *J. Polym. Sci., Part A: Polym. Chem.*, 1997, **35**, 2711.
- 9 M. Barrere and K. Landfester, *Polymer*, 2003, **44**, 2833.
- 10 F. Tiarks, K. Landfester and M. Antonietti, *J. Polym. Sci., Part A: Polym. Chem.*, 2001, **39**, 2520.
- 11 M. Barrere and K. Landfester, *Macromolecules*, 2003, **36**, 5119.
- 12 J. M. Whelan Jr., M. Hill and R. J. Cotter, *US Pat.*, 3 072 613, 1963.
- 13 G. Rokicki and R. Lazinski, *Angew. Makromol. Chem.*, 1989, **170**, 211.
- 14 G. Rokicki and C. Wojciechowski, *J. Appl. Polym. Sci.*, 1990, **41**, 627.
- 15 N. Kihara and T. Endo, *J. Polym. Sci., Part A: Polym. Chem.*, 1993, **31**, 2765.
- 16 N. Kihara, Y. Kushida and T. Endo, *J. Polym. Sci., Part A: Polym. Chem.*, 1996, **34**, 2173.
- 17 B. Ochiai, J. Nakayama, M. Mashiko, T. Nagasawa, Y. Kaneko and T. Endo, *J. Polym. Sci., Part A: Polym. Chem.*, DOI: 10.1002/pola21078. For aminolysis of cyclic carbonates with diethylenetriamine, see ref. 20.
- 18 Although the selectivity of the model reaction seems not enough for the quantitative formation of polymers, polymerization will be advantageous to promote the heterogeneity of the system that increases the opportunity of nucleophilic addition over hydrolysis. The lower selectivity in the aminolysis of 4-phenoxyethyl-1,3-dioxolan-2-one also supports this hypothesis.
- 19 T. Iwasaki, N. Kihara and T. Endo, *Bull. Chem. Soc. Jpn.*, 2000, **73**, 713.
- 20 D. C. Webster and A. L. Crain, *Prog. Org. Coat.*, 2000, **40**, 275.

A green process for chlorine-free benzaldehyde from the solvent-free oxidation of benzyl alcohol with molecular oxygen over a supported nano-size gold catalyst

Vasant R. Choudhary,* Anirban Dhar, Prabhas Jana, Rani Jha and Balu S. Uphade

Received 27th June 2005, Accepted 22nd September 2005

First published as an Advance Article on the web 4th October 2005

DOI: 10.1039/b509003b

Benzyl alcohol is oxidized selectively to benzaldehyde with high yield, with a little formation of benzylbenzoate, by molecular oxygen over a reusable nano-size gold catalyst supported on U_3O_8 , MgO, Al_2O_3 or ZrO_2 in the absence of any solvent.

Liquid phase oxidation of benzyl alcohol is an important preferred reaction practically for the production of chlorine-free benzaldehyde, without loss of carbon in the form of CO_2 (a greenhouse gas). The preparation of benzaldehyde by reacting benzyl alcohol with stoichiometric or excess amounts of potassium or ammonium permanganate in aqueous acidic medium¹ is not environmentally benign at all, because of the formation of a large amount of toxic waste. A few studies on the benzyl alcohol-to-benzaldehyde oxidation by H_2O_2 or O_2 in the presence of organic solvent, using different solid catalysts, such as Pd/C,² Pd(II) hydrotalcite,³ Pd-Ag/pumice,⁴ Ru-Co-Al hydrotalcite,⁵ Ni-containing hydrotalcite^{6,7} and nano-size NiO_2 ,⁸ have been reported. However, because of the use of organic solvent, the benzaldehyde production in these cases is not environmentally benign, even though an environmentally clean oxidant (O_2 or H_2O_2) is used. Recently, Choudhary *et al.*^{9,10} have reported the solvent-free oxidation of benzyl alcohol to benzaldehyde over MnO_4^- -exchanged hydrotalcite⁹ and transition metal containing layered double hydroxides and/or mixed hydroxides,¹⁰ using *tert*-butylhydroperoxide (TBHP) as the oxidant; after consumption TBHP leaves *tert*-butanol as a co-product and hence it is not a clean oxidizing agent. To be a cost effective and environmentally-friendly (or green) process, the benzyl alcohol-to-benzaldehyde oxidation with high selectivity and yield must be accomplished under solvent-free conditions, using molecular oxygen (which is not only a clean agent but also the cheapest oxidizing agent) as the oxidant and also using a highly active solid catalyst (which is easily separable and also reusable) in the process. This has been achieved in the present investigation. We report in this Communication a totally green process for the liquid phase selective oxidation of benzyl alcohol to benzaldehyde, with high selectivity and yield, by molecular oxygen using easily separable and reusable supported nano-size gold catalysts (*viz.* Au supported on U_3O_8 , MgO, Al_2O_3 or ZrO_2) in the absence of any solvent.

Results showing the solvent-free liquid phase oxidation of benzyl alcohol to benzaldehyde by molecular oxygen over nano-size gold supported over different metal oxides are presented in Table 1. In the absence of any catalyst, the benzyl alcohol conversion was 4% with 96% and 5% selectivity for benzaldehyde and benzylbenzoate, respectively. The preparation (by homogeneous deposition precipitation of gold on support) and characterisation of the supported nano-size gold catalysts are given earlier.¹¹ The liquid phase oxidation of benzyl alcohol over the supported Au catalysts, was carried out in a magnetically stirred reactor (capacity: 10 cm³), provided with a mercury thermometer for measuring the reaction temperature and reflux condenser, at the following reaction conditions: reaction mixture = 29 mmol benzyl alcohol + 0.1 g catalyst, temperature = 130 °C, pressure = 1.5 atm, and reaction time = 5 h. After the reaction, the catalyst was removed from the reaction mixture by filtration and the reaction products and unconverted reactants were analysed by gas chromatography with a flame ionisation detector, using a SE-30 column and N_2 as carrier gas.

From the results in Table 1 the following important observations can be made:

- Among the gold catalysts, the Au/ U_3O_8 catalyst showed the best performance [both high activity (53% conversion) and selectivity (95%)] in the oxidation of benzyl alcohol to benzaldehyde. The other supported gold catalysts, particularly Au/MgO, Au/ Al_2O_3 and Au/ ZrO_2 also showed good activity in the benzyl alcohol-to-benzaldehyde oxidation.
- The highest activity (benzyl alcohol conversion of 68.9%) was shown by the Au/ Al_2O_3 catalyst. However, this catalyst showed somewhat lower benzaldehyde selectivity (65%).
- The Au/ Fe_2O_3 catalyst showed very high selectivity (100%) for benzaldehyde but low activity (16.2% conversion) in the oxidation.
- The order of the catalysts for the benzaldehyde formation (benzaldehyde yield) is Au/ U_3O_8 (50.4%) > Au/ Al_2O_3 (44.8%) > Au/ ZrO_2 (44.1%) > Au/MgO (43.9%) > Au/ZnO (37.6%), Au/BaO or Au/ La_2O_3 (35.5%) > Au/ MnO_2 (34.5%) > Au/ Sm_2O_3 (33.3%) > Au/ Eu_2O_3 (32.4%) > Au/CaO (30.4%) > Au/CoO (26.7%) > Au/NiO (25.0%) > Au/CuO (18.6%) > Au/ Fe_2O_3 (16.2%).

The results reveal a strong influence of metal oxide support on the catalytic performance (both the benzyl alcohol conversion activity and product selectivity in the oxidation of benzyl alcohol to benzaldehyde) of the supported gold catalysts. However, since the supported gold catalysts do not have the same gold loading, their comparison may not be valid. It is, however, interesting to note that the Au/ ZrO_2 catalyst shows

Chemical Engineering and Process Development Division, National Chemical Laboratory, Pune-411008, India. E-mail: vrc@che.ncl.res.in; vrc@ems.ncl.res.in; Fax: +91 20 25893041; Tel: +91 20 25893300 (extn. 2318)

Table 1 Results of the oxidation of benzyl alcohol-to-benzaldehyde by O₂ over different metal oxide supported nano-size gold catalysts in the absence of any solvent

Nano-gold catalyst	Conc. of gold (wt.%)	Gold particle size/nm	Conversion of benzyl alcohol (%)	Selectivity (%)		Benzaldehyde yield (%)	TOF ^a /mol g(Au) ⁻¹ h ⁻¹
				Benzaldehyde	Benzylbenzoate		
Au/MgO	7.5	8.9 ± 0.7	51.0	86.0	14.0	43.9	0.34
Au/CaO	4.7	9.6 ± 1.2	33.3	91.3	8.6	30.4	0.38
Au/BaO	5.3	7.1 ^a	43.5	81.5	18.5	35.5	0.39
Au/Al ₂ O ₃	6.4	3.6 ± 1.1	68.9	65.0	35.0	44.8	0.41
Au/ZrO ₂	3.0	4.5 ± 1.20	50.7	87.0	13.0	44.1	0.85
Au/La ₂ O ₃	6.5	n.d.	51.6	68.8	31.3	35.5	0.32
Au/Sm ₂ O ₃	4.2	7.9 ± 0.5	44.4	75.0	25.0	33.3	0.46
Au/Eu ₂ O ₃	6.6	n.d.	37.5	87.5	12.5	32.4	0.29
Au/U ₃ O ₈	8.0	9.4 ± 3.2	53.0	95.0	5.0	50.4	0.37
Au/MnO ₂	4.1	6.1 ± 1.7	39.7	88.8	11.1	34.5	0.49
Au/Fe ₂ O ₃	6.1	5.8 ± 0.3	16.2	100	—	16.2	0.15
Au/CoO	7.1	5.7 ± 1.3	28.3	95.2	4.8	26.7	0.22
Au/NiO	6.2	23.1 ± 3.7	32.0	78.0	22.0	25.0	0.23
Au/CuO	6.8	11.7 ± 2.6	27.0	69.0	31.0	18.6	0.16
Au/ZnO	6.6	5.9 ^a	40.5	92.8	7.2	37.6	0.33

^a Rate of the formation of benzaldehyde per unit mass of the deposited gold per unit time.

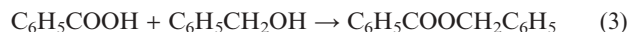
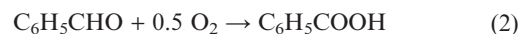
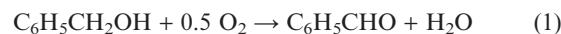
high activity (much higher than many of the supported Au catalysts) in spite of the fact that its Au loading is the lowest. This may be because of the lower Au particle size of the Au/ZrO₂. A comparison of the data also indicates that there is no direct relationship between the Au loading and the performance (in the benzyl alcohol-to-benzaldehyde oxidation) of the supported Au catalysts.

When the supported Au catalysts were compared for their turn-over-frequency (TOF), measured in terms of the rate of benzaldehyde formation per unit mass of gold deposited on the different metal oxide support, the supported Au catalysts show the following order: Au/ZrO₂ > Au/MnO₂ > Au/Sm₂O₃ > Au/Al₂O₃ > Au/BaO > Au/CaO > Au/U₃O₈ > Au/MgO > Au/ZnO > Au/La₂O₃ > Au/Eu₂O₃ > Au/NiO > Au/CoO > Au/CuO > Au/Fe₂O₃. The interaction between the supported gold and the support is expected to play an important role in deciding both the gold particle size and catalytic performance of the supported gold catalysts.

When the promising supported nano-size gold catalysts, Au/U₃O₈, Au/MgO, Au/Al₂O₃ and Au/ZrO₂, were reused in the benzyl alcohol-to-benzaldehyde oxidation, the variation in the benzaldehyde yield and selectivity was within 3–5%, indicating an excellent reusability of the catalysts. For the Au/U₃O₈ catalyst, the benzaldehyde yield after 1st, 3rd and 5th reuse was 50.1, 50.3 and 49.8%, respectively. The supports (*viz.* MgO, Al₂O₃, ZrO₂ and U₃O₈) alone showed negligible small activity for the oxidation of benzyl alcohol. Also, when the catalysts from the reaction mixture were removed after the initial reaction period of 30 min, there was no further appreciable increase in the conversion or yield, indicating that the reaction is essentially catalyzed by the heterogeneous supported gold. Use of supported gold catalysts has also been reported earlier for the selective oxidation by molecular oxygen of glycerol to glyceric acid,¹² polyhydroxylated aliphatics to monocarboxylates¹³ and aliphatic/aromatic aldehydes to carboxylic acids.¹⁴

It is interesting to note that benzyl benzoate is the only other product formed apart from benzaldehyde and the formation of benzoic acid was not at all detected in GC and/or in GC-MS

analysis. The reactions involved in the oxidation process are as follows:



The absence of benzoic acid in the GC and GC-MS analysis indicates that, as soon as benzoic acid is formed (reaction (2)), it reacts immediately with benzyl alcohol, which is available in much higher concentration, forming benzyl benzoate (reaction (3)).

The organic solvent-free preparation of chlorine-free benzaldehyde from the selective oxidation of benzyl alcohol by molecular oxygen using the supported nano-size gold catalyst, particularly nano-size gold supported on U₃O₈, MgO, Al₂O₃ or ZrO₂, is a totally clean process. Also, no operational problems are foreseen for use of this green process in the large scale production of benzaldehyde. The process may be carried out at higher oxygen pressure (>1.5 atm) to increase both the conversion and product yield or to reduce the reaction time.

References

- (a) L. Kotai, B. Kazinczy, A. Keszler, H. Sandor, I. Gacs and K. Banerji, *Z. Naturforsch., B*, 2001, **56**, 823; (b) A. Corma, V. Lambies, F. V. Melo and J. Palou, *An. Quim., Ser. A*, 1980, **76**, 304.
- N. S. Bijlani and S. B. Chandalia, *Indian Chem. Eng.*, 1981, **23**, 44.
- T. Nishimura, N. Kakiuchi, M. Inoue and S. Uemura, *Chem. Commun.*, 2000, 1245; T. Nishimura, N. Kakiuchi, M. Inoue and S. Uemura, *Bull. Chem. Soc. Jpn.*, 2001, **74**, 165.
- L. F. Liotta, A. M. Venezia, G. Deganello, A. Longo, A. Martorana, Z. Schay and L. Guzzi, *Catal. Today*, 2001, **66**, 271.
- I. Matsushita, K. Ebitani and K. Kaneda, *Chem. Commun.*, 1999, 265.
- B. M. Choudary, M. Lakshmi Kantum, Ateeq Rahman, Ch. Venkat Reddy and K. Koteswara Rao, *Angew. Chem. Int. Ed. Engl.*, 2001, **40**, 763.
- T. Kawabata, Y. Shinozuka, Y. Ohishi, T. Shishido, K. Takaki and K. Takehira, *J. Mol. Catal. A*, 2005, **236**, 206.
- H. Ji, T. Wang, M. Zhang, Y. She and L. Wang, *Appl. Catal. A*, 2005, **282**, 25.

- 9 V. R. Choudhary, D. K. Dumbre, V. S. Narkhede and S. K. Jana, *Catal. Lett.*, 2003, **86**, 229.
- 10 V. R. Choudhary, D. K. Dumbre, B. S. Uphade and V. S. Narkhede, *J. Mol. Catal. A*, 2004, **215**, 129.
- 11 (a) N. S. Patil, R. Jha, B. S. Uphade, S. K. Bhargava and V. R. Choudhary, *Appl. Catal. A*, 2004, **275**, 87; (b) N. S. Patil, B. S. Uphade, P. Jana, S. K. Bhargava and V. R. Choudhary, *J. Catal.*, 2004, **223**, 236; (c) N. S. Patil, B. S. Uphade, P. Jana, R. S. Sonawane, S. K. Bhargava and V. R. Choudhary, *Catal. Lett.*, 2004, **94**, 89; (d) N. S. Patil, B. S. Uphade, P. Jana, S. K. Bhargava and V. R. Choudhary, *Chem. Lett.*, 2004, **33**, 400; (e) N. S. Patil, B. S. Uphade, D. G. McCulloh, S. K. Bhargava and V. R. Choudhary, *Catal. Commun.*, 2004, **5**, 681.
- 12 (a) S. Carrettin, P. McMorn, P. Johnston, K. Griffin and G. J. Hutchings, *Chem. Commun.*, 2002, 696; (b) S. Carrettin, P. McMorn, P. Johnston, K. Griffin, C. J. Kiely, G. A. Attard and G. J. Hutchings, *Top. Catal.*, 2004, **27**, 131.
- 13 S. Biella, G. L. Castiglioni, C. Fumagalli, L. Prati and M. Rossi, *Catal. Today*, 2002, **72**, 4314.
- 14 A. Corma and M. E. Domine, *Chem. Commun.*, 2005, 4042.

Ammonium carbamate; mild, selective and efficient ammonia source for preparation of β -amino- α,β -unsaturated esters at room temperature

Mladen Litvić,* Mirela Filipan, Ivan Pogorelić and Ivica Cepanec

Received 19th July 2005, Accepted 6th September 2005

First published as an Advance Article on the web 22nd September 2005

DOI: 10.1039/b510276f

Ammonium carbamate can be used as a very effective reagent for preparation of different substituted β -amino- α,β -unsaturated esters in methanol at room temperature. The product is isolated without aqueous work-up in high purity and excellent yield. The method is simple and easily scaled-up.

Introduction

Hantzsch 1,4-dihydropyridines (1,4-DHPs) are an important class of heterocyclic compounds due to their pharmacological activity as calcium channel antagonists.¹ Therefore, they are found to be of use in the treatment of atherosclerosis and other coronary diseases. Recently, their other pharmacological activities have been reported such as: antitumor,² bronchodilating,³ antidiabetic,⁴ antiviral,⁵ antianginal⁶ among others.⁷ The Hantzsch 1,4-dihydropyridine synthesis is the most convenient route to the preparation of symmetrical 1,4-DHPs. It is accomplished by condensation of aliphatic or aromatic aldehydes with an excess of β -ketoesters and ammonia.⁸ For the synthesis of chiral, 3,5-unsymmetrically substituted 1,4-DHPs, equal amounts of β -amino- α,β -unsaturated esters† (1) and β -ketoesters‡ (2) are used in condensation with an appropriate aldehyde.⁹ β -Amino- α,β -unsaturated esters (1) have found important application as substrates for asymmetric hydrogenation to produce β -aminoesters which can be converted into chiral β -aminoacids.¹⁰

With growing interest towards better methodologies for preparation of 1,4-DHPs it is also important to find fast and practical methods for preparation of β -amino- α,β -unsaturated esters. Although most of the simple β -amino- α,β -unsaturated esters (1) are commercially available in large quantities, industrial chemicals always contain traces of ammonia and corresponding β -ketoesters as products of hydrolysis. From that point 1,4-DHPs synthesised by Hantzsch condensation contain considerable amounts of two symmetrical diesters as principal impurities, depending on the purity of the starting β -amino- α,β -unsaturated ester. Purification to the level of >99% includes at least a few recrystallisation steps and therefore causes drastic environmental impact by decreasing the overall yield as well as by usage of large quantities of volatile solvents. Due to the fact that 1,4-DHPs as well as their intermediates are today produced in tonnage amounts, better selectivity of the Hantzsch synthesis and development of facile

and “green” synthetic methods to β -amino- α,β -unsaturated esters are still demanded.

From the literature, few different methods are known for the preparation of *N*-unsubstituted β -amino- α,β -unsaturated esters. The condensation of β -ketoesters with excess ammonium acetate as the ammonia source in methanol¹¹ or acetic acid¹² is often used. Introduction of gaseous ammonia into the solution of β -ketoester in methanol,^{13,14} dichloromethane¹⁵ or chloroform¹⁶ at 0 °C is a milder method used for that purpose. To improve the yield and increase the reaction speed some other methods have been developed including reaction of β -ketoesters with gaseous ammonia catalysed with *p*-toluenesulfonic acid in toluene^{17,18} or benzene¹⁹ with azeotropic removal of water. Aqueous ammonia and a catalytic amount of acetic acid²⁰ in methanol²¹ or ethanol²² as solvent have also been used. Silica gel²³ and K-10 montmorillonite²⁴ catalysed enamination of β -dicarbonyl compounds have recently been developed.

However, the application of these methods suffers from one or more disadvantages such as prolonged heating, use of excess ammonia or ammonium salts, unsatisfactory yields and necessity of extractive work-ups of the reaction mixture. The purification of crude product is often required due to the fact that conversion in most cases is not complete.^{15,16} Vacuum distillation of crude product is a good and economic industrial method yielding pure product but its main drawback is the use of expensive equipment and high temperatures.¹⁸ To avoid this purification step, a mild, practical and rapid method yielding pure β -amino- α,β -unsaturated esters would be a good approach for these valuable chemicals, especially in the form of a one-pot Hantzsch 1,4-dihydropyridine synthesis.

Results and discussion

Our aim was to find a solid ammonia source which is selective enough in stoichiometric amounts to form β -amino- α,β -unsaturated esters from β -ketoesters without a catalyst. We began our study with ammonium salts such as ammonium acetate, formate and other salts of weak or moderately strong acids. All of them were able to convert β -ketoesters to appropriate β -amino- α,β -unsaturated esters even at room temperature but isolation of product required aqueous work-up due to the nonvolatility of the acids formed as

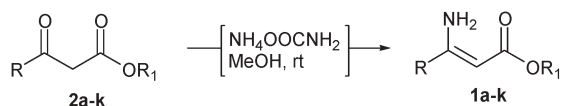
BELUPO Pharmaceuticals & Cosmetics Inc., Research Department, Radnička c. 224, 10000 Zagreb, Croatia.

E-mail: mladen.litvic@belupo.hr; Fax: +385 1 2408074;

Tel: +385 1 2404176

† 3-Aminocrotonic acid ester is the commonly used name for this type of compounds.

‡ Acetoacetic acid esters.



Scheme 1

reaction side products. Similar results in the same reaction were obtained by employing a few equivalents of ammonium carbamate ($\text{NH}_4\text{OOCNH}_2$), the ammonium salt of unstable carbamic acid (NH_2COOH), according to Scheme 1. In comparison to other ammonium salts, excess of ammonium

carbamate as well as ammonium hydrogencarbonate formed in reaction were simply removed during evaporation of the reaction mixture above $60\text{ }^\circ\text{C}$.²⁵ Ammonium carbamate, also called the “anhydride” of ammonium carbonate²⁴ is an industrially important chemical as an intermediate in the synthesis of urea, one of the most important artificial fertilizers. Although the world production of ammonium carbamate exceeds a few millions of tons it is very rarely used in organic synthesis. Some authors have used it as a mild ammonia source in lipase catalysed ammonolysis of esters²⁶ or synthesis of β -glycosylamines.²⁷

Table 1 Formation of β -amino- α,β -unsaturated esters employing ammonium carbamate

Entry	β -Ketoester 2	Product 1	Reaction time/min	Yield ^a (%)	mp/ ^o C
a			15	94	89–90 (83–84) ¹²
b			15	99	Oil ^b (Oil) ²³
c			15	98	Oil ^b (Oil) ¹³
d			15	98	Oil ^b (Oil) ¹⁸
e			15	95	Oil ^b (Oil) ¹³
f			15	94	Oil ^b (Oil) ¹³
g			15	98	86–88 (88) ²⁰
h			30	90	86–87
i			30	99	34–36 (36–37) ²³
j			10	95	31–32 (30–32) ²³
k			30	90	88–90 (90–92) ³⁰

^a All products were characterized by ^1H NMR, ^{13}C NMR and IR spectra and compared with authentic samples. ^b Crystallizes upon standing in refrigerator.

Herein we would like to report that ammonium carbamate efficiently and in mild conditions converts different types of β -ketoesters (**2a–k**) to β -amino- α,β -unsaturated esters (**1a–k**) in methanol at room temperature (Scheme 1).²⁸

As a result of preliminary studies methanol is chosen as the most convenient solvent due to the highest solubility of ammonium carbamate, shorter reaction time and the lowest boiling point in comparison to other alcohols studied such as ethanol, propan-2-ol, isobutanol *etc.*²⁹ The optimisation of the reaction showed that 1 equivalent of ammonium carbamate is sufficient to complete the reaction. To explore the scope of this method we decided to test it on a series of β -ketoesters (**2a–k**). Most of them are used as starting materials in Hantzsch synthesis of pharmaceutically important 1,4-dihydropyridines. The results presented in Table 1 indicate the generality of the method and efficacy of ammonium carbamate as very mild but selective ammonia source and dehydrating agent. The main characteristics of the reaction are short reaction time (usually 15 min), excellent yield (>90%) and high purity of crude products. This method was successfully applied to enamination of simple linear β -ketoesters with different ester groups (**2a–h**), a cyclic β -ketoester (**2i**) and a β -diketone (**2j**). Although most of the literature methods for preparation of β -amino- α,β -unsaturated esters are acid catalysed,^{12,17–23} we have been able to carry out this reaction in almost neutral conditions. In comparison to gaseous ammonia, ammonium carbamate is a much milder ammonia source due to its lower basicity and therefore allows preparation of β -amino- α,β -unsaturated esters in the presence of acid or base sensitive groups such as in **2f** and **2k**. The other advantage of the method employing ammonium carbamate compared to other methods is the high conversion (~100%) of starting β -ketoesters due to the fact that water formed in the reaction is converted to ammonium hydrogencarbonate which prevents hydrolysis of the product.

Furthermore, we extended our studies to explore the possibility of scaling up this new approach to β -amino- α,β -unsaturated esters. We decided to test the method for preparation of ethyl-3-aminocrotonate (**1b**). On 1 mol scale the reaction was completed within 45 minutes and after evaporation of the reaction mixture the product was isolated in 98.6% yield without any change in purity compared to the 10 mmol scale. The fact that **1b** is a very strong lachrymator and a very hygroscopic compound increases the importance of this new “green” method towards β -amino- α,β -unsaturated esters.

Conclusion

In summary, this paper describes an efficient and practical process for the synthesis of β -amino- α,β -unsaturated esters through the reaction of β -ketoesters with ammonium carbamate as a novel ammonia source and dehydrating agent. The reaction is carried out at room temperature in methanol as solvent without catalyst. The most important advantages of this method are short reaction times, mild reaction conditions, clean products, high yields and minimisation of waste due to elimination of the aqueous work-up to isolate the products. The method is easily scaled up and the crude product is isolated in high purity allowing its use in one-pot Hantzsch 1,4-DHP synthesis.

Experimental

IR spectra were recorded on a Perkin-Elmer Spectrum One spectrometer. ¹H NMR and ¹³C NMR were recorded on a Bruker 600 for CDCl₃ solutions, shifts are given in ppm downfield from TMS as an internal standard. Elemental analyses were done by the Central Analytical Service (CAS) at Ruder Bošković Institute, Zagreb. Compounds **2a–f**, **2i** and **2j** were purchased from Merck (Darmstadt, Germany). Compounds **2g**, **2h** were prepared from diketene³¹ and appropriate alcohol while **2k** was prepared according to the literature method.³²

General procedure for the preparation of β -amino- α,β -unsaturated esters (**1a–j**)

To a solution of β -ketoesters (**2a–j**; 10 mmol) in methanol (10 mL) at room temperature ammonium carbamate (0.78 g, 10 mmol) was added immediately. The resulting suspension was stirred at room temperature for the time indicated in Table 1. During that time all solid material is dissolved giving a clear solution. The reaction mixture was then evaporated to dryness. The crude product was isolated with a purity of >99%.

1h. Yield 93% as pale-yellow crystals, mp 86–87 °C, [α]_D²² –79.71 (*c* 1.00 in CH₂Cl₂). IR (KBr): ν 3441, 3333, 3230, 2945, 2894, 2868, 2850, 1651, 1554, 1448, 1371, 1326, 1292, 1174, 1106, 1082, 1040, 1010, 994, 924, 899, 881, 844, 789 cm⁻¹. ¹H NMR (600 MHz 298 K, CDCl₃): δ 0.77 (d, 3H, *J* = 7.0 Hz), 0.88–0.90 (m, 6H), 0.95–0.99 (m, 2H), 1.03–1.14 (m, 2H), 1.33–1.42 (m, 1H), 1.49–1.53 (m, 1H), 1.64–1.69 (m, 2H), 1.90 (s, 3H), 2.00–2.02 (m, 1H), 4.51 (s, 1H), 4.60–4.75 (m, 1H), 7.93 (br s, 2H). ¹³C NMR (600 MHz 298 K, CDCl₃): δ 16.42; 20.61; 21.93; 22.17; 23.61; 26.18; 31.32; 34.42; 41.41; 47.16; 71.76; 84.53; 159.20; 169.77.

Acknowledgements

The authors wish to express their gratitude to Belupo Pharmaceuticals & Cosmetics Inc. for financial support of this research.

References

- G. Grün and A. Fleckenstein, *Arzneim. Forsch.*, 1972, **22**, 334; F. Bossert, H. Meyer and E. Wehinger, *Angew. Chem.*, 1981, **93**, 755; R. A. Janis and D. J. Triggle, *J. Med. Chem.*, 1983, **26**, 755.
- T. Tsuruo, H. Iida, M. Nojiri, S. Tsukagoshi and Y. Sakurai, *Cancer Res.*, 1983, **43**, 2905.
- R. W. Chapman, G. Danko and M. I. Siegels, *Pharmacology*, 1984, **29**, 282.
- W. J. Malaise and P. C. F. Mathias, *Diabetologia*, 1985, **28**, 153.
- A. Krauze, S. Germane, O. Eberlins, I. Sturms, V. Klusa and G. Duburs, *Eur. J. Med. Chem.*, 1999, **34**, 301.
- R. Peri, S. Padmanabhan, S. Singh, A. Rutledge and D. J. Triggle, *J. Med. Chem.*, 2000, **43**, 2906.
- X. Zhou, L. Zhang, E. Tseng, E. Scott-Ramsay, J. J. Schentag, R. A. Coburn and M. E. Morris, *Drug Metab. Dispos.*, 2005, **33**, 321.
- A. Hantzsch, *Justus Liebigs Ann. Chem.*, 1882, **215**, 1.
- W. C. Wong, G. Chiu, J. M. Wetzel, M. R. Marzabadi, D. Nagarathnam, D. Wang, J. Fang, S. W. Miao, X. Hong, C. Forray, P. J. J. Vaysse, T. A. Brancheck and C. Gluchowski, *J. Med. Chem.*, 1998, **41**, 2643; D. Nagarathnam, J. M. Wetzel,

- S. W. Miao, M. R. Marzabadi, G. Chiu, W. C. Wong, X. Hong, J. Fang, C. Forray, T. A. Brancheck, W. E. Heydorn, R. S. L. Chang, T. Broten, T. W. Schorn and C. Gluchowski, *J. Med. Chem.*, 1998, **41**, 5320.
- 10 Y. Hsiao, N. R. Rivera, T. Rosner, S. W. Krska, E. Njolito, F. Wang, Y. Sun, J. D. Armstrong, E. J. J. Grabowski, R. D. Tillyer, F. Spindler and C. Malan, *J. Am. Chem. Soc.*, 2004, **126**, 9918; Y. J. Zhang, J. H. Park and S. Lee, *Tetrahedron: Asymmetry*, 2004, **15**, 2209.
- 11 G. Zhu, Z. Chen and X. Zhang, *J. Org. Chem.*, 1999, **64**, 6907; P. G. Garaldi, D. Simoni and S. Manfredini, *Synthesis*, 1983, 902; S. Marchalin and J. Kuthan, *Collect. Czech. Chem. Commun.*, 1983, **48**, 3112; S. Marchalin and J. Kuthan, *Collect. Czech. Chem. Commun.*, 1984, **49**, 1395.
- 12 H. Rodríguez, O. Reyes, M. Suarez, H. E. Garay, R. Pérez, L. J. Cruz, Y. Verdecia, N. Martín and C. Seoane, *Tetrahedron Lett.*, 2002, **43**, 439.
- 13 M. Iwanami, T. Shibanuma, M. Fujimoto, R. Kawai, K. Tamazawa, T. Takenaka, K. Takahashi and M. Murakami, *Chem. Pharm. Bull.*, 1979, **27**, 1426.
- 14 S. Ohno, O. Komatsu, K. Mizukoshi, K. Ichihara, Y. Nakamura, T. Morishima and K. Sumita, *Chem. Pharm. Bull.*, 1986, **34**, 1589; A. P. Beresford, P. V. Macrae, D. Alker and R. J. Kobylecki, *Arzneim. Forsch.*, 1989, **39**, 201.
- 15 A. Leonardi, G. Motta, R. Pennini, R. Testa, G. Sironi, A. Catto, A. Cerri, M. Zappa, G. Bianchi and D. Nardi, *Eur. J. Med. Chem.*, 1998, **33**, 399.
- 16 Y. S. Sadanandam, M. M. Shetty, K. Ram Mohan Reddy and L. Leelavathi, *Eur. J. Med. Chem.*, 1994, **29**, 975.
- 17 R. Tacke, A. Bentlage, R. Towart and E. Möller, *Eur. J. Med. Chem.*, 1983, **18**, 155; R. Shan, S. E. Howlett and E. E. Knaus, *J. Med. Chem.*, 2002, **45**, 955.
- 18 H. Meyer, F. Bossert, E. Wehinger, K. Stoepel and W. Vater, *Arzneim. Forsch.*, 1981, **31**, 407.
- 19 M. Milan and M. Viktor, *7th International Electronic Conference on Synthetic Organic Chemistry (ECSOC-7)*, 2003, A032.
- 20 A. Sobolev, M. C. R. Franssen, B. Vigante, B. Cekavicus, R. Zhalubovskis, H. Kooijman, A. L. Spek, G. Duburs and A. de Groot, *J. Org. Chem.*, 2002, **67**, 401.
- 21 H. Cho, M. Ueda, A. Mizuno, T. Ishihara, K. Aisaka and T. Noguchi, *Chem. Pharm. Bull.*, 1989, **37**, 2117.
- 22 K. Meguro, M. Aizava, T. Sohma, Y. Kawamatsu and A. Nagaoka, *Chem. Pharm. Bull.*, 1985, **33**, 3787.
- 23 Y. Gao, Q. Zhang and J. Xu, *Synth. Commun.*, 2004, **34**, 909.
- 24 M. E. F. Braibante, H. S. Braibante, L. Missio and A. Andricopulo, *Synthesis*, 1994, 898.
- 25 Ammonium carbamate is not stable above 60 °C and decomposes affording gaseous ammonia and carbon dioxide; *The Merck Index*, Merck Research Laboratories, Whitehouse Station, NJ, 12th edn, 1996.
- 26 M. J. J. Litjens, A. J. J. Straathof, J. A. Jongejan and J. J. Heijnen, *Chem. Commun.*, 1999, 1255; W. Du, M. Zong, Y. Guo and D. Liu, *Biotechnol. Appl. Biochem.*, 2003, **38**, 107; W. Du, M. H. Zong, Y. Guo and D. Liu, *Chin. J. Biotechnol.*, 2002, **18**, 242; W. Du, M. H. Zong, Y. Guo and D. Liu, *Biotechnol. Lett.*, 2003, **25**, 461; H. Peng, M. Zong, J. Wang and Y. Xu, *Biocatal. Biotransform.*, 2004, **22**, 183.
- 27 L. M. Likhoshesterov, O. S. Novikova and V. N. Shibaev, *Dokl. Chem.*, 2003, **389**, 73.
- 28 M. Litvić, I. Pogorelić, M. Filipan and I. Capanec, *Ammonium carbamate; Efficient Ammonia Source for Preparation of Enamino Esters*, XIX Croatian Meeting of Chemists and Chemical Engineers, Opatija, 2005.
- 29 The reaction carried out in propan-2-ol as solvent is much slower (>24 h) than in methanol.
- 30 Esteve Quimica S. A, L. Coppi, Y. Gasanz Guillen and J. Campon Pardo, *World Pat.*, WO 00/24714, 2000.
- 31 A. B. Boese, *Ind. Eng. Chem.*, 1940, **32**, 16.
- 32 J. E. Arrowsmith, S. F. Campbell, P. E. Cross, J. K. Stubbs, R. A. Burges, D. G. Gardiner and K. J. Blackburn, *J. Med. Chem.*, 1986, **29**, 1696.

Volumetric behaviour of the environmentally compatible lubricants pentaerythritol tetraheptanoate and pentaerythritol tetranonanoate at high pressures

Olivia Fandiño, Alfonso S. Pensado, Luis Lugo, Enriqueta R. López* and Josefa Fernández

Received 14th June 2005, Accepted 1st September 2005

First published as an Advance Article on the web 15th September 2005

DOI: 10.1039/b508402d

Knowledge of proper lubricant selection and its handling can substantially influence the reliability of a refrigeration system. In this sense the awareness of several thermophysical properties of refrigerants, lubricants, and their mixtures under different conditions of pressure and temperature is highly important for designing refrigeration systems. Polyol ester oils have been proposed as lubricant candidates for refrigeration systems. In this work, we have studied the density of two polyol esters, pentaerythritol tetraheptanoate and pentaerythritol tetranonanoate, in the range $278.15 \leq T/K \leq 353.15$ and $0.1 \leq p/\text{MPa} \leq 45$. In addition, the behaviour of two other essential volumetric properties, namely the thermal expansion coefficient and the isothermal compressibility coefficient, as well as the internal pressure have been analysed.

Introduction

All mechanical devices require lubrication to prevent overheating and wear over solid surfaces in contact. Where any two solid surfaces move in contact with each other, the created friction generates heat and causes wear. The lubricant is a substance inserted between moving components that has as major functions: lubricate, protect from wear, clean, and seal. A lubricant is a result of the blending between base stocks and additives, which will enhance specific aspects of an oils performance. Mineral-oil-based lubricating oils, greases, and hydraulic fluids are found in widespread use. However, these products are not readily biodegradable and are frequently toxic. Because of these characteristics, if these materials escape into the environment, the impacts tend to be accumulative and consequently harmful to living things.^{1–4}

For these reasons, in recent years, advances in green chemical technology are leading to the development of synthetic lubricants that offer industrial users significant advantages in demanding applications, such as better performance and minimization of the environmental impact. Synthetic lubricants^{5,6} are manufactured from a number of differing chemical bases. Several classes of compounds have been developed to provide base stocks for commercial synthetic fluids such as polyalphaolefins, PAO, esters, especially polyol esters, POE, or polyalkylene glycols, PAG, among others. Different studies point out^{3,7–9} that they can be really called green lubricants because they optimize energy efficiency and minimize wear in the machinery.⁷

Among these green lubricants, POEs seem to be the lubricants of choice for use with the natural refrigerant CO₂ or with non-chlorine refrigerants, such as HFCs, for reasons of

miscibility and also because of their inherently good lubricity.^{10,11} Polyol esters can extend the high temperature operating range of a lubricant by as much as 50–100 °C, due to their superior stability and low volatility. One of the major applications for polyol esters is as jet engine lubricants where they have been used exclusively for more than 30 years.^{12,13} They are also renowned for their film strength and increased lubricity, which is useful in reducing energy consumption in many applications.^{12,14} Polyol ester base oils combine both excellent performance, including for high temperature applications, and biodegradability.^{3,12,15,16} POEs are less toxic than mineral oils^{2–4} and can be obtained using a significant proportion of raw materials derived, or potentially derivable, from renewable resources.^{3,17,18} Other benefits include extended life, reduced maintenance and downtime, lower energy consumption, and reduced smoke and disposal.

Commercial lubricants based on POEs are obtained usually by esterifying a mixture of acids with one or two polyfunctional alcohols. Subsequently, several antiwear additives, copper deactivators, acid catchers and anti-oxidants can be added. A better knowledge of the thermophysical properties of pure POE fluids in broad temperature and pressure ranges is needed to develop POE lubricants more suitable for their different applications. Furthermore, a major problem in developing predictive methods for phase and viscosity behaviour of lubricants and their mixtures with refrigerants and other gases is the identification of the components that are included in commercial lubricant blends. Commercial oils and their performance properties can vary widely depending on the source and identity of the components present in the lubricant mixture. In addition, there are very little thermophysical property data available for the pure fluids used to formulate the oil. Such data are essential for the development and evaluation of predictive and correlation models.^{5,19} Subsequently, the models developed could be used for commercial lubricants.

Laboratorio de Propiedades Termofísicas, Dpto. de Física Aplicada, Facultad de Física, Universidad de Santiago, 15782 Santiago de Compostela, Spain. E-mail: faelopez@usc.es; Fax: +34 981 520676; Tel: +34 981 563100 Ext.14046

There are several families of pure POEs^{12,16} depending on the multifunctional alcohol used in their synthesis: trimethylolpropane, neopentylglycol, pentaerythritol or dipentaerythritol. In this work we will study two pentaerythritol esters: pentaerythritol tetraheptanoate and pentaerythritol tetranonanoate, which have four ester groups and four linear chains in their molecules. We should also point out that the POE lubricants are also named as esters neopentyl polyol esters.¹⁶

Thermophysical properties such as miscibility, solubility, viscosity or volumetric data of refrigerants, lubricants and their mixtures are needed to determine the suitability of refrigerant–lubricant combinations for use in refrigeration systems.^{5,9,20} These systems operate at different pressures and temperatures depending on the stage of the cycle, and thus the temperature and pressure effects on the thermophysical properties must be considered. Density is used in lubrication to identify oils, or oil fractions, and is also necessary to determine the experimental dynamic viscosity. Furthermore, density values are needed to apply the equations for the calculation of temperature rises in an oil film, of the Reynolds number, and of the heat transfer coefficient.¹⁴

Therefore, the aim of this work is to study the density of two polyol esters, pentaerythritol tetraheptanoate and pentaerythritol tetranonanoate, in the range $278.15 \leq T/K \leq 353.15$ and $0.1 \leq p/\text{MPa} \leq 45$. In addition, we have analysed the behaviour of three other volumetric properties: the thermal expansion coefficient, the isothermal compressibility coefficient and the internal pressure.

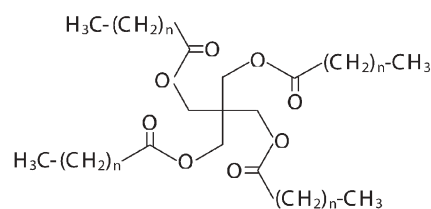
Results and discussion

Products

The two pentaerythritol tetraalkyl esters studied in this work (pentaerythritol tetraheptanoate, PEC7, and pentaerythritol tetranonanoate, PEC9) were synthesized by means of a reaction between a carboxylic acid and pentaerythritol catalysed by *p*-toluenesulfonic acid. The method used is basically that described by Wahlström and Vamling^{21,22} following the procedure proposed previously by Black and Gunstone²³ with the exception that the products were distilled under vacuum instead of separating them by chromatography, and *p*-xylene was used instead of *m*-xylene.

For the synthesis of PEC7 and PEC9 the employed products were: pentaerythritol (Aldrich, purity 98%), *p*-toluenesulfonic acid (Aldrich 99%), *p*-xylene (Aldrich >99%), and heptanoic (Aldrich 99%) or nonanoic acid (Fluka, mole fraction purity $\geq 97\%$), depending on the compound synthesized, PEC7 or PEC9. The distilled product was analysed by ¹H and ¹³C NMR as well as IR spectroscopy, and the purity was estimated to be greater than 95%. The molecular structures of the two POEs are represented in Scheme 1.

Furthermore, *n*-heptane (Aldrich $\geq 99.5\%$) was used to verify the experimental method and water (purified using a Milli-Q Plus system, with a resistivity of 18.2 MΩ cm at 298.15 K) was used as reference fluid. All the chemicals were partially degassed before use with a Branson 2210 ultrasonic bath.



Scheme 1 For $n = 5$: pentaerythritol tetraheptanoate, PEC7, $\text{C}_{33}\text{H}_{60}\text{O}_8$, $M_r = 584.82 \text{ g mol}^{-1}$; $n = 7$: pentaerythritol tetranonanoate, PEC9, $\text{C}_{41}\text{H}_{76}\text{O}_8$, $M_r = 697.04 \text{ g mol}^{-1}$.

Densities

Density measurements for both POEs were performed in the experimental range $278.15 \leq T/K \leq 353.15$ and $0.1 \leq p/\text{MPa} \leq 45$. Due to the significant viscosity values²⁴ of both products, it was necessary to apply a correction factor to the density values.²⁵ As in previous work²⁵ eqn (1), recommended by Anton Paar for the DMA 512P densimeter, has been used to calculate the correction factor $\Delta\rho$:

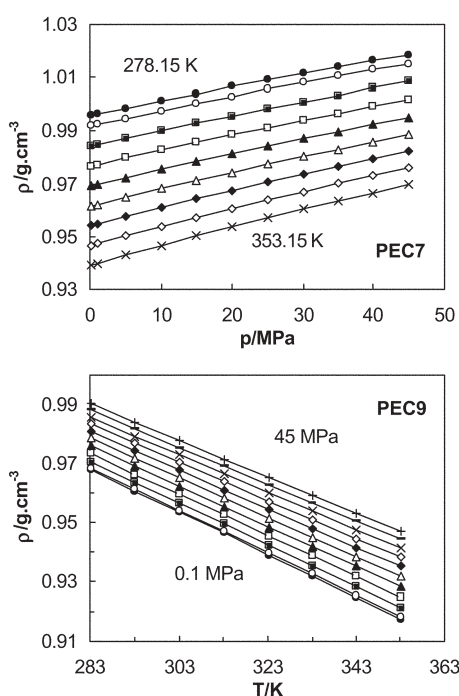
$$\frac{\Delta\rho}{\rho} = [-0.5 + 0.45\sqrt{\eta}]10^{-4} \quad (1)$$

where ρ represents the density value obtained from the densimeter calibration and the measured periods, $\Delta\rho$ is the difference between this ρ value and the “corrected” density value due to the effect of viscosity, and η is the dynamic viscosity of the sample in mPa s. The viscosity values for both POEs have been taken from Pensado *et al.*²⁴ The correction factor, $\Delta\rho$, ranges from 6×10^{-5} to $5 \times 10^{-4} \text{ g cm}^{-3}$ for PEC7 and from 8×10^{-5} to $5 \times 10^{-4} \text{ g cm}^{-3}$ for PEC9. Corrected experimental data are reported in Table 1 and plotted in Fig. 1. Taking into account the uncertainties in temperature, pressure, period, density data of water and the applied vacuum, the uncertainty of the density data was estimated to be $1 \times 10^{-4} \text{ g cm}^{-3}$ in the whole T - p range.

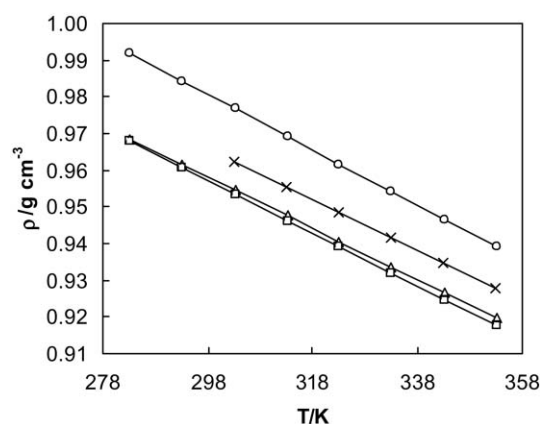
As usual, the density of each pure fluid decreases when the temperature rises along isobars and increases when the pressure increases at constant temperature. Moreover, the densities of POEs decrease with the increase of alkyl-chain length. This fact is opposite to the behaviour of alkanes,^{26,27} for which the density increases when the molecular mass increases due to a decrease of the free volume. Alkane molecules interact only through dipole-induced forces, which are basically proportional to the length of the carbon chain. In the case of POEs the increase of CH_2 groups causes both a dilution of the intermolecular forces among the ester groups and a loosening of the closely packed arrangement of the molecules by disrupting the local configurational order of the $-\text{COO}-$ group, and hence a less efficient packing (bigger molar volume).²⁷ Moreover, although the molecular mass increases simultaneously with the length of the acid chains, the ratio of heavy atoms to the number of carbons in the molecule diminishes, which also contributes to lower density values.²⁸ Thus, Shobha and Kishore²⁷ attribute the opposite trends of density with chain length of alkanes and POEs to the dilution of the $-\text{COO}-$ groups with the successive addition of $-\text{CH}_2-$ groups, since $\rho_{\text{COO}} \gg \rho_{\text{CH}_2}$.

Table 1 Experimental densities, $\rho/\text{g cm}^{-3}$, for PEC7 and PEC9 for pressures up to 45 MPa and temperatures from 278.15 to 353.15 K

p/MPa	T/K								
	278.15	283.15	293.15	303.15	313.15	323.15	333.15	343.15	353.15
PEC7									
0.10	0.9959	0.9919	0.9843	0.9768	0.9692	0.9615	0.9541	0.9465	0.9391
1.00	0.9964	0.9925	0.9848	0.9773	0.9697	0.9621	0.9547	0.9472	0.9398
5.00	0.9987	0.9947	0.9872	0.9798	0.9724	0.9648	0.9576	0.9502	0.9430
10.00	1.0014	0.9976	0.9901	0.9828	0.9755	0.9681	0.9611	0.9538	0.9467
15.00	1.0040	1.0003	0.9930	0.9858	0.9786	0.9713	0.9644	0.9573	0.9504
20.00	1.0066	1.0029	0.9957	0.9886	0.9815	0.9744	0.9676	0.9607	0.9538
25.00	1.0091	1.0055	0.9984	0.9914	0.9844	0.9774	0.9707	0.9639	0.9572
30.00	1.0116	1.0080	1.0010	0.9941	0.9872	0.9803	0.9737	0.9670	0.9604
35.00	1.0140	1.0105	1.0035	0.9967	0.9899	0.9832	0.9766	0.9701	0.9636
40.00	1.0163	1.0128	1.0060	0.9992	0.9926	0.9859	0.9795	0.9730	0.9666
45.00	1.0186	1.0151	1.0084	1.0017	0.9952	0.9886	0.9822	0.9759	0.9696
PEC9									
0.10		0.9679	0.9606	0.9536	0.9464	0.9389	0.9319	0.9247	0.9176
1.00		0.9684	0.9611	0.9541	0.9469	0.9395	0.9325	0.9254	0.9183
5.00		0.9706	0.9635	0.9566	0.9494	0.9421	0.9353	0.9282	0.9213
10.00		0.9733	0.9664	0.9595	0.9524	0.9453	0.9386	0.9317	0.9249
15.00		0.9760	0.9690	0.9623	0.9554	0.9484	0.9419	0.9351	0.9284
20.00		0.9785	0.9717	0.9651	0.9582	0.9514	0.9450	0.9383	0.9318
25.00		0.9810	0.9743	0.9678	0.9611	0.9543	0.9480	0.9415	0.9350
30.00		0.9834	0.9768	0.9704	0.9638	0.9571	0.9509	0.9445	0.9382
35.00		0.9858	0.9792	0.9729	0.9664	0.9599	0.9537	0.9474	0.9412
40.00		0.9881	0.9817	0.9754	0.9690	0.9625	0.9565	0.9502	0.9441
45.00		0.9903	0.9840	0.9778	0.9715	0.9651	0.9591	0.9530	0.9470

**Fig. 1** Experimental density data for PEC7 and PEC9.

In previous work²⁵ we have determined the density of pentaerythritol tetra(2-ethyl hexanoate) PEB8, which is a ramified isomer of pentaerythritol tetraoctanoate, PEC8 ($\text{C}_{37}\text{H}_{68}\text{O}_8$, $M_r = 640.93 \text{ g mol}^{-1}$). As can be seen in Fig. 2, the density values of PEB8 are lower than those of PEC8²⁷ and very close to that of PEC9, showing that an increase in the branching of the chains also diminishes the efficacy of the packing.²⁷

**Fig. 2** Density, ρ , versus temperature at atmospheric pressure for: (○) PEC7, (□) PEC9, (△) PEB8²⁵ and (×) PEC8.²⁷

The densities of both POEs have been correlated using the Tammann–Tait (TT) type eqn (2):

$$\rho(T, p) = \frac{\rho(T, p_{\text{ref}})}{1 - C \ln\left(\frac{B(T) + p}{B(T) + p_{\text{ref}}}\right)} \quad (2)$$

The reference pressure p_{ref} was 0.1 MPa. For the density correlation $\rho(T, p_{\text{ref}})$ at the reference pressure and for $B(T)$ the following polynomial functions of temperature were considered:

$$\rho(T, p_{\text{ref}}) = \sum_{i=0}^m A_i T^i \quad (3)$$

$$B(T) = \sum_{j=0}^n B_j T^j \quad (4)$$

The A_i values were determined by smoothing the parameters to the experimental densities at atmospheric pressure with a

Table 2 A_i , B_i , C coefficients and standard deviations, s and s^* , for eqn (2)–(4)

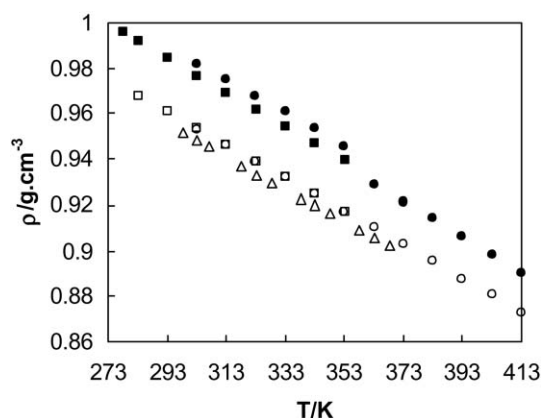
	PEC7	PEC9
$A_0/\text{g cm}^{-3}$	1.22459	1.17149
$-10^3 \times A_1/\text{g cm}^{-3} \text{K}^{-1}$	0.87443	0.71918
$10^6 \times A_2/\text{g cm}^{-3} \text{K}^{-2}$	0.18705	—
$10^4 \times s/\text{g cm}^{-3}$	0.7	1
C	0.080951	0.081002
B_0/MPa	444.666	384.798
$-B_1/\text{MPa K}^{-1}$	1.45886	1.07955
$10^3 \times B_2/\text{MPa K}^{-2}$	1.3235	0.73807
$10^4 \times s^*/\text{g cm}^{-3}$	0.4	0.8

standard deviation s lower than or equal to $1 \times 10^{-4} \text{ g cm}^{-3}$. The parameters B_j and C for each POE have been obtained by fitting eqn (2) by a least squares method using a Marquardt–Levenberg-type algorithm²⁹ to all the experimental data at pressures other than atmospheric. The standard deviations, s^* , from the Tammann–Tait correlations were lower than or equal to $8 \times 10^{-5} \text{ g cm}^{-3}$. The F -test for additional terms was used to determine the number of A_i and B_j parameters. The set of fitting coefficient values (A_i , B_j , C) and the standard deviations s and s^* are listed in Table 2.

We have only compared our experimental densities with those in the literature at atmospheric pressure,^{22,27} because literature values for these lubricants at other pressures are not known. For comparison, we have interpolated the densities using eqn (3) at the same temperature conditions as the literature values. In Fig. 3 experimental and literature data for the two POE at the atmospheric pressure are presented.

For PEC9 our results are in excellent agreement with the data presented by Shobha and Kishore,²⁷ with an absolute average deviation (AAD) of only 0.03%, whereas with the data of Wahlström and Vamling²² it is 0.60%.

For PEC7 the AAD between our data and those of Shobha and Kishore²⁷ is 0.64%, although we must point out that the data of these authors are exceedingly scattered. An inspection of Fig. 3 reveals that the temperature dependence of the Shobha and Kishore data at higher temperatures agrees with our $\rho(T)$ values better than with their own data at lower temperatures. This is due to an unexpected decrease of the densities, which occurs in their set of values²⁷ at 353.15 K.

**Fig. 3** Experimental and literature density data at 0.1 MPa for PEC7 (filled symbols) and PEC9 (unfilled symbols). (■, □) this work; (●, ○) Shobha and Kishore;²⁷ (▲, △) Wahlström and Vamling.²²

On the other hand, density values of PEC7 and PEC9 are higher than typical data of mineral oils.^{6,30–32} The higher density of synthetic lubricants contributes to more efficient oil separation and lower carry-over. In addition, according to the simplified Sieder–Tate equation,¹⁴ the higher the density value, the better the heat-transfer coefficient.

Derived properties

Two other fundamental oil properties related to density are the thermal expansion coefficient and the bulk modulus (or its inverse, the coefficient of isothermal compressibility). Both properties vary with pressure, temperature, and molecular structure.

The thermal expansion coefficient, α_p , is useful³⁰ for determining the size of a container in which the oil is heated. In Hydrodynamic Lubrication (HDL), the thermal expansion of the oil in the clearance of a bearing increases the hydraulic pressure. Thus, some researchers³⁰ discuss the “thermal wedge” mechanism of film formation and apply it to parallel sliding surfaces, especially flat, non-tilting, thrust bearings.

From the thermal expansion coefficient definition according to eqn (5)

$$\alpha_p = \frac{1}{V_m} \left(\frac{\partial V_m}{\partial T} \right)_p = -\frac{1}{\rho} \left(\frac{\partial \rho}{\partial T} \right)_p \quad (5)$$

and eqns. (2)–(4), it is easy to determine this property at different temperatures and pressures inside the experimental range through eqn (6):

$$\alpha_p = -\frac{\sum_{i=1}^m i A_i T^{i-1}}{\sum_{i=0}^m A_i T^i} - \frac{C(p_{\text{ref}} - p)}{(B+p)(B+p_{\text{ref}})} \frac{\sum_{j=1}^n j B_j T^{j-1}}{\left[1 - C \ln \left(\frac{B+p}{B+p_{\text{ref}}} \right) \right]} \quad (6)$$

In order to verify our procedure for determining the thermal expansion coefficient, we have determined this property for *n*-heptane in the same experimental T – p range in the present work, by using the experimental densities reported previously by us.²⁵ Subsequently, these α_p values have been compared with those of the literature obtained by densimetry and other methods.^{33–36}

Verdier and Andersen³³ have determined α_p for *n*-heptane at 303.15 K and pressures up to 30 MPa by calorimetry. Sun *et al.*³⁴ evaluated the thermal expansion coefficient of *n*-heptane from the speeds of sound in the temperature range of 180–320 K and at pressures ≤ 260 MPa. Pecar and Dolecek³⁵ obtained α_p for *n*-heptane by densimetry for temperatures between 298.15 and 348.15 K and up to 40 MPa. Finally, Malhotra and Woolf³⁶ have determined the isobaric expansivities of *n*-heptane from the volumetric data obtained by using a volumeter for temperatures from 278.15 to 338.15 K and pressures up to 400 MPa.

The comparison reveals that the values obtained by calorimetry are always lower than ours (AAD = bias), with an AAD of 2.2% presenting a maximum deviation of 2.7%. However, the values of Pecar and Dolecek are always larger than ours (AAD = –bias) the AAD being 4.8% and the maximum deviation 6.0%. The AAD between our data and those of Sun *et al.* is 1.4% whereas the corresponding bias is

–1.3% and the maximum deviation is 2.9%. The comparison with the data from Malhotra and Woolf,³⁶ presents an AAD of 0.92%, with a maximum deviation of 2.5%, but it must be pointed out that with this set of data, positive and negative deviations were found. Taking into account that the literature uncertainties of this property vary between 2 and 10%, we consider that the comparison is satisfactory.

Using eqn (6) with the parameters reported in Table 2, we have calculated α_p for PEC7 and PEC9 at the experimental conditions except the extreme ones. In Table 3 the values obtained for this property are reported at a range of temperatures and pressures.

In Fig. 4, we present α_p versus pressure (PEC7) and temperature (PEC9). The different isotherms present a crossing point around 10 MPa for PEC7, as can be seen in Fig. 4, and around 26 MPa for PEC9. Consequently, the temperature dependence of α_p for isobars, below and up to the pressure crossing point, is inverse. For lower pressures the thermal expansion coefficient increases with the temperature, whereas α_p diminishes with T for higher pressures, being constant at the crossing pressure. This fact means that there is a change in the sign of $(\partial\alpha_p/\partial T)_p$. Some authors³⁷ have attributed the change of sign in $(\partial\alpha_p/\partial T)_p$ to the predominant influence of the anharmonicity of the intermolecular vibrations and to the variation of the intermolecular potential with the pressure due to the anharmonic effects. Furthermore, the decreasing dependency of α_p with the temperature is related to the behaviour of c_p with pressure.³⁴ Thus, the heat capacity at constant pressure is related to the isobaric thermal expansion coefficient through eqn (7):

$$\left(\frac{\partial c_p}{\partial p}\right)_T = -T \left(\frac{\partial^2 V_m}{\partial T^2}\right)_p = -TV_m \left(\alpha_p^2 + \frac{\partial\alpha_p}{\partial T}\right)_p \quad (7)$$

with V_m as the molar volume of the fluid.

So, a change in the sign of $(\partial\alpha_p/\partial T)_p$ allows that $(\partial c_p/\partial p)_T$ becomes zero, then the heat capacity at constant pressure presents a minimum for certain combinations of T and p .

It is expected that the decrease of the density of POEs when the lengths of the acid chains increase, implies an increase in the molar volume, with the corresponding increase in the free

Table 3 Isobaric thermal expansivity, α_p , and isothermal compressibility, κ_T , of PEC7 and PEC9

p/MPa	$10^4 \alpha_p / \text{K}^{-1}$			$10^4 \kappa_T / \text{MPa}^{-1}$		
	T/K	T/K	T/K	T/K	T/K	T/K
	293.15	323.15	343.15	293.15	323.15	343.15
	PEC7					
1.00	7.74	7.80	7.84	6.15	7.20	8.03
10.00	7.47	7.48	7.48	5.79	6.71	7.42
20.00	7.22	7.16	7.13	5.43	6.24	6.85
30.00	6.97	6.89	6.83	5.12	5.84	6.37
40.00	6.76	6.65	6.58	4.98	5.48	5.95
	PEC9					
1.00	7.46	7.62	7.73	6.10	7.11	7.93
10.00	7.21	7.31	7.37	5.75	6.63	7.34
20.00	6.96	7.00	7.01	5.40	6.17	6.78
30.00	6.74	6.74	6.71	5.09	5.77	6.30
40.00	6.54	6.50	6.45	4.82	5.43	5.89

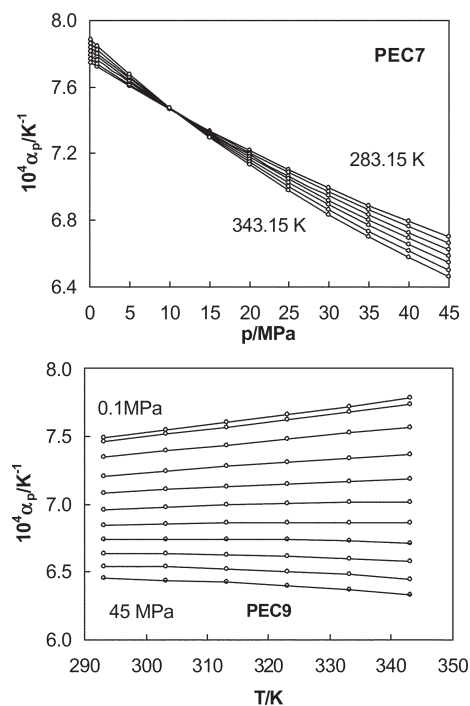


Fig. 4 Isobaric thermal expansivities, α_p , for PEC7 versus pressure, p and PEC9 versus temperature, T .

intermolecular space. Consequently, the capacity of the liquid to expand or contract would be also increased.³⁸ Nevertheless, α_p decreases when the length of the POE acid chains increase. In Fig. 4 it can be seen that PEC7 is slightly more expansible than PEC9. This fact is due to the opposite trends of V_m^{-1} and $(\partial V_m/\partial T)_p$ with the size of the molecular chains (Fig. 5 and 6). Thus, the decreasing of α_p implies that the increase in $(\partial V_m/\partial T)_p$ is not enough to counteract the decrease in V_m^{-1} when the acid chains of POE lengthen.

On the other hand, α_p values of PEC7 and PEC9 (with four linear acid chains) are larger than those of PEB8,²⁵ which has four branched chains. It can be seen in Fig. 5 and 6 that the V_m^{-1} and $(\partial V_m/\partial T)_p$ values for PEB8 are lower than the expected values for its isomer with linear chains PEC8. These two effects originate in the fact that PEB8 presents the lowest expansivity values (Fig. 7). On the other hand, for the three POEs α_p decreases with increasing pressure (Fig. 7). This is due to the observation that the capacity of a liquid to expand diminishes when the pressure increases, due to the diminution

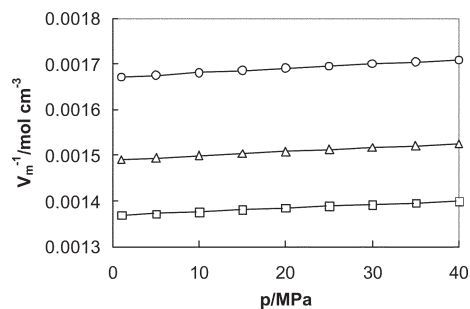


Fig. 5 V_m^{-1} vs. p for: (○) PEC7, (□) PEC9 and (△) PEB8²⁵ at 303.15 K.

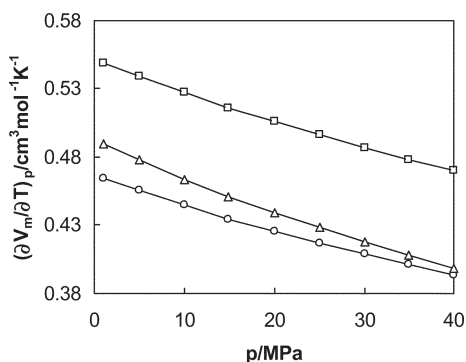


Fig. 6 $(\partial V_m/\partial T)_p$ versus pressure for: (○) PEC7, (□) PEC9 and (△) PEB8²⁵ at 303.15 K.

of free intermolecular space. The decrease of $(\partial V_m/\partial T)_p$ with increasing pressure is large enough to counteract the increase of V_m^{-1} (see Fig. 5 and 6).

It is interesting to point out that the typical values³⁰ of the coefficients of thermal expansion of mineral oils are around $6.4 \times 10^{-4} \text{ K}^{-1}$. Thus, PEC7 and PEC9 present slightly higher values for this property.

On the other hand, bulk modulus expresses the resistance of a fluid to a decrease in volume due to compression. The coefficient of isothermal compressibility (or simply isothermal compressibility) is the reciprocal of bulk modulus, and expresses the capacity of the fluid to contract. A fluid that is sponge-like and easily compressed has a low bulk modulus and consequently a high isothermal compressibility. The potential of a lubricant for energy loss and heat production increases with its compressibility. This is especially true in hydraulic and lube oil circulating systems. Bulk modulus is a factor used in several film thickness calculations.³⁰ Moreover, bulk modulus is used to estimate the pressure–viscosity coefficient of lubricants.^{39,40} Recently, Schmelzer *et al.*⁴⁰ have derived an equation that allows quantitative determination of the pressure dependence of viscosity, which requires, in the simplest case, only knowledge of the temperature dependence of viscosity at constant pressure, the thermal expansion coefficient, and the isothermal compressibility of the liquid.

From the definition of the isothermal compressibility, κ_T ,

$$\kappa_T = -\frac{1}{V_m} \left(\frac{\partial V_m}{\partial p} \right)_T = \frac{1}{\rho} \left(\frac{\partial \rho}{\partial p} \right)_T \quad (8)$$

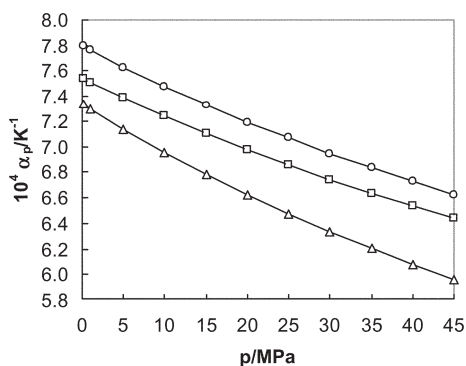


Fig. 7 Isobaric thermal expansivity, α_p , versus pressure for: (○) PEC7, (□) PEC9 and (△) PEB8²¹ at 303.15 K.

and eqn (2)–(4), this coefficient can be expressed as:

$$\kappa_T = \frac{C}{(B(T) + p) \left[1 - C \ln \frac{B(T) + p}{B(T) + p_{\text{ref}}} \right]} \quad (9)$$

Again, we have tested this method comparing our κ_T values of *n*-heptane with literature values.^{34–36} Comparing with the data reported by Pecar and Dolecek³⁵ up to 30 MPa, we have obtained an AAD of 1.4% and bias -0.1% , whereas with the data from Sun *et al.*³⁴ the AAD = $-$ bias was 1.7% up to 40 MPa. The comparison with the data of Malhotra and Woolf,³⁶ presents an AAD of 0.81%, with a maximum deviation of 2.7%. Deviations up to 6% for this property are usual in the literature. In average our deviation is considerably lower, therefore the values of this property provided by the Tait equation are compatible with those obtained by other procedures.

Using eqn (9) with the parameters reported in Table 2, we have calculated κ_T at the experimental conditions except the extreme ones. In Table 3 we report the values at a range of temperatures and pressures.

In Fig. 8 we have plotted the isothermal compressibility versus temperature at different pressures. For each compound, the κ_T values increase with temperature at constant pressure and along isotherms, decrease with the pressure. The capacity of a liquid to contract diminishes when the pressure increases or the temperature decreases, due to the diminution of free intermolecular space. The decrease of $[-(\partial V_m/\partial p)_T]$ with increasing pressure (or decreasing temperature) is enough to counteract the increase in V_m^{-1} .

As in the case of thermal expansion coefficient, κ_T values are small, and consequently both POE are slightly compressible.

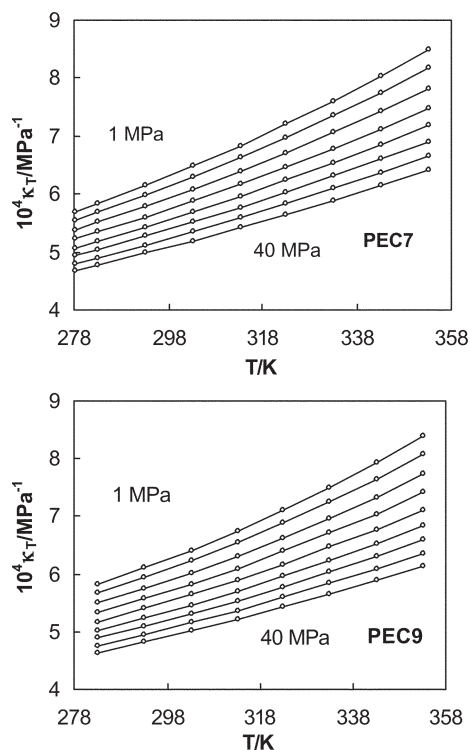


Fig. 8 Isothermal compressibility, κ_T , for PEC7 and PEC9.

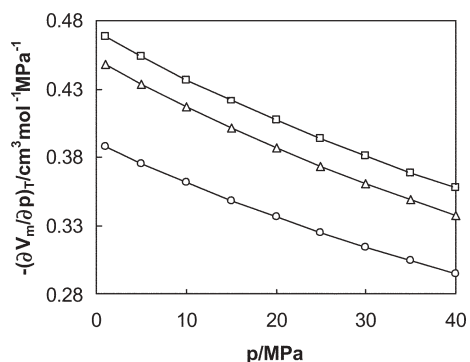


Fig. 9 $[-(\partial V_m/\partial p)_T]$ versus pressure for: (○) PEC7, (□) PEC9 and (△) PEB8²¹ at 303.15 K.

In fact, the isothermal compressibilities of these POEs are lower than those of other fluids previously studied by us, such as polyalkylene glycol dimethyl ethers^{41,42} or dialkyl carbonates.⁴² Comparing κ_T for both compounds, we observe that this property takes very similar values for both POEs, although PEC7 is slightly more compressible than PEC9. Similar to the thermal expansion coefficients, V_m^{-1} and $[-(\partial V_m/\partial p)_T]$ present an opposite trend when the size of the acid chains of POEs increases (Fig. 5 and 9) and the increase of $[-(\partial V_m/\partial p)_T]$ is not large enough to counteract the decrease in V_m^{-1} when the acid chains of POE lengthen.

On the other hand, it is interesting to note that the branching of the chains contributes differently to the isothermal compressibility and to the thermal expansion coefficient. Thus, the isothermal compressibility values of both PEC7 and PEC9, are lower than those of PEB8²⁵ (Fig. 10), contrary to the trend for α_p values. This is due to the fact that $[-(\partial V_m/\partial p)_T]$ values for PEB8 are significantly larger than the expected values for its isomer with linear chains, PEC8 (Fig. 9), whereas the opposite occurs for $(\partial V_m/\partial T)_p$ (Fig. 6).

An equation for the estimation of the bulk modulus as a function of pressure and temperature for a traditional mineral oil used as a hydraulic fluid is presented in ref. 32. Using this equation, in Fig. 11 the isothermal compressibility for the traditional mineral oil was plotted together with the corresponding ones of PEC7 and PEC9 at 10 MPa and 20 MPa, versus temperature. As can be observed, the κ_T values of both

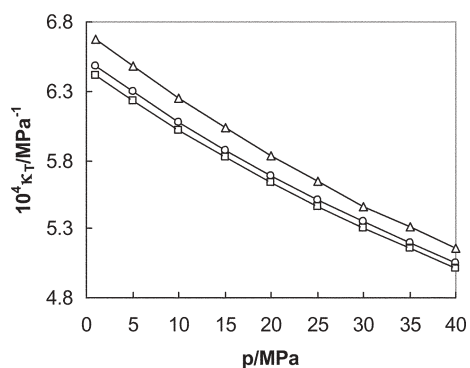


Fig. 10 Isothermal compressibility, κ_T , vs. p for: (○) PEC7, (□) PEC9 and (△) PEB8²⁵ at 303.15 K.

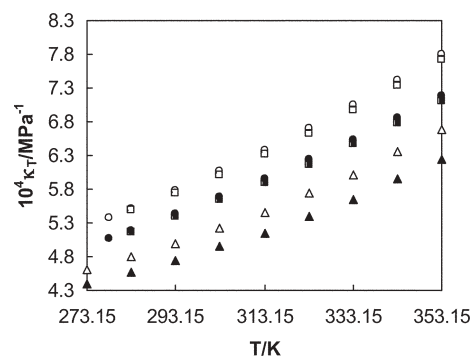


Fig. 11 Isothermal compressibility, κ_T , for: (▲, △) mineral oil,³² (●, ○) PEC7 and (■, □) PEC9 versus temperature, T , at 10 MPa (unfilled symbols) and 20 MPa (filled symbols).

POEs are very close to each other, and are slightly greater than the estimated mineral oil data. Nevertheless, in ref. 31 the isothermal compressibilities of other mineral based hydraulic fluids are presented at 295.15 K and two pressures, 14 MPa ($6.7 \times 10^{-4} \text{ MPa}^{-1}$) and 30 MPa ($6.3 \times 10^{-4} \text{ MPa}^{-1}$). Hence, this mineral hydraulic fluid is more compressible than PEC7 and PEC9. Comparing these mineral oil data with those of the POEs, it can be concluded that an increase of pressure affects more strongly the compressibility of mineral oils than that of POEs.

Finally, we have estimated another property, the internal pressure, π , which provides essential information on the intensity of intermolecular interactions. This property reflects the change in internal energy as the volume of the substance changes, *i.e.* $\pi = (\partial U/\partial V)_T$, and it is considered as a measure of the cohesive forces in the fluid. Knowing the values of isothermal compressibilities and isobaric thermal expansivities at the same T - p conditions, the internal pressure can be evaluated as $\pi = (\alpha_p/\kappa_T)T - p$.

In Fig. 12 the behaviour of the internal pressure versus pressure and temperature is presented. For both POEs, PEC7 and PEC9, the internal pressure values increase weakly with pressure and decrease significantly with the temperature. Nevertheless, for PEB8,²⁵ the trend of π with changing temperature and pressure is slightly different at lower and higher temperatures. In fact, Fandiño *et al.*²⁵ found that the slope of isothermal $\pi(V_m)$ curves for PEB8 is positive in almost all of the isotherms whereas the contrary happens with PEC7 and PEC9.

As can be observed in Fig. 12, the sequence of the values of this property is PEC7 > PEC9 > PEB8 in almost all the T - p conditions. This fact clearly indicates that stronger attractive molecular interactions exist in PEC7, as we pointed out before, and lower ones exist in PEB8, as a result of the branching of the chains.

Conclusions

In this work, different volumetric thermophysical properties of PEC7 and PEC9, that is, the pVT surface, isothermal compressibilities, thermal expansion coefficients, and internal pressures have been determined from density measurements in the range $278.15 \leq T/\text{K} \leq 353.15$ and $0.1 \leq p/\text{MPa} \leq 45$.

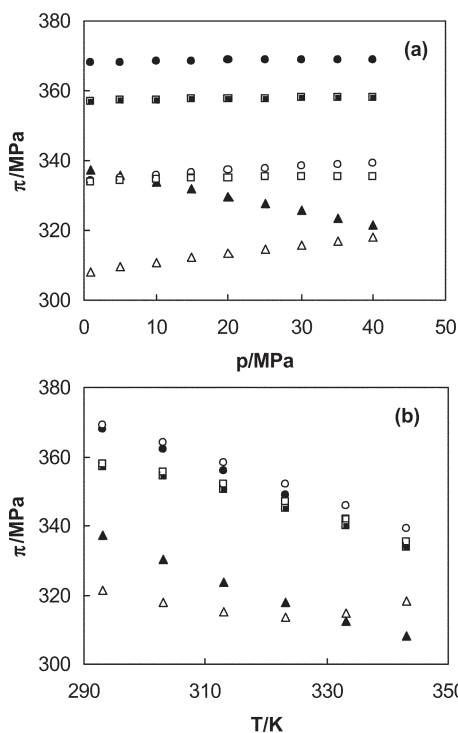


Fig. 12 Internal pressures, π , of: (●, ○) PEC7, (■, □) PEC9 and (▲, △) PEB8,²⁵ (a) versus pressure at 293.15 K (filled symbols) and 343.15 K (unfilled symbols), and (b) versus temperature at 1 MPa (filled symbols) and 40 MPa (unfilled symbols).

In all T - p ranges, ρ , α_p , κ_T , and π values of the linear POE compounds (PEC7 and PEC9) diminish with the increase in the number of CH₂ groups, whereas $(\partial V_m/\partial T)_p$ and $[-(\partial V_m/\partial p)_T]$ increase. The branching of the acid chains leads to lower ρ , α_p , π , and $(\partial V_m/\partial T)$ values as well as to higher κ_T and $[-(\partial V_m/\partial p)_T]$ values. The trends for ρ , π , $(\partial V_m/\partial T)_p$ and $[-(\partial V_m/\partial p)_T]$ are due to the increase of CH₂ groups, which causes a dilution of the intermolecular forces among the ester groups, hence a less efficient packing. The branching of the acid chains also diminishes the efficacy of the packing. In order to explain the trends of α_p and κ_T with the size and branching of the POE molecule as well as with the pressure and the temperature, one has to take into account the fact that opposite trends of V_m^{-1} and $(\partial V_m/\partial T)_p$ (and/or $[-(\partial V_m/\partial p)_T]$) occur.

Another interesting fact is the existence of crossing points in α_p isotherms in the pressure range studied. Thus, crossing points were found for PEC7 and PEC9 at 10 and 26 MPa respectively.

These properties, together with other important ones, should be taken into account in the best base fluid choice for environmentally adapted lubricants (EAL). It was found that in the case of POEs all the properties (density, thermal expansion coefficient, and isothermal compressibility) are slightly larger than those of traditional mineral oils (which usually are considered to be incompressible), whereas the last two properties are lower than those corresponding to other fluids previously studied by us, such as polyalkylene glycol dimethyl ethers or dialkyl carbonates.

Experimental

The Anton Paar DMA 60/512P vibrating tube densimeter was used to determine the experimental densities. This type of densimeter can be used to perform measurements from (263.15 to 423.15) K and up to 70 MPa, but requires the construction and setup of several pieces of equipment and peripherals. A complete experimental assembly of the apparatus and the experimental procedure have been previously described in detail.^{43,44}

The temperature inside the cellblock was measured with an Anton Paar CKT100 platinum resistance thermometer with a resolution of ± 0.001 K and an uncertainty of ± 0.01 K due to its calibration. The pressure was measured by means of an HBM-PE300 differential pressure gauge, which can operate at pressures up to 50 MPa. This gauge was calibrated with an uncertainty of 0.02 MPa. In this work, the calibration parameters of the densimeter cell were determined using the more precise of the two calibration methods developed by Lagourette *et al.*⁴⁵ For this method it is only necessary to know the density as a function of temperature and pressure for a reference fluid (water⁴⁶) and also the temperature dependence of the period for the cell under vacuum. Taking into account the uncertainties in temperature, pressure, and the literature water density, together with the reproducibility of the oscillation periods, an uncertainty of $\pm 10^{-4}$ g cm⁻³ has been estimated.

Acknowledgements

The authors wish to express their gratitude to Prof. F. J. Sardina (Departamento de Química Orgánica, Universidad de Santiago de Compostela) for his aid in the synthesis and analysis of PEC7 and PEC9. This work was carried out under the financial support received from the Spanish Ministry of Education and Science, Xunta de Galicia, and the European Union (FEDER) (PPQ2002-03262 and PGIDIT03PXIC20608PN Research Projects).

References

- 1 F. Haus, J. German and G.-A. Junter, *Chemosphere*, 2001, **45**, 98–990.
- 2 K. Vercammen, K. Van Acker, A. Vanhulsel, J. Barriga, A. Arnsek, M. Kalin and J. Meneve, *Tribol. Int.*, 2004, **37**, 983–989.
- 3 A. Willing, *Chemosphere*, 2001, **43**, 89–98.
- 4 *Engineering and Design-Lubricants and Hydraulic Fluids*, Manual of the Department of the Army, US Army Corps of Engineers, Washington, 1999, <http://www.usace.army.mil/inet/usace-docs/eng-manuals/em110-2-1424/c-8.pdf>.
- 5 K. N. Marsh and M. E. Kandil, *Fluid Phase Equilib.*, 2002, **199**, 319–334.
- 6 *Synthetic Lubricants and High-Performance Functional Fluids*, ed. L. R. Rudnick and R. L. Shubkin, M. Dekker, New York, 2nd edn, 1999, vol. 77.
- 7 S. Boyde, *Green Chem.*, 2002, **4**, 293–307.
- 8 G. D. Yadav and N. S. Doshi, *Green Chem.*, 2002, **4**, 528–540.
- 9 S. J. Randles, S. J. McTavish and T. W. Dekleva, *A Critical Assessment of Synthetic Lubricant Technologies for Alternative Refrigerants*, Proceeding in the ASHRAE 2003 Winter Meeting, Chicago, USA, January 27–29, 2003.
- 10 S. J. Randles, *Refrigeration Lubes*, in *Synthetic Lubricants and High-Performance Functional Fluids*, M. Dekker, New York, 2nd edn, 1999, vol. 77, pp. 563–594.

- 11 J. Hinrichs, *Lubricant screening for CO₂ automotive AC-systems, aspects from a compressor manufacturer point of view*, VDA Alternating Refrigerant Winter Meeting, Saalfelden, Austria, February 23–24, 2004.
- 12 S. J. Randles, *Esters*, in *Synthetic Lubricants and High-Performance Functional Fluids*, M. Dekker, New York, 2nd edn, 1999, vol. 77, pp. 63–101.
- 13 R. M. Mortier and S. T. Orszulik, *Chemistry and Technology of Lubricants*, Blackie Academic and Professional, Glasgow, 1992.
- 14 S. J. Randles, *Value Creation from a Technology Viewpoint (How Esters Can Save You Money)*, Proceeding in Lubricants of the Future and Environment, 6th International Congress, Brussels, Belgium, June 2–4, 1999.
- 15 V. Eychenne, Z. Mouloungui and A. Gaset, *Ol. Corps Gras, Lipides*, 1996, **3**, 57–63.
- 16 V. Eychenne and Z. Mouloungui, *Ind. Eng. Chem. Res.*, 1998, **37**, 4835–4844.
- 17 R. Carceller, *Esters based on vegetable oils*, First Workshop on New Applications for Vegetable Oils, September 8–9, 1998, Copenhagen, Denmark.
- 18 M. Schneider and P. Smith, *Plant oils as base fluids-lubricants and hydraulic fluids*, in Government–Industry Forum on Non-Food uses of Crops (GIFNFC 7/7), Final Report, May 16, 2002; <http://www.nnfcc.co.uk/nnfcclibrary/productreport/index.cfm>.
- 19 S. E. Quiñones-Cisneros, J. García, J. Fernández and M. A. Monsalvo, *Int. J. Refrig.*, 2005, **28**, 714–724.
- 20 A. Hauk and E. Weidner, *Ind. Eng. Chem. Res.*, 2000, **39**, 4646–4651.
- 21 A. Wahlstrom and L. Vamling, *J. Chem. Eng. Data*, 1999, **44**, 823–828.
- 22 A. Wahlstrom and L. Vamling, *J. Chem. Eng. Data*, 2000, **45**, 97–103.
- 23 K. D. Black and F. D. Gunstone, *Chem. Phys. Lipids*, 1990, **56**, 169–173.
- 24 A. S. Pensado, M. J. P. Comuñas, L. Lugo and J. Fernández, *Study of some lubrication properties of pentaerythritol esters at high pressures*, presented at Thermodynamics 2005, April 6–8, 2005, Sesimbra, Portugal.
- 25 O. Fandiño, A. S. Pensado, L. Lugo, M. J. P. Comuñas and J. Fernández, *J. Chem. Eng. Data*, 2005, **50**, 939–946.
- 26 M. J. Assael, J. H. Dymond and D. Exadaktilou, *Int. J. Thermophys.*, 1994, **15**, 155–164.
- 27 H. K. Shobha and K. Kishore, *J. Chem. Eng. Data*, 1992, **37**, 371–376.
- 28 R. F. Daley and S. J. Daley, *Organic Chemistry*, e-book: <http://homepages.wvc.edu/staff/daleri/index.html>.
- 29 D. W. Marquardt, *J. Soc. Ind. Appl. Math.*, 1963, **11**, 431–441.
- 30 D. Godfrey and W. R. Herguth, *Lubr. Eng.*, 1995, **51**, 493–496.
- 31 *Hydraulic Fluids and Lubricants* - Technical Information, Sauer Danfoss DKMH.PN.980.A2.02 520L0463 Rev.G, 11/2003, <http://www.sauer-danfoss.com>.
- 32 N. Manring, *Hydraulic Control Systems*, Wiley, New York, 2005.
- 33 S. Verdier and S. I. Andersen, *J. Chem. Eng. Data*, 2003, **48**, 892–897.
- 34 T. F. Sun, S. A. R. C. Bominaar, C. A. Seldam and S. N. Biswas, *Ber. Bunsen-Ges. Chem. Phys.*, 1991, **95**, 696–704.
- 35 D. Pecar and V. Dolecek, *Fluid Phase Equilib.*, 2003, **211**, 109–127.
- 36 R. Malhotra and L. A. Woolf, *J. Chem. Thermodyn.*, 1991, **23**, 49–57.
- 37 M. Taravillo, V. G. Baonza, M. Cáceres and J. Núñez, *J. Phys.: Condens. Matter*, 2003, **15**, 2979–2989.
- 38 E. Aicart, E. Junquera and T. M. Letcher, *J. Chem. Eng. Data*, 1995, **40**, 1225–1227.
- 39 W. G. Johnston, *ASLE Trans.*, 1981, **24**, 232–238.
- 40 J. W. P. Schmelzer, E. D. Zanotto and V. M. Fokin, *J. Chem. Phys.*, 2005, **122**, 074511/1–074511/11.
- 41 M. J. P. Comuñas, A. Baylaucq, C. Boned and J. Fernández, *J. Chem. Eng. Data*, 2003, **48**, 1044–1049.
- 42 M. J. P. Comuñas, A. Baylaucq, C. Boned and J. Fernández, *Int. J. Thermophys.*, 2001, **22**, 749–768.
- 43 M. J. P. Comuñas, E. R. López, P. Pires, J. García and J. Fernández, *Int. J. Thermophys.*, 2000, **21**, 831–851.
- 44 L. Lugo, M. J. P. Comuñas, E. R. López and J. Fernández, *Fluid Phase Equilib.*, 2001, **186**, 235–255.
- 45 B. Lagourette, C. Boned, H. Saint-Guirons, P. Xans and H. Zhou, *Meas. Sci. Technol.*, 1992, **3**, 699–703.
- 46 W. Wagner and A. Pruss, *J. Phys. Chem. Ref. Data*, 2002, **31**, 387–535.

Preparation and catalytic activity of active carbon-supported Mo₂C nanoparticles

A. Celzard,^{*a} J. F. Marêché,^a G. Furdin,^a V. Fierro,^b C. Sayag^c and J. Pielaszek^d

Received 7th June 2005, Accepted 22nd September 2005

First published as an Advance Article on the web 7th October 2005

DOI: 10.1039/b507971c

Mo₂C nanoparticles dispersed on two kinds of active carbon were prepared and their catalytic properties were tested. One carbonaceous support is a commercial active carbon: NC100, supplied by the French company Pica, while the other is a highly porous monolith derived from compressed expanded graphite. Both materials were impregnated with MoCl₅ in the vapour phase, followed by reduction-carburization at high temperature with a stream of hydrogen. Molybdenum carbide nanoparticles (1–5 nm wide) were thus obtained all over the surface. Such particles were also prepared by impregnation of the monolithic active carbon by (NH₄)₆Mo₇O₂₄·4H₂O in aqueous solution, followed by reduction-carburization in the same conditions. The effect on the catalytic properties of the carbonaceous support on one hand, and that of the precursor of the carbide on the other hand, could thus be investigated. For that purpose, studies of hydrodenitrogenation (HDN) of indole were carried out. The results showed that the monolithic support impregnated in the vapour phase is the best catalyst. Its catalytic activity was finally also studied in hydrodesulfuration (HDS) of dibenzothiophene. For both hydrotreatment reactions, Mo₂C was shown to be a very efficient, with a low hydrogenating activity, hence with a low consumption of hydrogen with respect to more conventional catalysts.

1. Introduction

For more than two decades, carbonaceous materials are known to be valuable catalyst supports for various applications.^{1–5} Such materials indeed possess several advantages, namely chemical stability, adjustable porosity and surface area, and mechanical strength. Besides, preparing catalysts by impregnation can be tailored due to the frequent presence of carbon–oxygen surface chemical groups, which strongly influence the adsorption of metallic elements. Hence, since the dispersion of the active phase is influenced accordingly, both high activity and high selectivity may be expected with suitably chosen carbonaceous supports.

This present experimental study is devoted to the preparation of catalysts designed for application in the refining of petroleum feedstock, especially for hydrodesulfuration (HDS) and hydrodenitrogenation (HDN). Classical industrial catalysts for the above processes (mainly the so-called sulfured “Ni–Mo” and “Co–Mo” supported on alumina) are indeed not efficient enough, given the new European standards for fuels, which impose very low contents for sulfur and nitrogen. Molybdenum carbide is a valuable catalyst for both HDS and

HDN and hence is of prospective use for this purpose.^{6,7} Supporting Mo₂C onto a carbonaceous material has two major advantages. A good dispersion of the active phase may be obtained; on the other hand, preparation of the carbide is easier than on any other support.⁸ Finally, recovery of the metal is possible by burning the carbonaceous matter after use of the catalyst.

In a previous work,⁹ a synthesis was suggested in which a commercial active carbon powder was directly impregnated by ammonium heptamolybdate. The latter was subsequently reduced and carburized under a hydrogen stream. In the present paper, a new preparative method for Mo₂C supported on active carbon is presented, using vapour of molybdenum pentachloride as a precursor. Two impregnation techniques were tested, namely from the vapour and from the liquid phases, using the same support. Then, the carbonaceous support was carburized under a flow of hydrogen at temperatures up to 700 °C. Next, the influence of the impregnating method on the catalytic activity of the carbide phase in HDN reaction of indole was investigated. Additionally, the role of the supporting material, being either a laboratory-made monolith or a commercial granular material, was studied in the same catalytic test. Finally, the performances in HDS of the vapour-phase impregnated monolith were also investigated.

2. Experimental

2.1. Carbonaceous materials

The preparation of Mo₂C nanoparticles was performed on two kinds of active carbon. One is a granular commercial material, termed NC100, and supplied by the French company Pica; it originates from the physical activation of coconut shell chars.

^aLaboratoire de Chimie du Solide Minéral, UMR CNRS 7555, Université Henri Poincaré - Nancy I, BP 239, Vandoeuvre-lès-Nancy, 54506, France. E-mail: Alain.Celzard@lcsm.uhp-nancy.fr; Fax: +33 (0) 3 83 68 46 19

^bDepartament d'Enginyeria Química, Universitat Rovira i Virgili, Campus Sescelades, Av. dels Països Catalans 26, Tarragona, 43007, Spain

^cLaboratoire Réactivité de Surface, UMR CNRS 7609, Université P. et M. Curie, 4 place Jussieu, 75252 Paris Cédex 05, France

^dInstitute of Physical Chemistry, Polish Academy of Sciences, Warszawa, Poland

Table 1 Elemental analyses (wt%) of the two carbonaceous supports. "neg." means negligible amount, *i.e.*, not detected by the chemical analysis

Active carbon	C	H	O	at. H/C	at. O/C	Ashes
NC100	91.7	0.8	2.4	0.10	0.02	1.4
Monolith	98.4	<0.3	<0.3	<0.04	<0.002	neg.

As seen in Table 1, such a material exhibits a rather low oxygen content, and thus should have a low amount of both surface functional groups and ashes (mainly oxides). The second one, referred to as the monolith, is obtained from expanded graphite compressed at a density of 0.11 g cm^{-3} , and next impregnated by furfuryl alcohol. The latter was polymerised to form a composite of porous graphite coated with polymer. Such a block was then pyrolysed and finally activated with steam at 50% burn-off. The resulting monolithic material, of which detailed preparation and features were described elsewhere,¹⁰ may be seen as a highly porous graphite backbone coated with a thin layer of active carbon. Its main advantages are: chemical purity (carbon content higher than 98 wt%, see Table 1) and high mechanical properties.¹¹

The textural parameters of all these materials were derived from adsorption isotherms, and are presented in Table 2; the micropore volumes were calculated from the theory of Dubinin–Radushkevitch¹² using the adsorption isotherms of carbon dioxide at 298 K, while the mesopore volumes were obtained by application of the Kelvin equation and capillary condensation theory^{13,14} to the adsorption isotherms of benzene at the same temperature. BET surface areas were calculated from nitrogen adsorption at 77 K. It may be seen that both materials are mainly microporous. However, while the microporosity of NC100 is homogeneous throughout the grains, that of the monolith is only a surface microporosity, since only a thin coating of coke (about 100 nm thick¹⁰) existing on the graphite surface was activated. Such a surface microporosity is thus assumed to be fully accessible through very wide and well-connected macropores.

2.2. Impregnation

The impregnation method in the liquid phase was carried out by the incipient wetness method.⁹ The carbonaceous material was impregnated by an aqueous solution of ammonium heptamolybdate $(\text{NH}_4)_6\text{Mo}_7\text{O}_{24}\cdot 4\text{H}_2\text{O}$ (10 wt.% of Mo) whose volume is exactly that of the pore space of the carbonaceous support. The latter was wetted by the solution, drop by drop, until complete soaking. The sample was next dried at 100°C in an oven for 24 h, then the impregnating salt was reduced and transformed into carbide upon heat-treatment in a hydrogen stream. In the aforementioned process, intermediate phases

Table 2 Pore textures of the two carbonaceous supports. "micro" and "meso" correspond to micropore and mesopore volumes, respectively

Active carbon	$V_{\text{micro}}/\text{cm}^3 \text{ g}^{-1}$	$V_{\text{meso}}/\text{cm}^3 \text{ g}^{-1}$	$S_{\text{micro}} + S_{\text{meso}}/\text{m}^2 \text{ g}^{-1}$	$S_{\text{BET}}/\text{m}^2 \text{ g}^{-1}$
NC100	0.58	0.08	$1615 + 49 = 1664$	1493
Monolith	0.33	0.066	$862 + 25 = 887$	795

like MoO_3 and MoO_2 occur before the metal, and finally the carbide, are formed. Since such intermediary oxides are rather volatile, they are suspected to coalesce, leading to the formation of large carbide clusters coexisting with much smaller particles dispersed on the carbon surface (see below). In order to avoid the formation of such large particles and to obtain the most homogeneous dispersion of very small Mo_2C crystallites, the oxygen-free precursor (MoCl_5) was used in the present work.

The molybdenum pentachloride used, supplied by Aldrich, was of purity better than 99.9%. It melts at 194°C and boils at 268°C , and is thus highly volatile at moderate temperatures. Due to its strongly hygroscopic character, any handling of MoCl_5 was done under dry nitrogen, in a glove bag. The sample to be impregnated in the gas phase was outgassed overnight at 10^{-4} – 10^{-5} Torr and 500°C , and introduced at one end of a two-bulb tube. MoCl_5 was then placed at the other end of the same tube, in such a quantity that the carbon is expected to be loaded at 10 wt.% of the metal, assuming a complete impregnation. The tube was subsequently sealed-off under vacuum, and was finally introduced in a two-temperature (245 – 250°C) horizontal furnace. The pentachloride was thus transported through vapour phase towards the active carbon, the latter being maintained 5°C higher than MoCl_5 in order to avoid the condensation of bulk chloride particles. After five days, the experiment was stopped and the doped sample was preserved in a tube sealed-off under vacuum before performing the final carburization step.

2.3. Reduction and carburization

The preparation of carbide may be easily achieved by heating the metallic element in a gaseous mixture of hydrogen and hydrocarbon (especially methane but also heavier molecules like ethylene or butane).^{15–17} However, early works have also shown the possibility of preparing carbide by diffusion of carbon inside a metal in a hydrogen atmosphere.^{18,19} In the present case, such a carburization was carried out through a simple heating of MoCl_5 deposited on carbonaceous supports in a hydrogen flow. Whatever the impregnation method, the supports were heated up to a maximum of 700°C at a rate of 1°C min^{-1} , under a stream of pure hydrogen flowing at 100 ml min^{-1} . The final temperature was maintained for two hours.

This way, the chloride was first reduced into metal which subsequently reacted with the carbonaceous support. After cooling, the samples were transferred into a glove bag filled with nitrogen. No pyrophoric behaviour could be observed with carburized supports submitted later to air exposure. This suggests that the samples were sufficiently passivated by residual oxygen in the glove bag ($\approx 50 \text{ ppm}$).

2.4. Catalytic tests

2.4.1. Hydrodenitrogenation (HDN). The supported catalysts were ground in a mortar, and only the grains having a size within the range 100 – $200 \mu\text{m}$ were collected. They were activated by heating up at 1°C min^{-1} in a flow of hydrogen ($25 \text{ cm}^3 \text{ min}^{-1}$) up to 450°C , the final temperature being maintained for 2 h. The catalytic tests were carried out

immediately after, at temperatures between 300 and 400 °C, under hydrogen pressure (50 bars). The reactor was fed with a mixture of gaseous hydrogen and a 1 wt.% indole solution in cyclohexane. The mixture obeyed the molar ratio hydrogen/indole = 600, and the flow of hydrogen was adjusted in order to control the contact time t_c , defined as:

$$t_c = \frac{\text{catalyst volume}}{\text{total flow (solution + hydrogen)}} \quad (1)$$

The catalyst volume was 0.67 cm³, and the flow of the feed was maintained so that t_c was in the range 0.4–4 s. At the outlet of the reactor, the gases were analysed with a gas-phase chromatograph (HP 5890 Series II) equipped with a FID detector.

2.4.2. Hydrodesulfuration (HDS). The supported catalysts were conditioned in the same way as detailed above (grinding and heat-treatment under hydrogen). The catalytic tests were performed at 340 °C under 40 bar of hydrogen. The reactor was fed with a mixture of gaseous hydrogen and a 1 wt.% dibenzothiophene (DBT) solution in decahydronaphthalene (*i.e.*, decaline). 1 wt.% dimethyldisulfide (DMDS) was also added to the feed as a supplementary source of sulfur. Both the flow of the feed (0.1–0.47 cm³ min⁻¹) and the amount of catalyst (200 and 800 mg) were varied in order to obtain contact times ranging from 0.2 to 3.5 s. The total sulfur content of the feed was adjusted at 0.5 wt.%, which is a rather high value for such catalytic tests (see below). At the outlet of the reactor, the liquid effluents were collected and analysed by gas chromatography.

3. Characterisation of the deposited phases

3.1. Impregnation from the liquid phase

The monolith impregnated with the molybdate salt was studied by XRD, and the corresponding pattern was found to be similar to that of the pure original carbonaceous material. No molybdenum phases could be evidenced, the deposited matter being either in the form of too small particles, or amorphous.

TEM studies coupled with X-ray microanalysis (EDAX) indeed revealed very well dispersed nanoparticles, typically 1 nm large. No cluster was evidenced, hence such an impregnation method was found to be very efficient, leading to the formation of fine well-dispersed particles.

3.2. Impregnation from the vapour phase

After vapour impregnation, Mo and Cl contents were measured by elemental analysis and compared with what

Table 3 Deposition yield of both elements Mo and Cl (calculated from elemental analyses and from initial amounts of MoCl₅ present in the vapour-phase impregnation reactor), and measured atomic Cl/Mo ratio

Active carbon	Mo deposition yield	Cl deposition yield	Atomic Cl/Mo
NC100	99.9%	80.5%	4.0
Monolith	96.0%	67.6%	3.5

could be expected if the pentachloride was fully deposited onto the carbonaceous material. Table 3 shows the deposition yield for each of the elements and each of the supports. It can be seen that the expected amount of deposited matter is not met exactly; the atomic Cl/Mo ratio is not 5 but rather within the range 3–4. XRD measurements on the residual salt remaining in the bulb and not transported to the impregnated support indeed showed the presence of molybdenum trichloride, probably originating from the thermal decomposition of MoCl₅ according to :



Since MoCl₃ is less volatile than MoCl₅, it was not fully transported towards the carbonaceous material. Weighing the residue remaining in the bulb previously containing the pentachloride and recalculating the amount of deposited molybdenum indeed confirmed the data presented in Table 3.

Just like in the previous impregnation method, XRD did not show the presence of Mo at the surface of the supports. TEM studies showed two kinds of deposited particles: one consisting of very small isolated particles (average size below 2 nm), the other one being made of clusters (average size 10 nm, exceptionally up to 50 nm). The presence of MoCl₃ was confirmed both by electron microdiffraction and EDAX performed on big clusters. From the latter method, an atomic Cl/Mo ratio ranging from 2.5 to 3 was found, in good agreement with the previous elemental analysis given in Table 3. Much finer and more dispersed particles were observed at the monolith surface, evidencing the strong influence of the support on the dispersion. Indeed, MoCl₅ is a strongly acidic compound, able to react easily with oxygen. Since the monolith is almost free of ashes or oxygenated surface groups contrary to the NC100, many more clusters were found on NC100.

3.3. Carburization

TEM observation of carburized monolith previously impregnated with aqueous heptamolybdate showed two kinds of regions, one displaying a number of small individual, well dispersed nanoparticles, and the other being characterised by clusters with an average size ranging from 10 to 20 nm (see Fig. 1).

XRD experiments were carried out on carburized materials obtained by vapour impregnation, using samples enclosed in sealed-off Lindemann glass tubes. As seen in Fig. 2, the characteristic reflections of hexagonal α -Mo₂C, being the only molybdenum-based phase which was found, are observed for both supports. It can be seen that the peaks from the monolith have higher intensity and resolution than those from NC100. TEM observations (see pictures in Fig. 3) show again the coexistence of a number of small individual well dispersed and very fine particles (\approx 1 nm in diameter) and some bigger grains or clusters, typically 5 nm large. Electron microdiffraction performed on the larger grains also confirmed the presence of the hexagonal α -Mo₂C phase, see Fig. 4. Besides, no chloride could be made evident from EDAX analyses on the same grains, suggesting that the experimental parameters were suitably optimised for a carburization process.

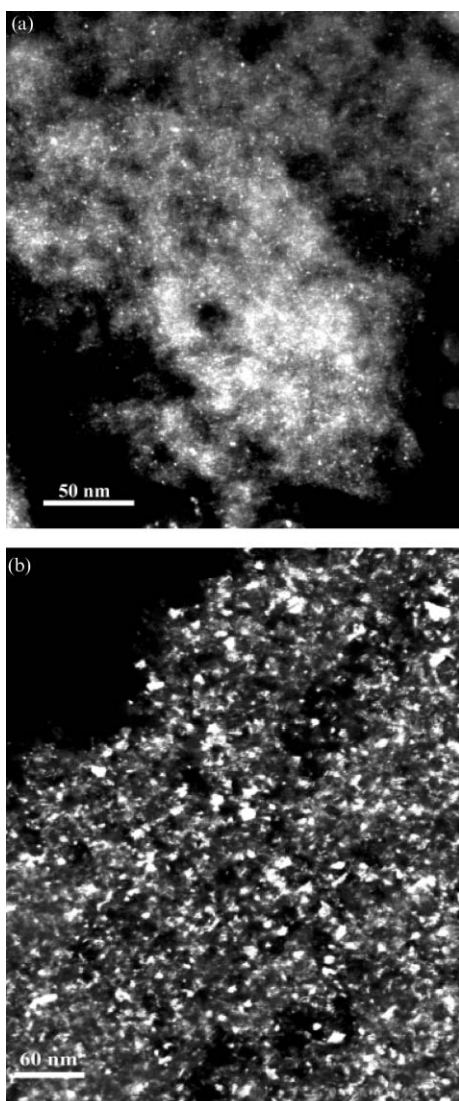


Fig. 1 TEM (dark field) pictures of dispersed nanoparticles (a) and large clusters (b) of molybdenum carbide prepared by liquid phase impregnation of the monolithic support.

At first sight, given that the impregnation in the vapour phase was thus leading to the finest and the most dispersed nanoparticles, the catalytic properties of derived carbide were expected to be better than those of the materials impregnated in the liquid phase. Concerning the role of the support, since monolith is almost oxygen-free, a lower clustering of the carbide particles occurred, and such a material was expected to present the highest catalytic activity.

4. Catalytic studies

4.1. HDN

Present in petroleum feedstock nitrogenated molecules which have to be eliminated are usually in the form of both saturated and unsaturated heterocycles, *e.g.*, pyridine, piperidine, quinoline, pyrrole, indole and carbazole. Among these, quinoline was the most studied, while indole is thought to lead to the most simple hydrodenitrogenation mechanisms.

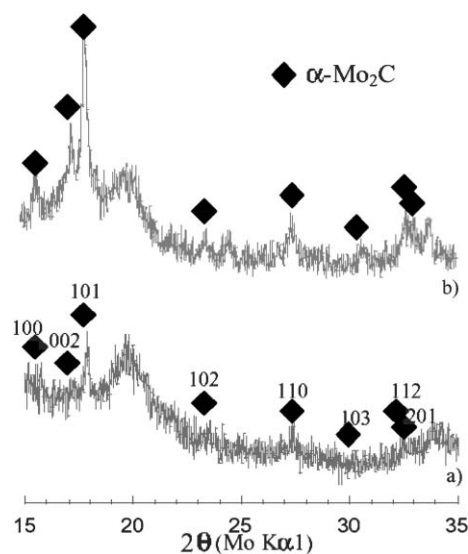


Fig. 2 XRD patterns of the carbide phase from carburized: (a) vapour-phase MoCl_5 -impregnated NC100; (b) vapour-phase MoCl_5 -impregnated monolith.

The catalytic activity of Mo_2C towards HDN of the quinoline reaction was already demonstrated;²⁰ a selectivity for saturated *vs.* unsaturated nitrogenated products lower than that of the traditional, so-called sulfured, NiMo or CoMo/alumina was shown. In other words, no preliminary hydrogenation of the unsaturated cycles is required, hence a lower hydrogen consumption. Keeping these features in mind, the HDN of indole was investigated on our carbide phase as a function of both: preparation method and carbonaceous support.

4.1.1. Reaction scheme. Several routes are possible for the HDN of indole,^{21–25} see Fig. 5. The first step is the hydrogenation of the heterocycle, leading to indoline, then hydrogenolysis essentially occurs, producing orthoethylaniline (OEA). The latter can next be denitrogenated according to two main routes, termed 1 and 2, with possible secondary reactions. Route 1 is that followed by classical sulfured CoMo/alumina catalysts, leading to evolution of NH_3 and saturated molecules; much hydrogen is thus required. By contrast, route 2 denitrogenates OEA, also leading to NH_3 , but without hydrogenation of the aromatic cycle, hence an economy of hydrogen.

4.1.2. Results. The influence of the carbonaceous support (monolith or NC100 impregnated in the vapour phase) on the catalytic activity was studied as a function of both contact time and reaction temperature. It should be recalled here that the doping of the carbons was the same, *i.e.*, 10 wt.% of Mo. Subsequently, the preparation method (monolith impregnated in vapour or in liquid phase) was investigated at a given temperature for several contact times.

Influence of the support at constant contact time. The feed flow was kept constant in order to fix $t_c = 1.58$ s; the molar concentrations of reagent (indole) and intermediary products (OEA, OMA, OECHA, aniline) were measured at the reactor outlet and the results are presented in Fig. 6. No indole could

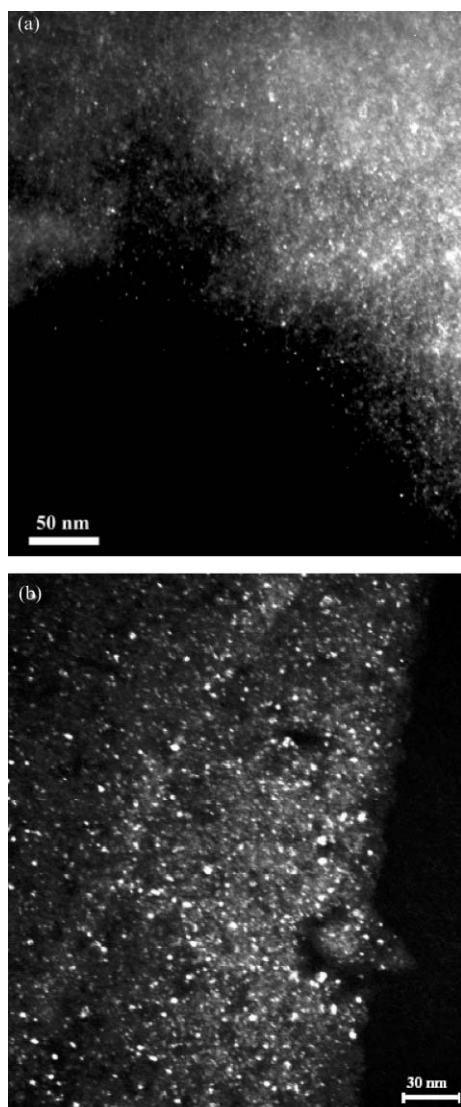


Fig. 3 Dispersed carbide nanoparticles (average size 1–5 nm) as seen by TEM (dark field) achieved on carburized vapour-phase MoCl_5 -impregnated (a) NC100 and (b) monolith.

be detected above 300 °C, because it is very rapidly converted into the main intermediary molecule OEA (no HHI was indeed found).

The HDN yield of the reaction was defined as:

$$\text{HDN yield (\%)} = \frac{m_{\text{ECH}} + m_{\text{EB}} + m_{\text{MCH}} + m_{\text{toluene}}}{m_{\text{indole initial}}} \times 100 \quad (3)$$

where m_x are the number of moles of the molecule x . As shown in Fig. 7(a), the HDN yield of the monolithic material increased very rapidly with temperature, and was found to be complete near 350 °C. That of the NC100 increased more slowly under strictly identical experimental conditions, leading to 100% HDN at 400 °C (see Fig. 7(b)).

Influence of the support at constant temperature. Kinetic studies could be achieved by varying the contact time at a constant temperature of 350 °C. Fig. 8(a) was obtained with vapour phase impregnated monolith: it shows that indole is

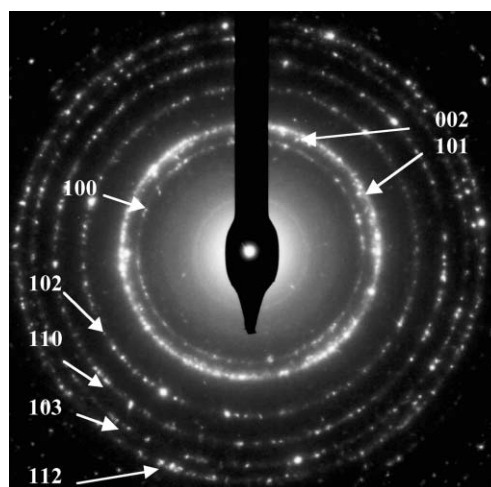


Fig. 4 Electron microdiffraction pattern of large grains of Fig. 3(b) (carburized vapour-phase made monolithic catalyst), showing well crystallised $\alpha\text{-Mo}_2\text{C}$.

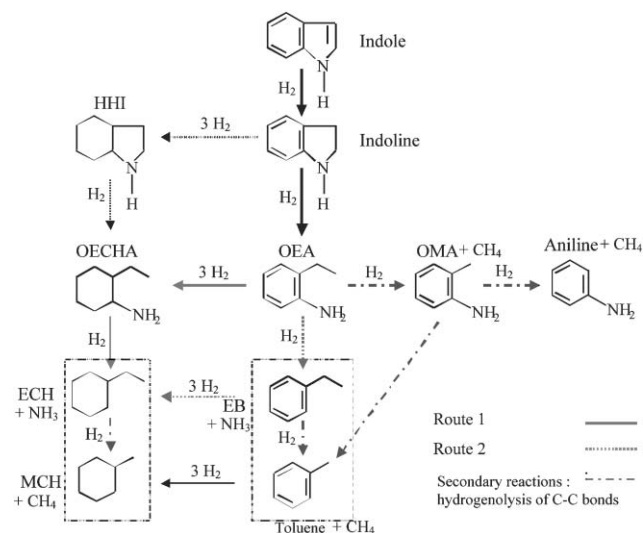


Fig. 5 Reaction scheme of HDN of indole. HHI = hexahydroindoline, OECHA = orthoethylcyclohexylamine, OEA = orthoethylaniline, OMA = orthomethylaniline, ECH = ethylcyclohexane, EB = ethylbenzene, MCH = methylcyclohexane.

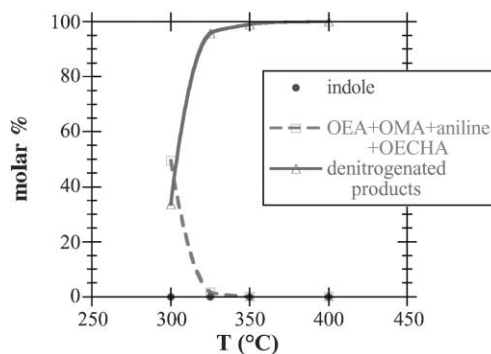


Fig. 6 Evolution of the molar percents of reagent (indole) and intermediary products at the outlet of the HDN reactor, for the vapour-phase made Mo_2C /monolith at a constant contact time of 1.58 s.

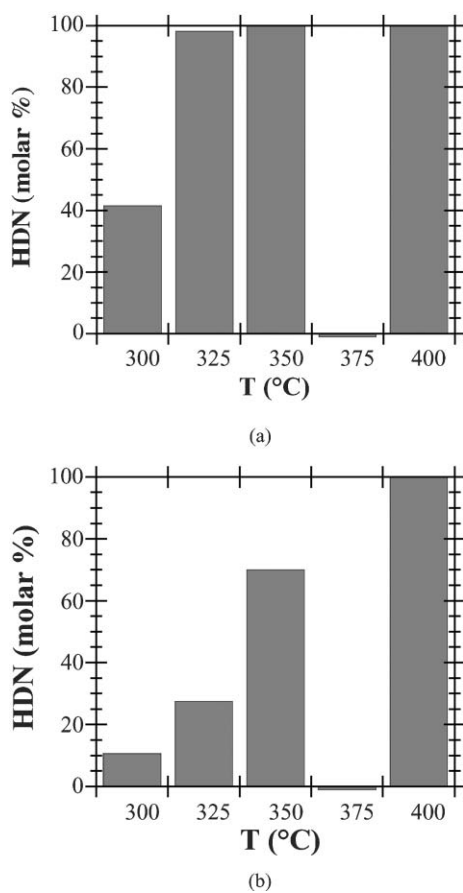


Fig. 7 HDN yield of indole at a contact time of 1.5 s as a function of temperature for vapour-phase made (a) Mo₂C/monolith, and (b) Mo₂C/NC100.

not detected at the outlet of the reactor for contact times as short as 0.4 s, thus evidencing a very high catalytic activity. Indole was indeed completely transformed either into nitrogenated intermediary products (mainly OEA), or into denitrogenated saturated (route 1) and unsaturated (route 2) molecules. The nitrogenated intermediary products themselves disappeared after only 1 s. The data in Fig. 8(a) also shows that, above 1 s, the formation of saturated compounds becomes predominant, hence stopping the reaction at $t_c = 1$ s may save hydrogen as compared with traditional HDN catalysts for which route 1 is the major mechanism. This finding may be very interesting from an industrial point of view.

As expected, the catalytic activity of the carbide deposited on NC100 is lower, since indole disappeared only after 1.5 s instead of 0.4 s as in the previous case. Such a difference can not be ascribed to the pore texture of the active carbon, since both supports are microporous. However, the carbide nanoparticles on the monolith are better crystallised (see Fig. 2), and are a little more dispersed and finer. However, the main effect could be the fact that, as explained at the beginning of this work, the monolith is a highly porous graphite backbone with a surfacic microporosity; diffusion in such a very wide and very well connected pore network is expected to be very easy, while NC100 grains are microporous throughout their volume, with a negligible fraction of wider pores.

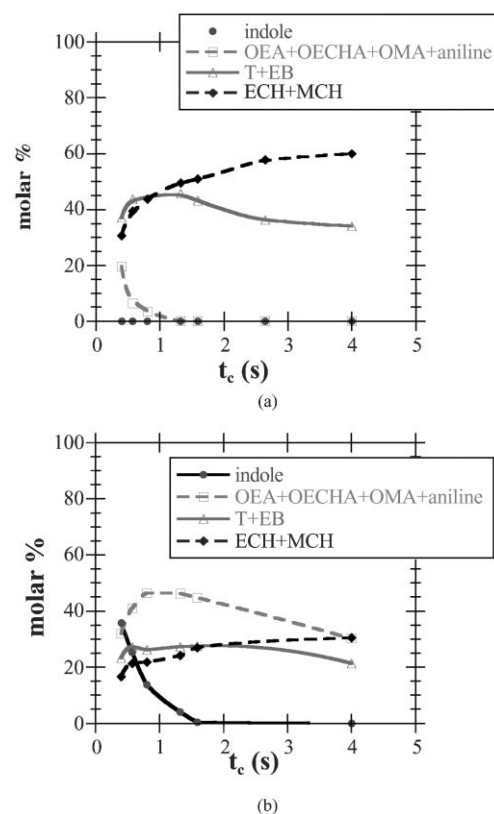


Fig. 8 Evolution of the molar percents of reagent (indole) and intermediary products at the outlet of the HDN reactor working at 350 °C for various contact times, for vapour-phase impregnated (a) Mo₂C/monolith and (b) Mo₂C/NC100.

Influence of the impregnation method at constant temperature.

The influence of the way the monolith was impregnated was investigated at 350 °C for various contact times, as seen in Fig. 9. The reaction products are the same as before, but the formation of saturated denitrogenated molecules now clearly prevails. In other words, route 1 is the main HDN mechanism even at low contact times, hence consuming much hydrogen.

The carbide derived from aqueous heptamolybdate has thus a higher hydrogenating potential, but a lower activity than that obtained from the MoCl₅ vapour. HDN is indeed complete at

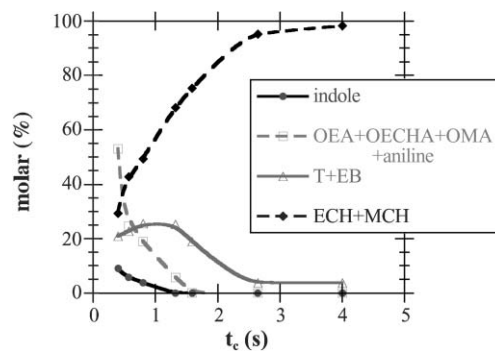


Fig. 9 Evolution of the molar percents of reagent (indole) and intermediary products at the outlet of the HDN reactor working at 350 °C for various contact times, for liquid-phase impregnated Mo₂C/monolith.

Table 4 Results derived from the chemisorption of CO on the monolith, depending on the impregnation mode

Impregnation mode of the monolith	wt.% of deposited Mo	Chemisorbed CO/ $\mu\text{mol g-catalyst}^{-1}$	% of accessible Mo
Vapour-phase	10.5	86	7.9
Liquid-phase	9.2	28	2.7

1.6 s, similarly as for NC100. Considering that the active phase is the same whatever the precursor, *i.e.*, hexagonal $\alpha\text{-Mo}_2\text{C}$, such a difference could be ascribed to the state of dispersion at the surface of the carbonaceous support, in agreement with what was seen in Fig. 1 and 3(b). Such an assumption was verified by CO chemisorption, a technique which was already shown to lead to reliable results with molybdenum carbides, either supported²⁶ or not.^{27,28} 10 vol% of CO in helium was injected every 10 min in the vessel containing the catalyst, until its surface was saturated; the amount of unchemisorbed CO was measured simultaneously. The number of fixed moles of CO was thus calculated, and the results are presented in Table 4. From these results, the fraction of available active phase was calculated according to :

$$f = \frac{\text{moles of chemisorbed CO}}{\text{moles of deposited Mo at the surface of the support}} \quad (4)$$

The amount of accessible Mo is higher with the chlorinated precursor because the particle size is lower than for the oxygenated one. Additionally, the impregnation in the vapour phase was probably more homogeneous, hence the higher catalytic activity of the catalyst presented in the present work.

4.2. HDS

The very promising results obtained in HDN encouraged us to study the HDS reaction, since the desulfurization of several molecules is difficult using classical supported sulfured NiMo and CoMo. Indeed, the actual sulfur content of the fuels should not exceed 50 ppm. In the following, HDS of dibenzothiophene (DBT), which is a molecule particularly hard to break up, is studied using vapour-derived $\text{Mo}_2\text{C}/\text{monolith}$.

4.2.1. Reaction scheme. HDS of DBT is based on reactions of hydrogenation and hydrogenolysis of C–S bonds,²⁹ as displayed in Fig. 10. Two routes are possible, a hydrogenating one (route 1) leading to the bicyclohexyl, and a desulfuring one (route 2) producing biphenyl. It was shown that no hydrogenation of the latter molecule occurs when $\text{Mo}_2\text{C}/\text{alumina}$ is used.³⁰

4.2.2. Results. *Catalytic activity of $\text{Mo}_2\text{C}/\text{monolith}$.* Fig. 11 presents both the conversion of DBT and the HDS yield, defined as :

$$\text{DBT conversion (\%)} = \frac{m_{\text{THDBT}} + m_{\text{biphenyl}} + m_{\text{CHB}} + m_{\text{BCH}}}{m_{\text{DBT initial}}} \times 100 \quad (5)$$

$$\text{HDS yield (\%)} = \frac{m_{\text{biphenyl}} + m_{\text{CHB}} + m_{\text{BCH}}}{m_{\text{DBT initial}}} \times 100 \quad (6)$$

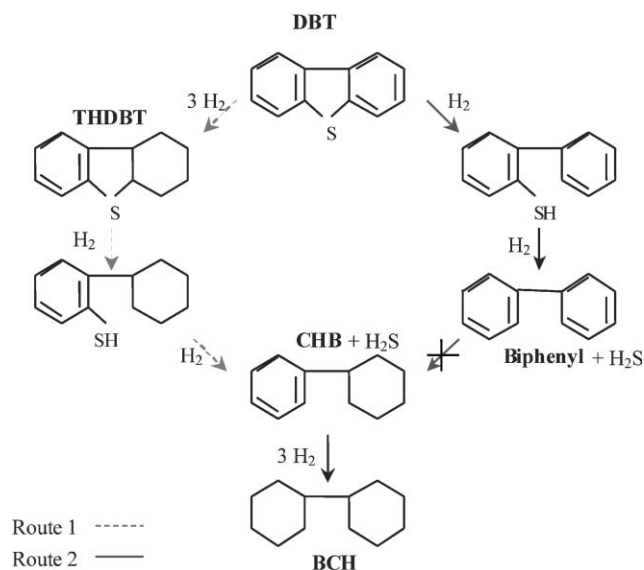


Fig. 10 Reaction scheme of HDS of DBT (dibenzothiophene). THDBT = tetrahydrodibenzothiophene, CHB = cyclohexylbenzene, BCH = bicyclohexyl.

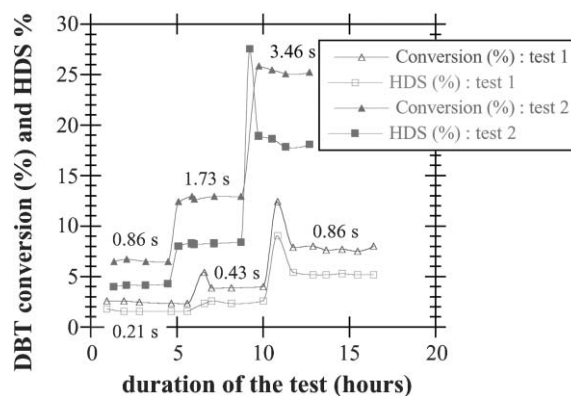


Fig. 11 Evolution of the conversion of DBT and the HDS yield (340 °C) for $\text{Mo}_2\text{C}/\text{monolith}$ as a function of contact time (indicated on the plot) and duration of the test. Tests 1 and 2 correspond to catalyst amounts of 200 and 800 mg, respectively.

as a function of contact time and duration of the catalytic test. It can be seen that, at constant contact time (here 0.86 s), both HDS yield and DBT conversion are unchanged, whatever is the amount of catalyst (200 mg and 800 mg in tests 1 and 2, respectively). Increasing the contact time makes the conversion and the yield increase proportionally. Upon changing t_c , the catalytic activity exhibits a jump then stabilises after about 1 h, and finally remains constant. At $t_c = 3.46$ s, conversion and yield are close to 26% and 18%, respectively; these values are rather low because of the high sulfur content of the feed (0.5 wt.%) and the high amount of DBT. The $\text{Mo}_2\text{C}/\text{monolith}$ catalyst does not behave like the carbides containing Ni or Mo whose surface is progressively modified by the presence of sulfur, and whose HDS activity increases with time. This latter effect was attributed to the gradual transformation of carbide into oxycarbosulfide, whose activity tends to resemble that of sulfides.³¹ Consequently, sulfuration of $\text{Mo}_2\text{C}/\text{monolith}$ does not seem to occur.

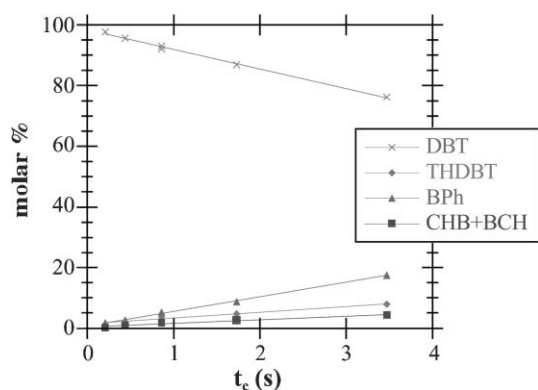


Fig. 12 Evolution of the molar percents of reagent (DBT) and intermediary products at the outlet of the HDS reactor working at 340 °C for various contact times, for vapour-phase impregnated Mo₂C/monolith.

The molar percents of the reagent (DBT) and the intermediary products are given in Fig. 12 as a function of contact time. While indole was consumed in an exponential way (see Fig. 8(b) and 9), corresponding to a reaction of order 1, the concentration of DBT decreases linearly with time, evidence of a reaction of order 0, already observed for P-doped Mo₂C/alumina.³⁰ The biphenyl (BPh on the plot) is the main reaction product, showing that the HDS mechanism preferentially occurs according to route 2, *i.e.*, the non-hydrogenating way. Such a selectivity is also that of Mo₂C/alumina,³⁰ suggesting that the carbides favour the direct breaking of the C–S bond, just like the molybdenum nitrides do.³² By contrast, the sulfured CoMo and NiMo present a much higher hydrogenating power, hence a higher consumption of hydrogen than Mo₂C.

Ageing of the Mo₂C/monolith catalyst. One more catalytic test was carried out with a real petroleum feedstock (liquid gasoline) in actual industrial conditions (micro-pilot reactor: catalyst volume 20 cm³, hydrogen pressure 55.5 bar, hourly spatial speed 1 h⁻¹) during 250 h. The initial sulfur and nitrogen contents of the feed were 245 and 62 ppm, respectively. Fig. 13 shows the conversion of the sulfured molecules

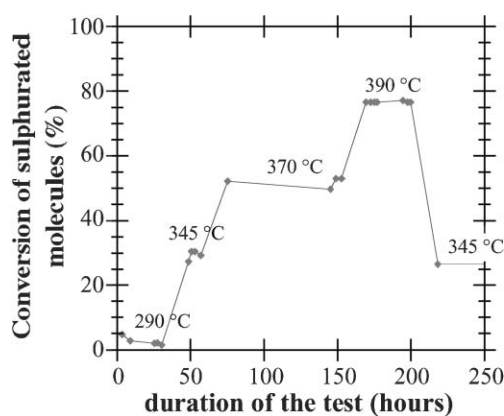


Fig. 13 Evolution of the conversion of sulfured molecules by Mo₂C/monolith in a real petroleum feedstock as a function of temperature and duration of the test.

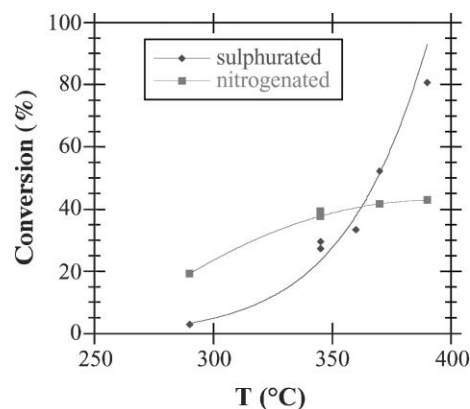


Fig. 14 Evolution of the conversion of sulfured and nitrogenated molecules by Mo₂C/monolith in a real petroleum feedstock as a function of temperature.

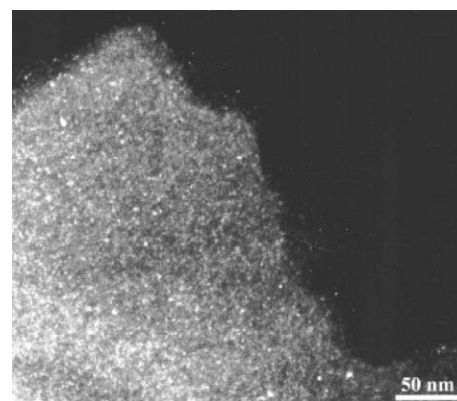


Fig. 15 Dispersed carbide nanoparticles (average size 1–7 nm) as seen by TEM (dark field) achieved on Mo₂C/monolith after 10 days of HDS reaction.

as a function of time and temperature. It can be seen that the conversion has not changed after more than 200 h of test, since the same yield was recovered at 345 °C. In other words, no deactivation of the catalyst was found. Fig. 14 presents the conversion of both nitrogenated and sulfured molecules as a function of temperature for the same gasoline feed in the same conditions. HDN hardly reaches 50% at 390 °C, but HDS attains 80%. In other words, 20% of the sulfured molecules were not converted, meaning that the remaining sulfur content of the feed is only 50 ppm, which was the target to reach.

XRD and TEM were used to characterise the catalyst after the test. The only phase evidenced by XRD was hexagonal α -Mo₂C, and no surface sulfuration could be observed. The corresponding detailed study is given in a separate work.³³ TEM showed that no clustering of the nanoparticles occurred, since only well-dispersed grains 1 to 7 nm large were seen (see Fig. 15).

5. Conclusions

In this work, a new preparation method of molybdenum carbide supported on a monolithic carbonaceous material is described, using MoCl₅ as a precursor. This method was also

tested on a commercial active carbon. Whatever the supporting material, hexagonal α -Mo₂C was obtained. The catalytic properties of this carbide, dispersed on the two supports, toward the HDN of indole were compared. For one of the supports (the monolithic one), comparison was also made between two impregnation techniques, namely MoCl₅ vapour and (NH₄)₆Mo₇O₂₄·4H₂O aqueous solution. The main advantages and disadvantages of each support and each impregnation technique are summed up below:

- The lab-made monolithic support is nearly ash-free and oxygen-free, hence minor clustering of the carbide particles was seen. The catalyst derived from the commercial active carbon presented more numerous and bigger clusters.

- A direct consequence of this was a higher activity of Mo₂C/monolith in the HDN of indole, which was very efficient: 100% HDN at 350 °C for a contact time of 1.6 s, and a complete vanishing of indole as soon as 0.4 s of working time was reached.

- Such a good catalytic performance was also attributed to the particular texture of the monolithic support, namely a very thin coating of active carbon on a highly porous graphite backbone, allowing an excellent diffusion of molecules throughout the pore network.

- Impregnation from the liquid phase leads to poor dispersion of the active phase, hence the catalytic activity of the same Mo₂C on the same monolithic support prepared this way was lower than that of the vapour phase made material.

The catalytic properties of Mo₂C/monolith prepared with the MoCl₅ precursor was also tested for the HDS reaction. Encouraging performances were found, especially with actual petroleum feedstock, since the desulfuration target was met at 390 °C. No decrease of the activity by sulfuration of the catalyst was observed even after 10 days of working time.

Finally, it was shown that molybdenum carbide supported on a carbonaceous support favours the HDN and HDS routes which consume a lower amount of hydrogen, since hydrogenation of the aromatic molecules might be avoided. This fact may have serious economical implications.

Acknowledgements

The authors acknowledge financial support from the company TotalFinaElf, and from the Polish Academy of Sciences (PAN) and the CNRS through the GDRE "Adsorbants Carbonés et Catalytiques pour l'Énergie et l'Environnement". G. Pérot, from LACO (CNRS-Poitiers, France) is thanked for having carried out part of the HDS experiments.

References

- 1 A. W. Miller, W. Atkinson, M. Barber and P. Swift, *J. Catal.*, 1971, **22**, 140.
- 2 M. Honalla and B. Delmon, *J. Phys. Chem.*, 1971, **84**, 2194.
- 3 I. E. Wachs, R. Y. Salch, S. S. Chan and C. C. Chersich, *Appl. Catal.*, 1985, **15**, 339.
- 4 G. Marcelin and J. E. Lester, *J. Catal.*, 1985, **93**, 270.
- 5 M. S. Spencer, *J. Catal.*, 1985, **93**, 216.
- 6 M. J. Ledoux, C. Pham-Huu, J. Guille and H. Dunlop, *J. Catal.*, 1992, **134**, 383.
- 7 K. R. McCrea, J. W. Logan, T. L. Tarbuck, J. L. Heiser and M. E. Bussell, *J. Catal.*, 1997, **171**, 255.
- 8 S. Puricelli, PhD Thesis, University of Nancy I, 2001.
- 9 D. Mordenti, D. Brodzki and G. Djéga-Mariadassou, *J. Solid State Chem.*, 1998, **141**, 181.
- 10 J. F. Maréché, D. Bégin, G. Furdin, S. Puricelli, J. Pajak, A. Albiniak, M. Jasienko-Halat and T. Siemieniewska, *Carbon*, 2001, **39**, 771.
- 11 A. Celzard, M. Krzesińska, D. Bégin, J. F. Maréché, S. Puricelli and G. Furdin, *Carbon*, 2002, **40**, 557.
- 12 M. M. Dubinin, E. D. Zaverina and L. V. Radushkevich, *J. Phys. Chem. (USSR)*, 1947, **21**, 1351.
- 13 S. J. Gregg and K. S. W. Sing, *Adsorption, surface area and porosity*, Academic Press, London, 1982.
- 14 P. J. M. Carrott, M. M. L. Ribeiro Carrott, I. P. P. Cansado and J. M. V. Nabais, *Carbon*, 2000, **38**, 465.
- 15 L. Volpe and M. Boudart, *J. Solid State Chem.*, 1985, **59**, 348.
- 16 J. G. Choi, J. R. Brenner and L. Thompson, *J. Catal.*, 1995, **154**, 33.
- 17 S. Decker, A. Löfberg, J. M. Bastin and A. Frennet, *Catal. Lett.*, 1997, **44**, 229.
- 18 P. N. Ross Jr and P. Stonehart, *J. Catal.*, 1977, **48**, 42.
- 19 L. Leclerc, M. Provost, H. Pastor, J. Grimblot, A. M. Hardy, L. Gengembre and G. Leclerc, *J. Catal.*, 1989, **117**, 371.
- 20 J. C. Schlatter, S. T. Oyama, J. E. Metcalfe III and J. M. Lambert Jr, *Ind. Eng. Chem. Res.*, 1988, **27**, 1648.
- 21 T. C. Ho, A. R. Katritzky and S. J. Cato, *Ind. Eng. Chem. Res.*, 1992, **31**, 1589.
- 22 H. Abe and A. T. Bell, *Catal. Lett.*, 1993, **18**, 1.
- 23 S. Li and J. S. Lee, *J. Catal.*, 1998, **173**, 134.
- 24 E. W. Stern, *J. Catal.*, 1979, **57**, 390.
- 25 E. O. Odeunmi and D. F. Ollis, *J. Catal.*, 1983, **80**, 76.
- 26 P. A. Aegerter, W. W. C. Quigley, G. J. Simpson, D. D. Ziegler, J. W. Logan, K. R. McCrea, S. Glazier and M. E. Bussell, *J. Catal.*, 1996, **164**, 109.
- 27 J. S. Lee, S. T. Oyama and M. Boudart, *J. Catal.*, 1987, **106**, 125.
- 28 J. S. Lee, L. Volpe, F. H. Ribeiro and M. Boudart, *J. Catal.*, 1988, **112**, 44.
- 29 F. Bataille, J. L. Lemberton, P. Michaud, G. Pérot, M. Vrinat, M. Lemaire, E. Schulz, M. Breyse and S. Kasztelan, *J. Catal.*, 2000, **191**, 409.
- 30 P. Da Costa, PhD Thesis, University of Paris VI, 2000.
- 31 B. Dhandapani, T. S. Clair and S. T. Oyama, *Appl. Catal. A*, 1998, **168**, 219.
- 32 M. Nagai, Y. Goto, H. Sasuga and S. Omi, *J. Eur. Ceram. Soc.*, 1997, **17**, 1983.
- 33 J. Pielaszek, B. Mierzwa, G. Medjahdi, J. F. Maréché, S. Puricelli, A. Celzard and G. Furdin, *Appl. Catal. A*, in press.

Influence of the metallic precursor in the hydrogenation of tetralin over Pd–Pt supported zirconium doped mesoporous silica

M. C. Carrión,^a B. R. Manzano,^a F. A. Jalón,^a D. Eliche-Quesada,^b P. Maireles-Torres,^b E. Rodríguez-Castellón^b and A. Jiménez-López^{*b}

Received 7th June 2005, Accepted 13th September 2005

First published as an Advance Article on the web 4th October 2005

DOI: 10.1039/b507495a

Palladium–platinum supported on zirconium doped mesoporous silica catalysts have been prepared by incipient wetness impregnation with two different precursors: (i) a dinuclear precursor [PdPtCl₂(μ-dppm)₂] where dppm = Ph₂PCH₂PPh₂; and (ii) PdCl₂ and H₂PtCl₆·6H₂O. The catalysts obtained with the bimetallic precursor show a much smaller metallic particle size than those prepared using monometallic precursors. The influence of the precursor in the hydrogenation of tetralin at high hydrogen pressure was studied. Both types of catalysts exhibit a good hydrogenation activity with a poor hydrogenolysis/ring opening activity. The type of precursor has a marked influence in the observed *trans*- to *cis*-decalin ratio being higher for catalysts prepared with monometallic precursors. Both types of catalysts show a good thiotolerance against dibenzothiophene, but the observed poisoning is more reversible in the case of catalysts prepared using monometallic precursors. A positive effect of the hydrogen pressure over the catalyst thiotolerance was observed, and using a *P*(H₂) of 6 MPa, the catalyst with a 2 wt% PdPt prepared from monometallic salts was found to be very resistant to sulfur poisoning, with a tetralin conversion higher than 95% in the presence of 1375 ppm of DBT in the feed, at 588 K.

Introduction

The current high demand for middle distillates for diesel applications and the stringent environmental legislations, directed at a reduction in aromatics and sulfur content of diesel, are the reasons for the many studies aimed at the preparation of new catalyst systems and the hydrotreating of Light Cycle Oil (LCO) streams.

Catalytic hydrogenation is an important process for reducing the aromatic content in liquid fuels or solvents,¹ because, after a deep desulfuration and denitrogenation treatment, they usually still contain a relatively high percentage of aromatics, which not only generate undesired emissions of particles in exhaust gases but also decrease the cetane number. For the new diesel fuel specifications, the maximum aromatic content level is limited to 1 v/v% by 2015.

An important aspect to be considered in the hydrotreating catalyst is the pore size distribution, the specific surface area and the acidity of the support, especially when processing heavy feedstocks. In this sense, the support is important in order to obtain not only a high dispersion of the active phase but also to allow the access of voluminous molecules through the pores to the active centres.

For this reason, the use of mesoporous acid solids as catalytic supports has given rise to a significant improvement for many reactions in comparison to conventional supports. As it is well-known, MCM-41 type solids display a hexagonal arrangement of cylindrical channels with diameters that vary between 16 and more than 100 Å, thus overcoming the small pore sizes of zeolites. These new supports also exhibit a very high surface area, mild acidity and high stability.^{2–3} Recently, many catalytic reactions have been successfully studied by using mesoporous silica or doped silica with different heteroatoms as supports of diverse active phases.^{4–11} Mesoporous MCM-41 silica is almost inactive as acid catalyst, due to the small number of acid sites. The introduction of heteroatoms such as Al, Ti or Zr increases the acidity of mesoporous solids. Particularly, Zr-MCM-41 has shown an excellent behaviour in such reactions.^{11–13}

On the other hand, the size of the aromatic molecules of diesel oil makes the pore size and topology of the catalyst have a strong influence on diffusion and, consequently, on activity and selectivity in ring opening reactions.¹⁴ Recently, MCM-41-type materials have been investigated in these catalytic processes.

Very recently, nickel impregnated Zr-MCM-41 catalysts have been successfully tested in the hydrogenation and ring opening of tetralin (THN) at high hydrogen pressures and 623 K,¹⁰ but they are poorly resistant to sulfur poisoning.

High activities and acceptable sulfur tolerances in the hydrogenation/ring opening reaction can be attained by using noble metal catalysts, mainly bimetallic PdPt supported on β-zeolite,^{15–17} silica-alumina,^{17–19} USY,^{1,14,20–22} γ-alumina,²³ Y-zeolite,²⁴ and a mixed γ-zirconium phosphate-silica.²⁵ These

^aDepartamento de Química Inorgánica, Orgánica y Bioquímica, Facultad de Químicas, Universidad de Castilla-La Mancha, Campus Universitario de Ciudad Real, 13071 Ciudad Real, Spain

^bDepartamento de Química Inorgánica, Cristalografía y Mineralogía (Unidad Asociada al Instituto de Catálisis y Petroleoquímica del CSIC), Facultad de Ciencias, Universidad de Málaga, Campus de Teatinos, 29071 Málaga, Spain. E-mail: Felix.Jalon@uclm.es; ajimenezl@uma.es; Fax: +34-952137534; Tel: +34-952131876

bimetallic PdPt catalysts have been claimed as the best in terms of activity and sulfur tolerance, and they have been chosen to be used in the second reactor of a two-stage process, where the feed still contains a concentration of about 50 ppm of sulfur.

Since monoaromatics are predominantly present in the hydrotreated LCO, tetralin has been selected as a model molecule in many catalytic studies.^{1,14,22–24,26} DBT (dibenzothiophene) was selected as a sulfur-poisoning agent because it is one of the main sulfur-containing compounds in diesel and its desulfuration chemistry is known.²⁷

The difficult hydrogenation of tetralin mainly produces *cis*- and *trans*-decalins, the *cis/trans* selectivity recently being considered as a useful probe for the study of electronic effects on metals and sulfided metal catalysts,^{24,28,29} and products derived from the hydrogenolysis/hydrocracking reactions, such as alkylbenzenes and alkylcyclohexanes, with a high cetane number.

In a previous paper, we have demonstrated that the use of a dinuclear PdPt complex as precursor gives rise to bimetallic catalysts supported on Zr-doped mesoporous silica with a high degree of metal dispersion, which are very selective in the gas-phase hydrogenation of acetonitrile.³⁰ Following with this study about the influence of the metal precursor on the catalytic performance, in the present work, we report their use in the hydrogenation and ring opening of tetralin at 548–623 K at a pressure of 6.0 MPa (H₂ pressure of 4.5 or 6.0 MPa). The choice of this support of moderate acidity lies in its stability against mechanical, hydrothermal and regeneration treatments. Moreover, this material, used as support of nickel, has already shown excellent results in the hydrogenation and ring opening of THN at high H₂ pressures.¹⁰

One of the main goals of the work was to evaluate the influence of introducing both metals (Pd/Pt) in the form of a dinuclear complex against the use of a mixture of salts on the catalytic performance. In that way, with the unique complex, the ratio 1 : 1 of metals would be already present in each molecule of the precursor and the homogeneity of the metallic dispersion could be improved. Other factors such as the metallic content, temperature, and effect of the hydrogen pressure will also be evaluated. The other aim of our work was to evaluate the thiotolerance (with the addition of DBT to the organic flow) of the catalysts prepared in the search for a catalytic system highly resistant to the sulfur poisoning.

Results and discussion

Catalysts characterization

The catalysts studied are listed in Table 1. In the name of each catalyst, the number indicates the final metal wt% in the

calcined material. After this number, the metals present are indicated and also the support (SiZr for SiZr-5 support). Catalysts obtained from the dinuclear complex are marked with B at the end of the name.

The characterization of the mesoporous support and the bimetallic catalysts studied in the present paper has been previously reported.^{13,30} These studies have shown that, after the incorporation and calcination of the active phase, the hexagonal arrangement of the mesoporous support is preserved, since the typical d_{100} low angle reflection is still observed in their powder X-ray diffraction patterns. In addition, the unreduced catalysts, except sample 2PdPtSiZr, and the reduced ones do not show diffraction signals ascribable to the presence of either metal oxide or metallic phase, indicating that a high dispersion is attained, mainly when the dinuclear precursor is employed. This fact is corroborated by transmission electron microscopy (TEM) which reveals that the catalysts prepared from the dinuclear complex exhibit average metal particles sizes lower than 3 nm, whereas the catalysts obtained from monometallic salts give rise to average values higher than 25 nm.³⁰ All the textural and metallic properties of the catalysts are compiled in Table 1.

Concerning the textural characteristics deduced from the N₂ adsorption–desorption at 77 K (Table 1), the evolution of the specific surface area and pore volume values indicates that, after the incorporation of the active phase, no drastic modifications of the corresponding values of the mesoporous support occur, especially when the dinuclear complex is used as precursor.

As it is reflected in Table 1, a decrease of the acidity after the incorporation of the metallic phase is observed in all cases, this effect being more marked when the dinuclear complex is used.³⁰

On the other hand, H₂ temperature programmed reduction (H₂-TPR) studies have demonstrated that the bimetallic catalysts obtained from the dinuclear precursor are less reducible than the analogous catalysts prepared from salts, because at higher temperatures, between 523–623 and 673–773 K, broad hydrogen consumption signals are detected, revealing a stronger interaction of the metallic particles with the support, and hence a higher dispersion.³⁰

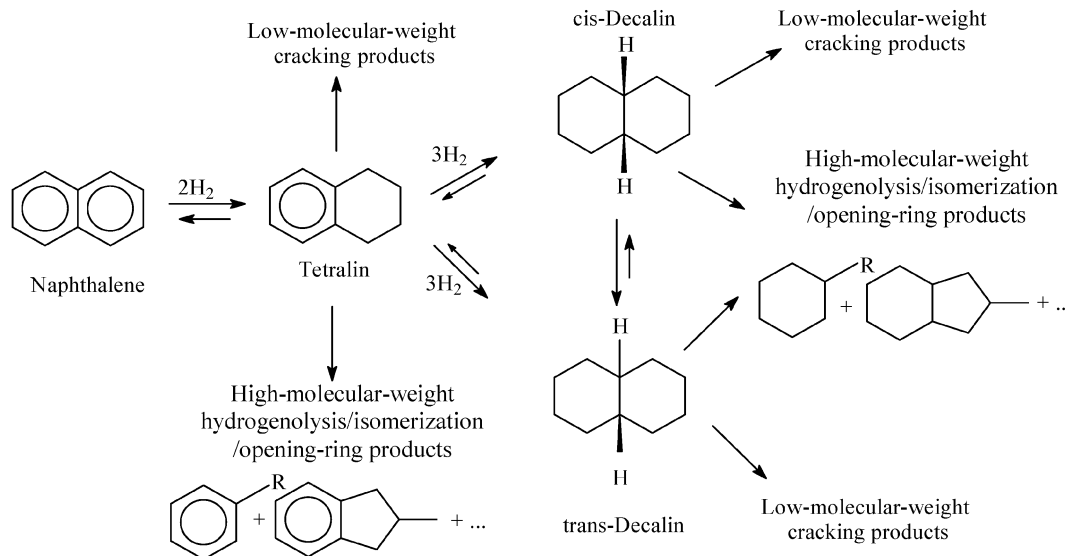
Catalytic hydrogenation of tetralin

The analysis of the liquid products obtained in the hydrogenation of tetralin allows detection of more than 70 compounds. They were classified into the following groups: (i) volatile compounds (VC) that includes non-condensable C₁–C₆ products which were calculated from the carbon balance of the reaction, (ii) hydrogenation products, that include *trans*- and *cis*-decalin, (iii) hydrogenolysis, isomerization and cracking

Table 1 Textural characteristics of the support and the bimetallic catalysts^a

—	$S_{\text{BET}}/\text{m}^2 \text{ g}^{-1}$	$S_{\text{ac}}^b/\text{m}^2 \text{ g}^{-1}$	$\sum V_{\text{p}}^b/\text{cm}^3 \text{ g}^{-1}$	$d_{\text{p}}(\text{av})^b/\text{nm}$	Acidity ^c /μmol NH ₃ g ⁻¹	Metal particles d_{av}/nm (TEM)
SiZr5	545	700	0.592	3.4	1349	—
1PdPtSiZr	493	579	0.442	3.0	—	14.8
2PdPtSiZr	495	649	0.552	3.4	721	26.3
1PdPtSiZr-B	545	781	0.723	3.7	491	2.1
2PdPtSiZr-B	534	679	0.695	4.1	478	2.9

^a From ref. 30. ^b By using the Cranston and Inkley method.³¹ ^c Total acidity of reduced catalysts, as deduced by NH₃-TPD.



Scheme 1 Main products detected in the hydrogenation and ring-opening of tetralin.

products (HC) that include primary products such as toluene, ethylbenzene, *o*-xylene, 1-ethyl-2-methylbenzene, 1-propenyl-2-methylbenzene, *n*-propylbenzene and *iso*-propylbenzene, and secondary products which derived from ring-opening reactions such as polyalkylolefins, decadiene and cyclo-hexene-1-butylidene and (iv) naphthalene (Scheme 1). Among the HC products, all C₁₀ compounds formed by isomerization of tetralin and decalins are included.^{32–34} Products heavier than decalins were never found. To evaluate the thiotolerance of the catalysts, the hydrogenation of tetralin was carried out in the same way, with 6.0 MPa of total pressure (4.5 or 6.0 MPa of hydrogen pressure), and different amounts of dibenzothio- phene (DBT) (425 and 1375 ppm) added to the organic feed.

The THN conversion values for the bimetallic catalysts obtained from the dinuclear complex are higher than 85% for the 2PdPtSiZr-B catalyst over the full range of temperatures studied. However, the decrease in conversion as the temperature rises from 588 to 623 K is attributed to thermodynamic restrictions since the hydrogenation reaction is exothermic (Fig. 1). These good results with the 2PdPtSiZr-B catalyst are in accordance to other studies, where an excellent hydrogenation activity for bimetallic PdPt systems was described.^{17,35}

Although the hydrogenation of aromatics is generally recognized to be a metal-catalysed reaction, many authors report that, in addition to the hydrogenation on metal centres, the acid sites of the support might also participate in the hydrogenation step,^{21,36–39} where aromatics molecules adsorbed on these acid sites can be hydrogenated by hydrogen spillover from the metal surface. Therefore, the small differences in the catalytic activity could be attributed not only to the higher average metal particle sizes but also to the slightly lower acidity of the 2PdPtSiZr-B compared with the 1PdPtSiZr-B catalyst, as measured by TPD-NH₃, since aromatic molecules could be adsorbed on acidic sites of the support close to the metallic particles.⁴⁰ Thus, the 1PdPtSiZr-B catalyst shows tetralin conversion, between 548 and 588 K, slightly higher than that obtained over 2PdPtSiZr-B. At 623 K, deactivation of the catalyst 1PdPtSiZr-B is important, giving a

conversion close to 80%. We will come back to this fact in the study of the evolution of the catalytic behaviour as a function of time-on-stream (see below).

In order to evaluate the influence of the precursor used in the preparation of the catalysts, as it was one of the goals of this work, results obtained with 2PdPtSiZr-B and 2PdPtSiZr were compared (Fig. 1). For these catalysts there are not important differences, but the catalyst prepared from the mixture of salts has at all temperatures a slightly lower activity. This fact can be due to the worse metallic dispersion for 2PdPtSiZr, as it has been demonstrated by TEM and DRX.

In all cases, the main reaction product is *trans*-decalin, whereas the *trans*- to *cis*-decalin ratio depends on the type of catalyst. For the 2PdPtSiZr-B catalyst, this ratio increases with temperature, while for 1PdPtSiZr-B is almost constant. In the case of 2PdPtSiZr the *trans*- to *cis*-decalin ratio is the highest, close to 10/1 over the range of temperature studied, according to the high acidity of this catalyst.³⁷ For the catalyst with 2 wt% metal content obtained from the dinuclear precursor, HC products are not detected, while they are produced with a yield of 5% on 1PdPtSiZr-B at 623 K, probably due to the higher

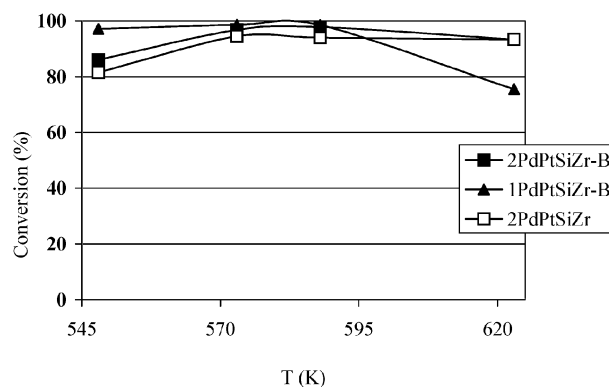


Fig. 1 Evolution of the conversion as a function of the reaction temperature in the hydrogenation of tetralin over bimetallic catalysts. H₂/THN = 10.1, P(H₂) = 6.0 MPa, contact time = 3.6 s.

acidity of 1PdPtSiZr-B, which favours these secondary reactions. The same can be argued for the more acidic catalyst, 2PdPtSiZr, which has a moderate yield (6%) of HC products. However, the amount of naphthalene is negligible in all cases. That is, these catalysts exhibit a very good hydrogenation activity toward decalins, with a poor activity to hydrogenolysis/ring opening compounds.

In order to study the stability of these PdPt catalysts, the analysis of the evolution of the conversion and selectivity with the time-on-stream was carried out at temperatures of 548 and 623 K. Taking into account that the conversion was similar in the full range of temperatures used in the preliminary studies, the temperature of 548 K was chosen in order to minimize the energetic spending. On the other hand, the temperature of 623 K was chosen in order to maximize the ring opening products, which is favoured at high temperatures.

At 548 K, all catalysts need a transient period before reaching the steady state with a conversion around 100% (Fig. 2). Among the catalysts with 2 wt% of metal content, that prepared from the dinuclear complex gets faster the steadier state. After 3 h of time-on-stream, the catalysts with 2 wt% of metal content still exhibit full tetralin conversion. The metallic content has a moderate influence, since the catalyst with 1 wt% required about 5 h to reach this situation, but at this moment the catalytic behaviour is similar to the other catalysts. However, the metal precursor used does not seem to have an important influence on the conversion, because both catalysts with 2 wt% of metal content have similar results in the steady state.

Nevertheless, at 548 K, the selectivity pattern strongly depends on the precursor used to prepare the bimetallic catalyst. As it has been described before, the PdPt catalysts show almost total selectivity to decalins, *trans*-decalin being the main product. For 2PdPtSiZr-B, the *trans*- to *cis*-decalin ratio is 1, while for 1PdPtSiZr-B is around 2 during the whole of the experiment. The best selectivity to this product, at this temperature, is observed for 2PdPtSiZr, with a value around 10 for the *trans*- to *cis*-decalin ratio. This result is different to the data reported for a PdPd supported on zirconium doped mesoporous silica, prepared from a mixture of salts but with a Pd/Pt molar ratio of 5.5, where the *trans*- to *cis*-decalin ratio was 7, working at 588 K.⁴¹

The influence of the metal content on the stability of the catalysts prepared from the dinuclear complex has been

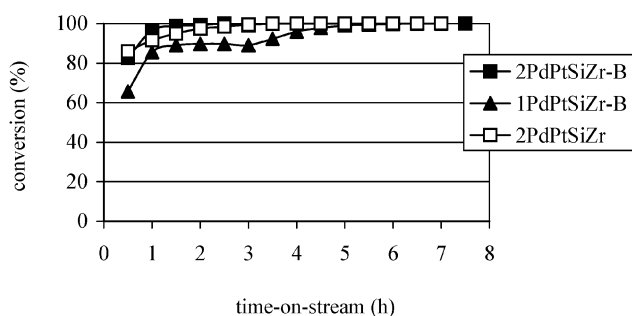


Fig. 2 Evolution of the conversion with the time-on-stream in the hydrogenation of tetralin for the PdPt catalysts. $T = 548$ K. $H_2/THN = 10.1$, $P(H_2) = 6.0$ MPa, contact time = 3.6 s.

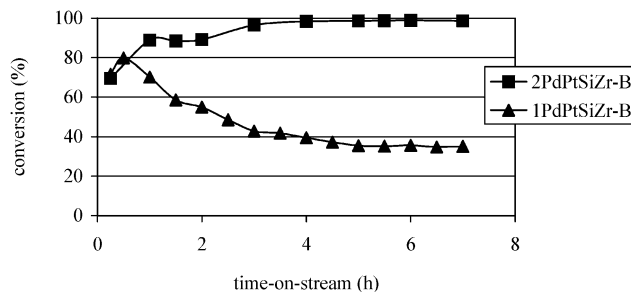


Fig. 3 THN conversion at 623 K as a function of time-on-stream over the PdPt catalysts. $H_2/THN = 10.1$, $P(H_2) = 6.0$ MPa, contact time = 3.6 s.

studied at 623 K (Fig. 3). The conversion for 2PdPtSiZr-B is similar to that obtained at 548 K, being almost 100% after reaching the steady state. However, for 1PdPtSiZr-B, a strong deactivation is observed, leading to a conversion value close to 35%, in the steady state after 7 h of time-on-stream. A plausible explanation for this observation would be the formation of a deposit of coke on the active centres, as confirmed by elemental CHN analysis of the spent catalyst, which showed for the 1PdPtSiZr-B sample a 4.13 wt% of C. A temperature raising produces for both catalysts an increment in the *trans*- to *cis*-decalin ratio. Naphthalene is not observed, and selectivity to HC products is low for 2PdPtSiZr-B (5%) and moderate for 1PdPtSiZr-B (11%), perhaps due to its higher acidity. Thus, the formation of HC products is very low, probably due to the covering of acid sites by the highly dispersed metal particles.

The influence of the hydrogen pressure was also studied. When this pressure was reduced from 6.0 MPa to 4.5 MPa at $T = 588$ K, the conversion on 1PdPtSiZr-B was reduced from 98.5% to 53% (Fig. 4). At 4.5 MPa, a variation in the selectivity is also observed, increasing the amount of *cis*-decalin and ring opening products, and decreasing that of *trans*-decalin. This result was expected because reducing the hydrogen pressure, the competitiveness of the hydrogen molecules for the metal centres is lower, and the formation of HC products from tetralin, by successive steps on active sites, is favoured. Thus, the hydrogen pressure seems to have a

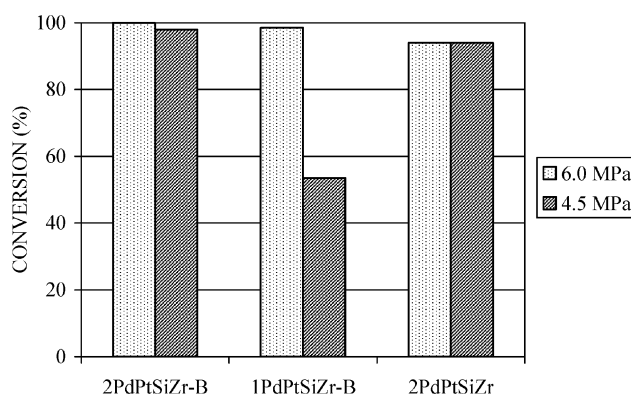


Fig. 4 Influence of the hydrogen pressure in the THN conversion over the PdPt catalysts. $T = 588$ K, $H_2/THN = 10.1$, contact time = 3.6 s.

strong influence on the catalytic results in the THN hydrogenation with this metallic content (1 wt%). When the 2PdPtSiZr-B and 2PdPtSiZr catalysts were tested at the lowest pressure and the results compared with those obtained at 6.0 MPa, at the same temperature, only a small decrease in the conversion and a similar change in selectivity were observed.

Thiotolerance studies

The thiotolerance of this set of catalysts in the hydrogenation of tetralin was evaluated by adding different amounts of DBT (425 and 1375 ppm, corresponding to 70 and 230 ppm of sulfur, respectively) to the organic feed. The reaction conditions initially used for these tests were: H_2/THN molar ratio = 10.1, contact time = 3.6 s, $T = 588$ K, $P(H_2) = 4.5$ MPa and total pressure of 6.0 MPa reached with N_2 . The time-on-stream for each test was 7 h.

The results for the catalysts with 2 wt% of metal content are displayed in Fig. 5. It can be observed that the deactivation, in the presence of 425 ppm of DBT, is important for both catalysts. Thus, after 7 h of TOS, the 2PdPtSiZr-B shows a THN conversion of 50%, about half the value obtained without sulfur. However, this deactivation is mainly reversible. With 1375 ppm of DBT, there is a drastic decrease in the activity. Concomitantly, a change in the selectivity pattern was also observed, decreasing the amount of *trans*-decalin and increasing that of *cis*-decalin.

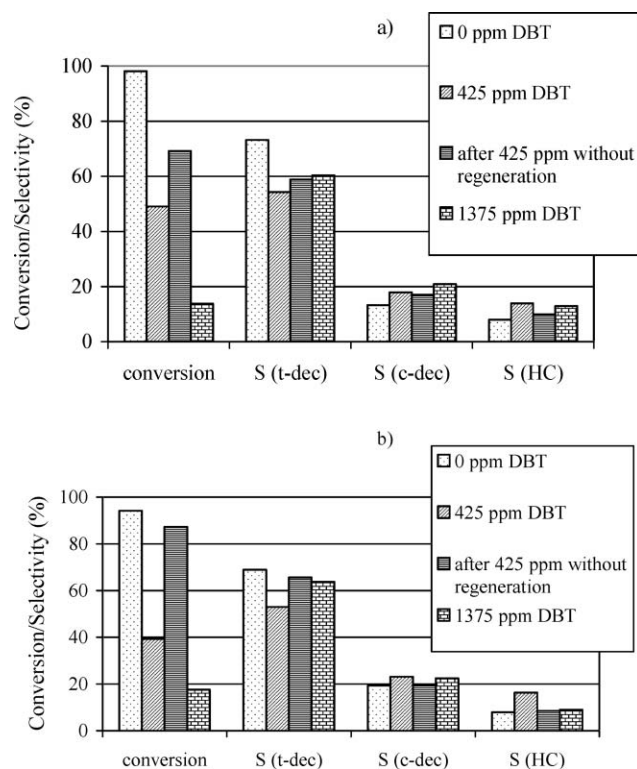


Fig. 5 Conversion and selectivity in the hydrogenation of tetralin for (a) 2PdPtSiZr-B catalyst and (b) 2PdPtSiZr catalyst, with different amounts of DBT. Reaction time: 7 h. $T = 588$ K, $H_2/THN = 10.1$, $P(H_2) = 4.5$ MPa, contact time = 3.6 s.

If the behaviour against the presence of sulfur of 2PdPtSiZr and 2PdPtSiZr-B is compared, the conclusion will be that the type of metal precursor used is not a very important parameter. However, 2PdPtSiZr-B is slightly more resistant than 2PdPtSiZr, leading to a 50% of conversion after 7 h of TOS with 425 ppm of DBT (40% for 2PdPtSiZr). This small difference can be due to the better metallic dispersion obtained from the dinuclear complex. After using a feed free from sulfur, the 2PdPtSiZr-B catalyst recovers partially their initial activity and, in the case of the 2PdPtSiZr, the initial value is nearly attained (Fig. 5). With 1375 ppm of DBT the 2PdPtSiZr-B catalyst is also almost inactive.

Taking into account the positive effect of the H_2 pressure over the hydrogenation process, previously observed, we decided to explore this factor in relation to the thiotolerance by studying the catalytic behaviour of the 2PdPtSiZr catalyst at a hydrogen pressure of 6.0 MPa (Fig. 6). This catalyst, under these experimental conditions, is very resistant to the presence of sulfur in the organic feed. Thus, by adding 425 ppm of DBT, there was no appreciable decrease in the conversion with a value around 100% (40% at a $P(H_2) = 4.5$ MPa, Fig. 5.b). In the presence of 1375 ppm of DBT in the organic feed, the conversion is around 95% after 7 h of time-on-stream (below 20% for the lower pressure). The evolution of the selectivity at 425 and 1375 ppm of DBT is similar to that observed in previous tests. With a feed free of sulfur, the conversion and selectivity is totally recovered without the need for catalyst regeneration. Therefore, it is possible to conclude that this catalyst can be considered as thiotolerant in the conditions used and that the hydrogen pressure is a very important factor, at least for our systems, concerning the resistance to sulfur poisoning.

The results of thiotolerance obtained with this catalyst are in contrast with those previously reported for an analogous PdPt catalyst,⁴¹ but with a Pd/Pt molar ratio of 5.5, whose conversion decreases until 32% with 1375 ppm of DBT, at 623 K and 6 MPa of hydrogen pressure. Apparently, the

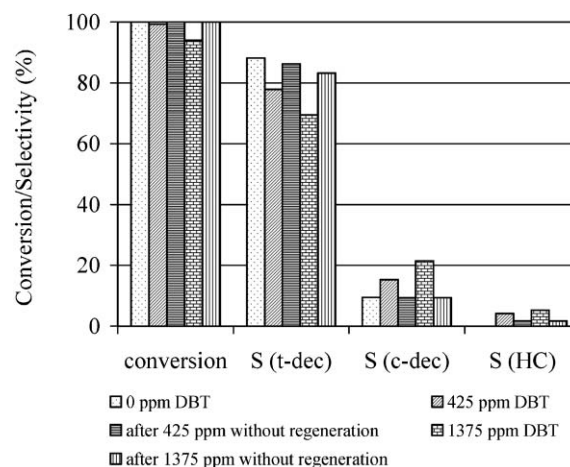


Fig. 6 Conversion and selectivity in the hydrogenation of tetralin for the 2PdPtSiZr catalyst with different amounts of DBT. Reaction time: 7 h. $T = 588$ K, $H_2/THN = 10.1$, $P(H_2) = 6.0$ MPa, contact time = 3.6 s.

ratio of metals is also an important factor governing the thiotolerance of these catalysts.

In the literature, two types of poisoning with thiophene or DBT are described. The first one is produced at high temperatures (above 473 K), where chemisorption of thiophene occurs through a strong bond with hydrogenolysis of the adsorbed molecule,⁴² leading to the final formation of a metallic sulfide on the catalyst surface. This type of poisoning is irreversible. The second mechanism takes place at temperatures lower than 473 K, where adsorption with a weak planar interaction of the thiophene molecule over the metallic atoms. This is a quick but reversible poisoning, that may be eliminated with a feed free of DBT.

In our systems, all the poisoning has been found to be reversible without the need for catalyst regeneration. Consequently, and although the temperature used in our experiments is 588 K and the first mechanism could be expected, the second mechanism must be operative and the hydrogenolysis of DBT does not take place, at least in an important percentage. A plausible explanation for that could be the lower tendency of the noble metals used to form metallic sulfides in comparison to other metals like nickel, for which the poisoning is usually irreversible.

After the thiotolerance study, the spent catalysts have been analyzed by elemental CHNS analysis, but after treating them with a tetralin feed free of DBT. The sulfur analysis gives percentages, in all cases, lower than 0.11 wt%, and coke deposition has clearly been observed. This fact confirms that interaction of DBT over catalysts is labile and hence the poisoning is reversible.

On the other hand, the Transmission Electron Microscopy technique reveals that the average sizes of the metallic particles, after the catalytic studies, are not modified in comparison with those of the fresh catalysts, and consequently there is not sintering of the active phase during the catalytic process.

Therefore, we can conclude that this family of PdPt catalysts are very active in the catalytic hydrogenation of tetralin, yielding decalin with high selectivity. Moreover, a clear effect of the hydrogen pressure has been found. The catalysts prepared from the dinuclear complex as precursor exhibit a much better metallic dispersion than those prepared from the mixture of salts. However, there are not clear differences in the catalytic behaviour between both types of catalysts, a fact that might be due to the high activity already obtained with the catalysts exhibiting lower dispersion.

With respect to the resistance to sulfur poisoning, we have found a catalyst that in certain conditions exhibits a high degree of thiotolerance, with the hydrogen pressure and Pd/Pt ratio being extremely important factors.

Experimental

Zirconium doped mesoporous silica support with a Si/Zr molar ratio of 5, SiZr-5, was obtained by following the procedure reported elsewhere.¹³ Catalysts were prepared by using incipient wetness impregnation over the powdered support. The dinuclear complex precursor, [PdPtCl₂(μ-dppm)₂],⁴³ where dppm = Ph₂PCH₂PPh₂, was incorporated as CH₂Cl₂ solution, while the monometallic precursors (PdCl₂ and H₂PtCl₆·6H₂O)

were introduced in aqueous solutions. After drying in air at 333 K for 12 h, and calcination at 773 K for 4 h (2 K min⁻¹ heating rate), samples were reduced at 673 K in a H₂ flow of 50 mL min⁻¹ for 60 min.

Powder X-ray diffraction patterns were obtained by using a Siemens D-501 diffractometer (Cu Kα source) provided with a graphite monochromator. Textural parameters have been calculated from N₂ adsorption-desorption at 77 K carried out in a conventional glass volumetric apparatus (outgassing at 473 K and 10⁻⁴ mbar overnight). Temperature-programmed desorption of ammonia (NH₃-TPD) was used to determine the total acidity of the supports and catalysts. Before the adsorption of ammonia at 373 K, the samples were treated at 823 K in a helium flow (50 mL min⁻¹) for 60 min. The NH₃-TPD was performed between 373 and 823 K, with a heating rate of 10 K min⁻¹. The evolved ammonia was analyzed by an on-line gas chromatograph (Shimadzu GC-14A) provided with a thermal conductivity detector.

Hydrogen temperature-programmed reduction (H₂-TPR) experiments were performed between room temperature and 823 K, by using a flow of Ar/H₂ (10 vol% of H₂, 40 mL min⁻¹) and a heating rate of 10 K min⁻¹. Water produced in the reduction was removed by passing the gas flow through a cold finger (188 K). The H₂ consumption was analyzed by an on-line gas chromatograph (Shimadzu GC-14A) provided with a TCD.

The purity of the dinuclear complex [PdPtCl₂(μ-dppm)₂] was verified by ¹H, ¹³C{¹H} and ³¹P{¹H}-NMR using the following NMR spectrometers: Gemini FT-200 (for ¹H-NMR), Varian Unity FT-300 (for all the nucleus), Gemini FT-400 (¹H-NMR) and Innova FT-500 (¹H- and ¹³C-NMR).

The hydrogenation of tetralin was performed in a high-pressure fixed-bed continuous-flow stainless steel catalytic reactor (9.1 mm id, 14.3 mm od and 230 mm length) operated in the down-flow mode. The reaction temperature was measured with an interior placed thermocouple in direct contact with the top part of the catalyst bed. The organic feed consisted of a solution of tetralin in *n*-heptane (10 vol%) and was supplied by mean of a Gilson 307SC piston pump (model 10SC). A fixed volume of catalyst (3 cm³ with particle size of 0.85–1.00 mm) without dilution was used in all the studies. Prior to the activity test, the catalysts were reduced *in situ* at atmospheric pressure with H₂ (flow rate 60 cm³ min⁻¹), heating from room temperature to 673 K with a heating rate of 10 K min⁻¹, and maintaining at 673 K until 1 h of total time.

Catalytic hydrogenation activities were measured at different temperatures under 6.0 MPa of hydrogen pressure, H₂/tetralin molar ratio of 10.1, and a contact time of 3.6 s. A liquid hourly space velocity (LHSV) of 6.0 h⁻¹ was used in all cases. The reaction was kept at steady state for 5–7 h in the studies of evolution of conversion and selectivity with time, or 1 h at each temperature in the evolution of conversion and selectivity with temperature. Liquid samples were collected and kept in sealed vials for posterior analysis by gas chromatography (Shimadzu GC-14A, equipped with a flame ionization detector and a capillary column TBR-1). First, the influence of reaction parameters, such as reaction temperature on the conversion and selectivity was studied. In previous

experiments, the variation of the amount of catalysts and the total flow rate, maintaining the space velocity constant, led to the conversion values being unmodified. As well, the catalytic behaviour was found to be independent of the particle diameter.

Acknowledgements

We are grateful to the Spanish DGES/MCyT (Project N. BQU-2002-00286), FEDER fund CICYT /E.U. (Ref. PB95-09011FD97-2207-CO2-O1, MAT) and MAT2003-2986, as well as to the European Union (GROWTH programme, contract GR5D-2001-00537), for financial support.

References

- H. Yasuda and Y. Yoshima, *Catal. Lett.*, 1997, **46**, 43–48.
- C. T. Kresge, M. E. Leonowicz, W. J. Roth, J. C. Vartuli and J. S. Beck, *Nature*, 1992, **359**, 710–712.
- J. Beck, J. C. Vartuli, W. J. Roth, M. E. Leonowicz, C. T. Kresge, K. D. Schmitt, C. T. W. Chu, D. H. Olson, E. W. Sheppard, S. B. McCullen, J. B. Higgins and J. L. Schlenker, *J. Am. Chem. Soc.*, 1992, **114**, 10834–10843.
- A. Corma, A. Martínez, V. Martínez-Soria and J. B. Montón, *J. Catal.*, 1995, **153**, 25–31.
- K. M. Reddy and C. Song, *Catal. Today*, 1996, **31**, 137–144.
- C. Song and K. M. Reddy, *Appl. Catal., A*, 1999, **176**, 1–10.
- A. Wang, Y. Wang, T. Kabe, Y. Chen, A. Ishihara and W. Qian, *J. Catal.*, 2001, **199**, 19–29.
- L. Ramírez, R. Contreras, P. Castillo, T. Klimova, R. Zárate and R. Luna, *Appl. Catal., A*, 2000, **197**, 69–78.
- T. Klimova, E. Rodríguez, M. Martínez and J. Ramírez, *Microporous Mesoporous Mater.*, 2001, **44–45**, 357–365.
- E. Rodríguez-Castellón, L. Díaz, P. Braos-García, J. Mérida-Robles, P. Maireles-Torres, A. Jiménez-López and A. Vaccari, *Appl. Catal., A*, 2003, **240**, 83–94.
- O. C. Bianchi, M. Campanati, P. Maireles-Torres, E. Rodríguez-Castellón, A. Jiménez-López and A. Vaccari, *Appl. Catal., A*, 2001, **220**, 105–112.
- D. J. Jones, J. Jiménez-Jiménez, A. Jiménez-López, P. Maireles-Torres, P. Olivera-Pastor, E. Rodríguez-Castellón and J. Rozière, *Chem. Commun.*, 1997, 431–432.
- E. Rodríguez-Castellón, A. Jiménez-López, P. Maireles-Torres, D. J. Jones, J. Rozière, M. Trombetta, G. Busca, M. Lenarda and L. Storaro, *J. Solid State Chem.*, 2003, **175**, 159–169.
- A. Corma, V. González-Alfaro and A. V. Orchilles, *J. Catal.*, 2001, **200**, 34–44.
- S. G. Kues, F. T. Clark and D. Hopkins, WIPO Patent 94/19429, 1994, Amoco Corp.
- J. K. Lee and H. K. Rhee, *J. Catal.*, 1998, **177**, 208–216.
- B. Pawelec, R. Mariscal, R. M. Navarro, S. van Bokhorst, S. Rojas and J. L. G. Fierro, *Appl. Catal., A*, 2002, **225**, 223–237.
- T. Fujikawa, K. Idei, T. Ebihara, H. Mizuguchi and K. Usui, *Appl. Catal., A*, 2000, **192**, 253–261.
- R. Navarro, B. Pawelec, J. M. Trejo, R. Mariscal and J. L. G. Fierro, *J. Catal.*, 2000, **189**, 184–194.
- C. Petitto, G. Giordano, F. Fajula and C. Moreau, *Catal. Commun.*, 2002, **3**, 15–18.
- M. A. Arribas and A. Martínez, *Appl. Catal., A*, 2002, **230**, 203–217.
- L. Le Bihan and Y. Yoshimura, *Fuel*, 2002, **81**, 491–494.
- J. L. Rousset, L. Stievano, F. J. Cadete Santos Aires, C. Geantet, A. J. Renouprez and M. Pellarin, *J. Catal.*, 2001, **202**, 163–168.
- C. C. Costa Augusto, J. L. Zotin and A. Da Costa Faro, *Catal. Lett.*, 2001, **75**, 1.
- S. Murcia-Mascarós, B. Pawelec and J. L. G. Fierro, *Catal. Commun.*, 2002, **2**, 305–311.
- K. Ito, Y. Kogasaka, H. Kurokawa, M. Ohshima, K. Sugiyama and H. Miura, *Fuel Process. Technol.*, 2002, **79**, 77–80.
- B. C. Gates, J. R. Katzer and G. C. A. Schuit, *Chemistry of Catalytic Processes*, McGraw-Hill, New York, 1979, p. 39.
- A. D. Schmitz, G. Bower and C. Song, *Catal. Today*, 1996, **31**, 45–56.
- L. Fischer, V. Harl and S. Kaztelan, *Stud. Surf. Sci. Catal.*, 1999, **127**, 261.
- M. C. Carrión, B. R. Manzano, F. A. Jalón, I. Fuentes-Perujo, P. Maireles-Torres, E. Rodríguez-Castellón and A. Jiménez-López, *Appl. Catal., A*, 2005, **288**, 34.
- R. W. Cranston and F. A. Inkley, *Adv. Catal.*, 1957, **9**, 143.
- G. B. McVicker, M. Daage, M. S. Touvelle, C. W. Hudson, D. P. Klein, W. C. Baird, Jr., B. R. Cook, J. G. Chen, S. Hantzer, D. E. W. Vaughan, E. S. Ellis and O. E. Feeley, *J. Catal.*, 2002, **210**, 137–148.
- D. Kubicka, N. Kumar, P. Mäki-Arvela, M. Tiitta, V. Niemi, T. Salmi and D. Y. Murzin, *J. Catal.*, 2004, **222**, 65–79.
- D. Kubicka, N. Kumar, P. Mäki-Arvela, M. Tiitta, V. Niemi, H. Karhu, T. Salmi and D. Y. Murzin, *J. Catal.*, 2004, **227**, 313–327.
- V. L. Barrio, P. L. Arias, J. F. Cambra, M. B. Güemez, B. Pawelec and J. L. G. Fierro, *Appl. Catal., A*, 2003, **242**, 17–30.
- K. C. Park, D. J. Yim and S. K. Ihm, *Catal. Today*, 2002, **74**, 281–290.
- P. Chou and M. A. Vannice, *J. Catal.*, 1987, **107**, 129–139.
- M. V. Arman and M. A. Vannice, *J. Catal.*, 1991, **127**, 251–266.
- J. Wang, Q. Li and J. Yao, *Appl. Catal., A*, 1999, **184**, 181–188.
- K. Thomas, C. Binet, T. Chevreau, D. Cornet and P. J. Gilson, *J. Catal.*, 2002, **212**, 63–75.
- E. Rodríguez-Castellón, J. Mérida-Robles, L. Díaz, P. Maireles-Torres, D. J. Jones, J. Rozière and A. Jiménez-López, *Appl. Catal., A*, 2004, **260**, 9–18.
- X. L. Seoane and A. Arcoya, *J. Chem. Technol. Biotechnol.*, 1993, **56**, 91.
- P. G. Pringle and B. L. Shaw, *J. Chem. Soc., Dalton Trans.*, 1983, 889.

The benzil–benzilic acid rearrangement in high-temperature water

Craig M. Comisar and Phillip E. Savage

Received 21st July 2005, Accepted 6th September 2005

First published as an Advance Article on the web 22nd September 2005

DOI: 10.1039/b510340a

The rearrangement of benzil is base (and not acid) catalyzed under conventional conditions (water–dioxane mixture around 100 °C). We examined this reaction in high-temperature water (HTW) between 300–380 °C with the intent of studying a reaction that proceeds solely by base catalysis in this more environmentally benign medium. The rearrangement proceeds in neutral HTW without addition of base, but the yield of rearrangement products is nearly insensitive to pH at near-neutral conditions. Adding larger amounts of base, however, leads to much higher yields and 100% selectivity to rearrangement products. Likewise, adding larger amounts of acid leads to comparable yields, but less than 100% selectivity. The selectivity to rearrangement products generally increased with pH at near-neutral and basic conditions whereas the selectivity to benzil decomposition products (a competing thermal pathway) exhibited a maximum at near-neutral conditions. We conclude that the benzil rearrangement is catalyzed by acid, base, and water in HTW. The dominant mechanism shifts as the pH changes. This system shows that mechanisms that are unimportant at conventional reaction conditions can become dominant in HTW. It also demonstrates the ability to use pH to direct the selectivity of a reaction in HTW.

Introduction

High-temperature water (HTW), defined here as liquid water above 200 °C, is a useful medium for chemical reactions. Relative to water at room temperature, HTW has a low dielectric constant, increased solubility for small organic compounds, and an increased ion product. All of these properties are temperature dependent and can be manipulated to optimize the reaction environment.

Although HTW and supercritical water ($T > 374$ °C, $P > 218$ atm) have been investigated for numerous acid-catalyzed reactions, much less research has been dedicated to exploring base-catalyzed reaction systems in these media. HTW, which has elevated levels of hydroxide ions, is an interesting medium for base-catalyzed reactions, such as the benzil–benzilic acid reaction.

This rearrangement has been widely studied with published work dating back to 1838.¹ In 1923 Lachman indicated that acids have no catalytic action on benzil at 100 °C.² In 1958, Hine and Haworth³ showed the reaction was faster in the more basic dioxane–D₂O than in dioxane–H₂O. They also showed through the deuterium kinetic isotope effect that the rate-controlling steps in the reaction could not include a proton transfer. From these observations, the benzil reaction system seemed like an appropriate one to test HTW as a medium for reactions that require a nucleophilic agent.

Benzil–benzilic acid type rearrangements are not known to occur in HTW. These reactions have industrial importance in the production of phenytoin, an antiepileptic drug.⁴ The benzil–benzilic acid rearrangement is related to other reactions such as the intramolecular Cannizzaro reaction. Both reactions involve the oxidation and reduction of an organic substrate

which contains a carbonyl group with no alpha hydrogen. The Cannizzaro reaction has been demonstrated in HTW.⁵ By elucidating the benzil–benzilic acid rearrangement, we broaden the general knowledge of organic chemical reactivity in HTW. This broadened understanding could facilitate the implementation of HTW as a more environmentally benign reaction medium.

Results

Benzil was reacted in neutral HTW between 300–380 °C for times between 0.5 and 8 hours. The reaction products included benzene, toluene, benzaldehyde, diphenylmethane, benzophenone, benzhydrol, and 2-phenylmethylphenol. We classify as rearrangement products those compounds with a single carbon atom linking two aromatic rings. These products include diphenylmethane, benzophenone, benzhydrol, and 2-phenylmethylphenol. We classify benzil decomposition products as compounds containing only one aromatic ring. These products include benzene, toluene, and benzaldehyde.

Table 1 shows experimental results obtained at different temperatures and batch holding times for the benzil–benzilic acid rearrangement. The results are the molar yields of the starting compound benzil, the combined yields of single-ring products formed by benzil decomposition, the yields of rearrangement products, and the aromatic ring balance. The uncertainties shown here and throughout the article are standard deviations calculated from multiple experiments at each set of reaction conditions.

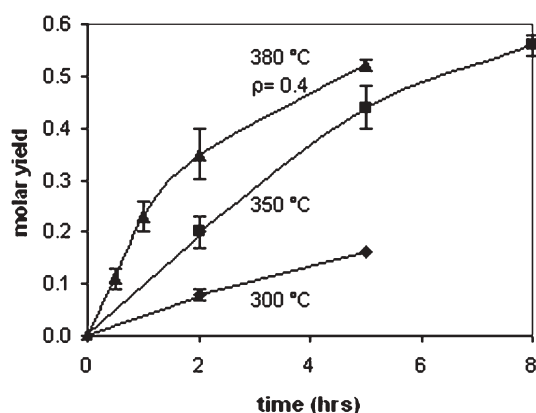
Benzil conversion increases with increased temperature and time. Splitting of the benzil diketone bridge to form single-ring compounds also increases with temperature and time as is evidenced by the yields of decomposition products at all conditions investigated. The yield of rearrangement products increases with both time and temperature as shown in Fig. 1.

Department of Chemical Engineering, University of Michigan, Ann Arbor, Michigan, USA. E-mail: psavage@umich.edu

Table 1 Molar yields of reactants and products from benzil–benzilic acid rearrangement in neutral high-temperature water

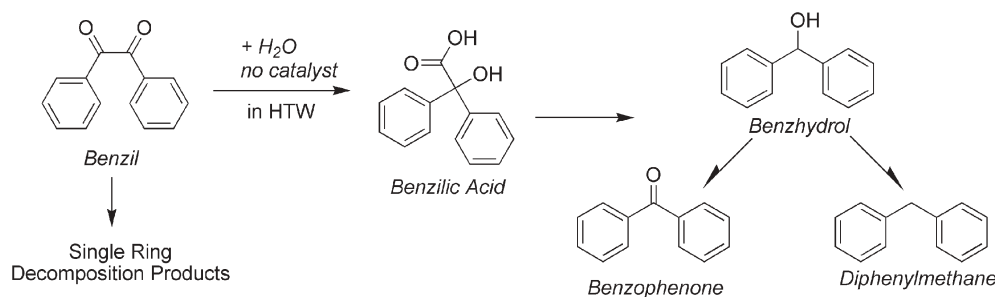
Temperature/°C	t/h	Molar yields						Total rearrangement products ^c	Ring balance
		Benzil	Benzil decomposition products ^a	Diphenylmethane	Benzophenone/benzhydrol ^b	2-Phenylmethylphenol			
300	2	0.84 ± 0.07	0.02 ± 0.01	0.02 ± 0.01	0.07 ± 0.01	Not detected	0.09 ± 0.02	0.93 ± 0.08	
	5	0.82	0.07	0.09	0.07	Not detected	0.16	1.01	
350	2	0.72 ± 0.11	0.10 ± 0.02	0.09 ± 0.03	0.07 ± 0.02	0.03 ± 0.02	0.19 ± 0.04	0.96 ± 0.13	
	5	0.27 ± 0.02	0.24 ± 0.02	0.32 ± 0.02	0.09 ± 0.03	0.04 ± 0.01	0.45 ± 0.04	0.84 ± 0.03	
380 (ρ = 0.4 g mL ⁻¹)	8	0.12 ± 0.04	0.24 ± 0.04	0.41 ± 0.01	0.09 ± 0.01	0.06 ± 0.01	0.56 ± 0.02	0.80 ± 0.03	
	0.5	0.66 ± 0.07	0.03 ± 0.05	0.02 ± 0.01	0.08 ± 0.02	0.01 ± 0.01	0.11 ± 0.02	0.79 ± 0.08	
380 (ρ = 0.4 g mL ⁻¹)	1	0.48 ± 0.05	0.11 ± 0.01	0.09 ± 0.01	0.12 ± 0.02	0.03 ± 0.01	0.24 ± 0.02	0.76 ± 0.01	
	2	0.26 ± 0.02	0.11 ± 0.01	0.17 ± 0.02	0.17 ± 0.04	0.03 ± 0.01	0.37 ± 0.05	0.66 ± 0.06	
	5	0.12 ± 0.01	0.17 ± 0.02	0.30 ± 0.01	0.17 ± 0.01	0.05 ± 0.01	0.52 ± 0.02	0.72 ± 0.02	

^a Benzil decomposition product yields consist of benzene, toluene, and benzaldehyde yields. ^b Early experimental runs did not resolve benzophenone/benzhydrol peaks. This value is a combination of the benzophenone and benzhydrol yields. ^c Rearrangement product yields consist of diphenylmethane, benzophenone/benzhydrol, and 2-phenylmethylphenol yields.

**Fig. 1** Temporal variation of rearrangement product yields in neutral HTW.

The product present in the highest yield is either benzophenone/benzhydrol or diphenylmethane. Benzophenone/benzhydrol yields are nearly time invariant at 300 and 350 °C, but this yield increases with time at 380 °C. Diphenylmethane yields increase with increased temperature and time. Diphenylmethane becomes the predominant product at longer times.

For the 300 °C and 350 °C experiments, the mean ring balance was 91 ± 12%. The ring balance becomes lower at more severe conditions. The decreasing ring balance could be due to reactions that form products either too small or too large to be detected in our analysis.

**Scheme 1** Reaction network for benzil in HTW.

Reaction pathways

From the results in Table 1 and the literature we developed the reaction network in Scheme 1 for the rearrangement of benzil in HTW. The generally accepted pathway from benzil to benzilic acid is base-catalyzed.³ While HTW can form OH⁻ ions, there also exists the possibility that the reaction at these higher temperatures is thermally activated.

To test the reactivity of benzil in the absence of HTW as an OH⁻ source, benzil was heated for 2 hours at 350 °C in trimethylbenzene in the presence of five times the stoichiometric amount of water. These experiments showed 9 ± 1% yield to decomposition products, but only 1 ± 1% conversion of benzil to rearrangement products (diphenylmethane only). We conclude that the rearrangement observed in HTW is not an uncatalyzed molecular rearrangement.

Since benzilic acid is the first product formed in Scheme 1, its reactivity in HTW is of interest. We performed reactions of benzilic acid in HTW. Benzilic acid reacts completely at 350 °C and 2 hours to form benzophenone/benzhydrol and diphenylmethane in roughly equal proportions, which is consistent with the reaction products observed from experiments with benzil. We found benzophenone and diphenylmethane to be stable at 350 °C and 2 hours in HTW, which is consistent with Katritzky *et al.*⁶ Benzhydrol, on the other hand, reacts completely at 350 °C and 2 hours to form diphenylmethane and benzophenone in roughly equal proportions. This result is consistent with Hatano *et al.*⁷ who found that benzhydrol forms equal proportions of benzophenone and diphenylmethane through a disproportionation reaction.

Table 2 Molar yields of reactants and products from benzil–benzilic acid rearrangement in near-critical water at 350 °C for 2 hours

Reaction pH	Molar yields									
	Benzil	Benzil decomposition products ^a			Diphenylmethane	Benzophenone	Benzhydrol	Phenylacetophenone	2-Phenylmethylphenol	Total rearrangement products ^c
1.7	0.03 ± 0.02	0.07 ± 0.01	0.02	0.29 ± 0.01	0.30 ± 0.03	Not detected	0.20 ± 0.03	0.02 ± 0.01	0.61 ± 0.03	0.87 ± 0.01
3.1	0.43 ± 0.04	0.07 ± 0.01	0.04	0.13 ± 0.05	0.06 ± 0.01	0.04 ± 0.03	Not detected	0.04 ± 0.02	0.27 ± 0.06	0.74 ± 0.04
4.2	0.69 ± 0.13	0.06 ± 0.01	0.06	0.06 ± 0.01	0.07 ± 0.01	± 0.03 ^b	Not detected	0.03 ± 0.02	0.16 ± 0.04	0.89 ± 0.12
4.8	0.75	0.04	0.05	0.05	0.08 ^b	0.08 ^b	Not detected	0.02	0.15	0.94
5.4	0.83 ± 0.10	0.06 ± 0.02	0.02	0.07 ± 0.02	0.10 ± 0.02 ^b	0.10 ± 0.02 ^b	Not detected	0.03 ± 0.01	0.20 ± 0.03	1.02 ± 0.09
6.1 (neutral)	0.72 ± 0.11	0.10 ± 0.02	0.02	0.09 ± 0.03	0.07 ± 0.02 ^b	0.07 ± 0.02 ^b	Not detected	0.03 ± 0.02	0.19 ± 0.04	0.96 ± 0.13
6.9	0.77 ± 0.18	0.05 ± 0.01	0.01	0.06 ± 0.01	0.10 ± 0.01 ^b	0.10 ± 0.01 ^b	Not detected	0.02 ± 0.01	0.18 ± 0.02	0.98 ± 0.17
7.5	0.71 ± 0.01	0.07 ± 0.01	0.01	0.09 ± 0.01	0.13 ± 0.02 ^b	0.13 ± 0.02 ^b	Not detected	0.02 ± 0.01	0.24 ± 0.02	1.00 ± 0.03
8.1	0.68 ± 0.08	0.07 ± 0.02	0.02	0.09 ± 0.03	0.16 ± 0.02 ^b	0.16 ± 0.02 ^b	Not detected	0.01 ± 0.01	0.26 ± 0.04	0.99 ± 0.07
9.2	0.03	0.04	0.01	0.20	0.20	0.45	Not detected	0.01 ± 0.01	0.85	0.90
10.6	Not detected	Not detected	0.01	0.61	0.61	0.39	Not detected	Not detected	1.00	1.00

^a Benzil decomposition product yields consist of benzene, toluene, and benzaldehyde yields. ^b Early experimental runs did not resolve benzophenone/benzhydrol peaks. This value is a combination of the benzophenone and benzhydrol yields. ^c Rearrangement product yields consist of diphenylmethane, benzophenone, benzhydrol, and 2-phenylmethylphenol yields.

Effect of pH

Table 2 displays the yields of observed chemical species from experiments at 350 °C and 2 hours wherein we varied the pH of the reaction solution. The amount of benzil remaining unreacted was about the same for all pH values investigated between 4.2 and 8.1. The benzil yields were much lower, though, at both lower and higher pH. In fact, 97% conversion was obtained at a pH of 1.7 and also at 9.2, but the conversion was only about 25% at near-neutral conditions.

The yield of benzil decomposition products was relatively insensitive to pH over the entire range investigated except for the experiment at the highest pH, where this yield is zero. At these strongly basic conditions, the rearrangement rate appears to be so fast that it proceeds to completion before the thermally driven decomposition reactions occur to any appreciable extent.

Fig. 2 shows that the yield of rearrangement products is about 0.2 over a range of near-neutral pH values. The yield increases with the addition of both strong acid and base, however. Higher yields with added base were expected because the reaction is base catalyzed.³ Higher yields with added acid were not expected. This result suggests that an acid-catalyzed mechanism is also operative in HTW. Further discussion of the mechanistic implications is deferred until the next section.

The rearrangement product benzhydrol was not detected at the lowest pH. Rather, it appears in higher yields in basic HTW solutions. Fig. 3, which shows the yields of individual rearrangement products, provides more detailed information about the effect of pH. The yield of diphenylmethane was zero at the most basic conditions but at its highest value at the most strongly acidic conditions. Conversely, the yield of benzhydrol was zero at the most strongly acidic conditions, but at its highest values at the most basic conditions. The increased yield of benzhydrol and decreased yield of diphenylmethane in more basic HTW is consistent with the reduction of benzhydrol to diphenylmethane being a reversible acid-catalyzed ionic substitution reaction.⁸ In basic solution, the rate of this path would be reduced, hence more benzhydrol would survive and less diphenylmethane would form.

In addition to rearrangement products, phenylacetophenone is produced in highly acidic HTW solutions. This product is

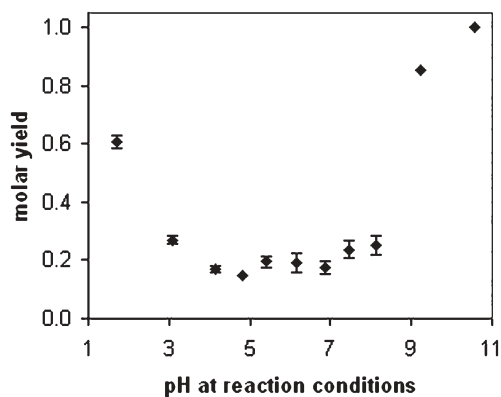


Fig. 2 Effect of pH on the yield of rearrangement products (350 °C, 2 hours).

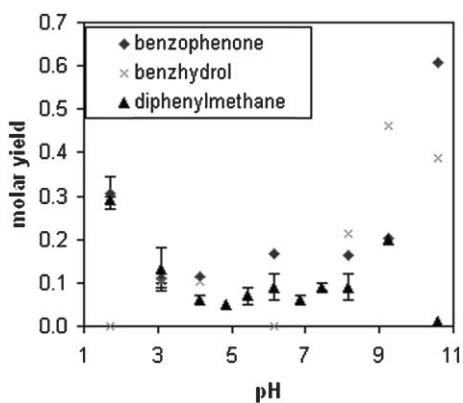


Fig. 3 Effect of pH on yields of individual rearrangement products at 350 °C and 2 hours.

most likely a direct reduction product of benzil. The two-carbon-atom bridge between the phenyl rings indicates the absence of a rearrangement mechanism. Fig. 4 shows the increase in phenylacetophenone yield with respect to time in 0.1 M HCl.

Fig. 5 displays the selectivity to benzil rearrangement products and benzil decomposition products at the different pH values explored experimentally. The error bars are large for some of the points because the conversions were low in these experiments. Nevertheless, the trends are clear. At pH 3 and above, the selectivity to rearrangement products increases with pH. This result is reasonable for a base-catalyzed reaction. Adding more base favors the base-catalyzed rearrangement, so its rate should increase more than those of competing non-base-catalyzed pathways. One such competing pathway is thermal and it leads to single-ring benzil decomposition products. The selectivity to these products is at a maximum (about 35%) at near-neutral conditions. At higher pH, the selectivity decreases, presumably because the base-catalyzed rearrangement becomes faster and more rearrangement occurs before decomposition can take place. At lower pH, the selectivity decreases, in part because the rearrangement rate

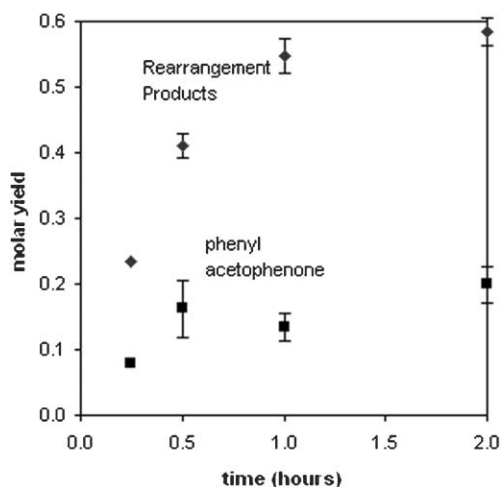


Fig. 4 Temporal variation of phenylacetophenone yield in 0.1 M HCl in HTW at 350 °C. Average ring balance was $95 \pm 8\%$.

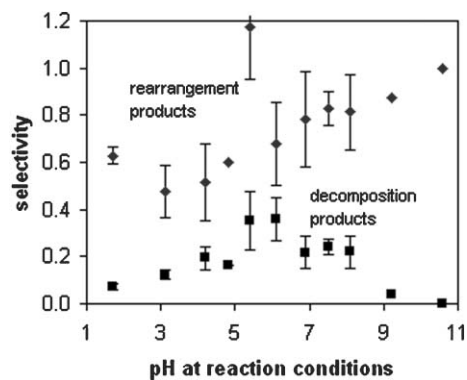


Fig. 5 Effect of pH on selectivity to rearrangement and decomposition products (350 °C, 2 hours).

increases but also in part because a new reaction path becomes available. This new path, which was observed only at the most acidic conditions investigated, leads to phenylacetophenone.

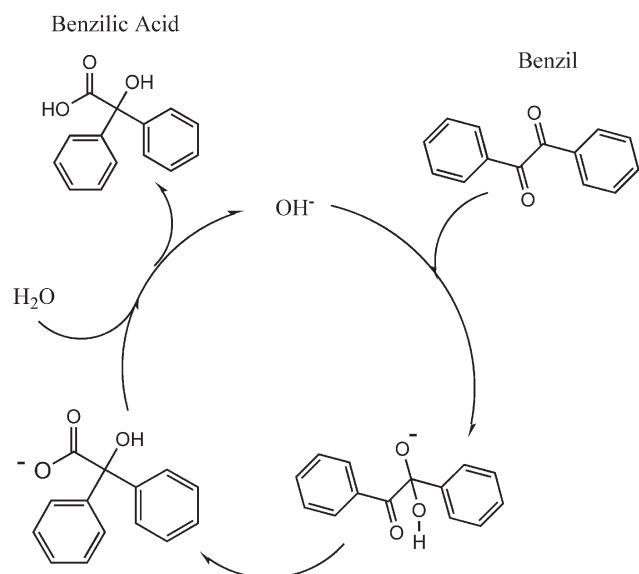
Reaction mechanisms

Fig. 2 shows that the yield of rearrangement products was always about 20% between pH 4–7. Within this region, the addition of hydronium or hydroxide ions does not greatly influence the formation of benzil rearrangement products. This insensitivity to pH suggests that the benzil rearrangement reaction does not follow a simple specific acid or base catalyzed mechanism at these conditions. Rather a water-catalyzed mechanism is more likely. At high concentrations of added acid or base, however, there are increased yields of rearrangement products suggesting the operation of specific acid/base mechanisms at these conditions.

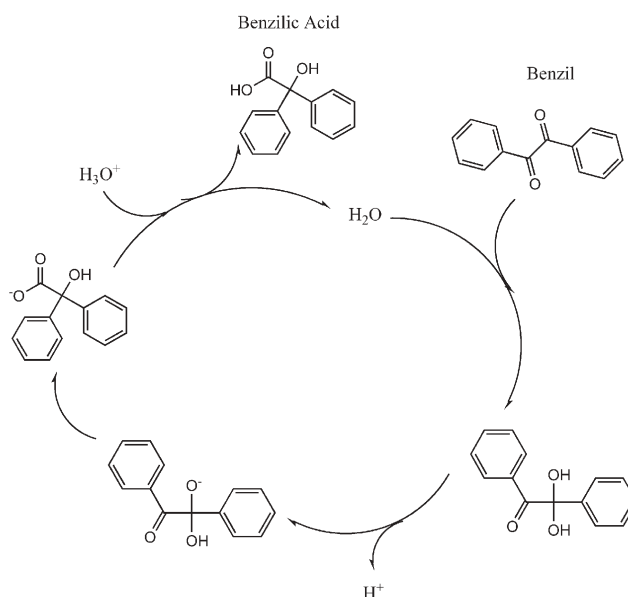
The accepted base catalyzed mechanism is shown in Scheme 2. To account for reaction at high acid concentrations and near neutral conditions, we propose mechanisms for acid- and water-catalyzed rearrangements. These mechanisms appear in Schemes 3 and 4. Acid catalysis has not been proposed previously for this reaction. Most previous benzil rearrangement experiments have been conducted in dioxane–water mixtures (~ 50 °C) where acid does not appear to cause the rearrangement of benzil to form benzilic acid. In HTW, however, one obtains significant rearrangement product yields with added acid. The increased temperature and solvent effect of HTW apparently allow for an acid catalyzed rearrangement mechanism to occur.

We propose an acid-catalyzed mechanism (Scheme 3) in which benzil reacts to form an enol, in the right-most catalytic cycle. The enol then participates in another acid-catalyzed reaction. The first intermediate formed in this second catalytic cycle undergoes either an alpha ketol rearrangement or a ketone rearrangement to form the intermediate that leads to benzilic acid.

The water induced reaction, first hypothesized by Westheimer⁹ and later probed by Roberts and Urey¹⁰ (but not as a catalytic cycle) involves a rapid reversible hydration and ionization of the hydrate followed by a rearrangement. We include the subsequent acid addition necessary to complete the cycle and form benzilic acid.



Scheme 2 Base catalysis mechanism for benzil–benzilic acid rearrangement.

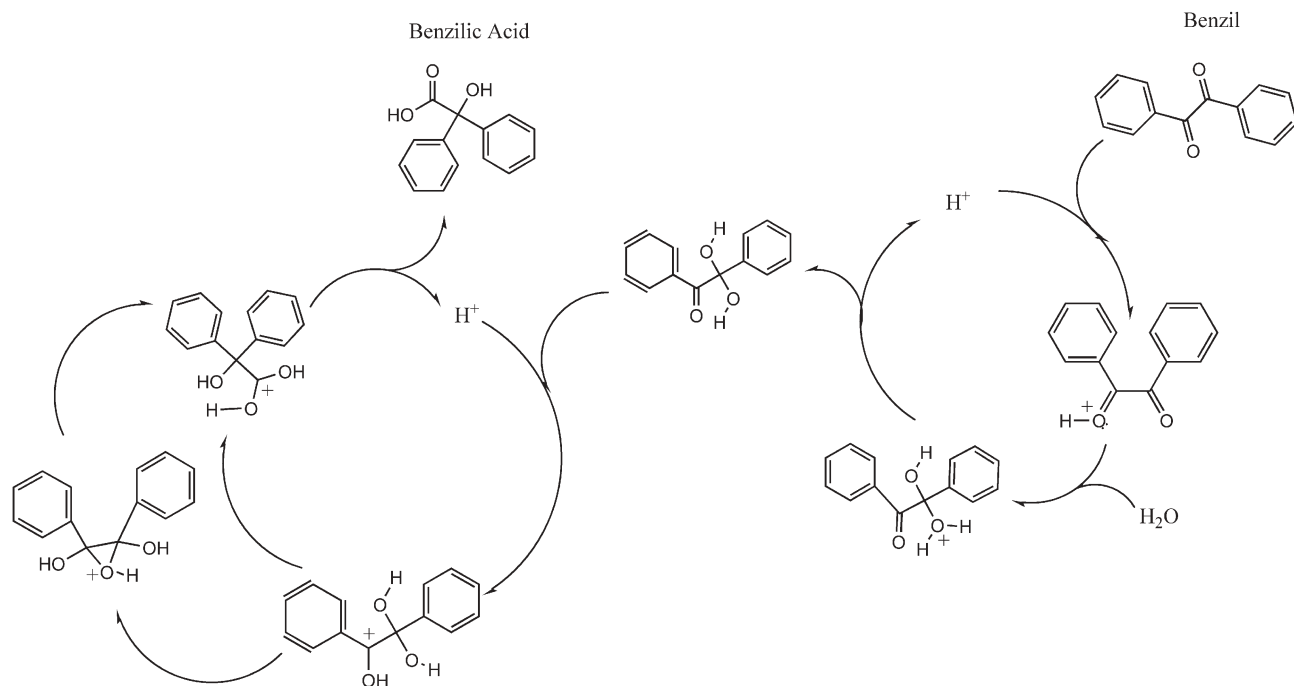


Scheme 4 Water catalysis mechanism for benzil–benzilic acid rearrangement.

Experimental

We performed batch reactor experiments in $\frac{1}{4}$ inch stainless steel Swagelok tube fittings. These reactors consisted of a port connector and two caps, which provided a 0.59 mL reactor volume. Prior to their use in experiments, all the reactors were loaded with water and conditioned for 1 hour at 300 °C. These reactors were then cleaned with acetone and dried prior to use. All chemicals were purchased from Aldrich in 98+% purity and used as received. Deionized water and HPLC grade acetone were used.

A carefully measured amount of benzil or reaction product (~ 10 mg) was added to the reactors, and then the reactors were placed inside a glove box filled with purified helium. Helium bubbled through deionized water in the glove box for 25 minutes to remove any dissolved oxygen and carbon dioxide, which could affect the reaction rate. We loaded 236–448 μL of water, precisely measured, in the reactors. The water loadings were selected such that 95% of the reactor volume would be occupied with liquid water at the subcritical reaction temperatures and the balance of the reactor will be occupied



Scheme 3 Acid catalysis mechanism for benzil–benzilic acid rearrangement.

with water vapor and helium. Water densities were taken from the steam tables.¹¹

In some experiments hydrochloric acid or sodium hydroxide solution was added to the reactors. A Beckman Φ 45 pH Meter was calibrated at pH 4.0 and 10.0 with commercial buffer solutions and then used to measure the pH of the standard acid and base solutions. The standard solutions were then diluted in deionized water to make solutions with the desired pH. The pH values reported in this article are those at reaction (not ambient) conditions.

Once loaded and capped, the reactors were stored in a $-10\text{ }^{\circ}\text{C}$ freezer (12 hours or less) until they could be placed in a Techne SBL-2 fluidized sand bath, preheated to the reaction temperature $\pm 1\text{ }^{\circ}\text{C}$. The reactor heat-up time is on the order of a few minutes,¹² which is very short compared to the reaction times investigated. Following the reaction period, the reactors were removed from the sand bath and submerged in room temperature water for 30–60 seconds. The cooled reactors were then stored in the freezer until they were opened and their contents recovered and analyzed.

Upon being opened, the reactors were filled with acetone. The reactor contents were then stirred to dissolve any solids in the reactors and the solution was removed from the reactor. This process was repeated 5–8 times. The solutions were then analyzed by an Agilent model 6890 gas chromatograph (GC). A $50\text{ m} \times 0.2\text{ mm} \times 33\text{ }\mu\text{m}$ HP-5 capillary column with helium carrier gas separated the sample constituents. We used a mass spectrometric (GC-MS) detector for product identification and a flame ionization detector (GC-FID) for quantitative analysis. An auto injector was used with both devices. The GC-FID injected $2\text{ }\mu\text{L}$ and used a split ratio of 25 : 1. The GC-MS injected $4\text{ }\mu\text{L}$ in splitless mode. There were two separate temperature programs used in analysis of the products. The initial temperature program consisted of the oven being heated for 7 minutes at $70\text{ }^{\circ}\text{C}$, a temperature ramp of $70\text{ }^{\circ}\text{C}$ per minute to $240\text{ }^{\circ}\text{C}$, and then holding the final temperature for 12 minutes. This program could separate benzil, diphenylmethane, and phenylacetophenone but, unknown to us at the time, benzophenone and benzhydrol did not separate. Subsequent analysis of extracted ion chromatograms for that peak, however, revealed the presence of both benzophenone and benzhydrol. After this discovery, we altered the GC oven temperature program to separate benzhydrol and benzophenone in further experiments. This modified temperature program consisted of the oven being heated for 4 minutes at $70\text{ }^{\circ}\text{C}$, a temperature ramp of $70\text{ }^{\circ}\text{C}$ per minute to $150\text{ }^{\circ}\text{C}$ and holding at this temperature for 30 minutes, a temperature ramp of $70\text{ }^{\circ}\text{C}$ per minute to $165\text{ }^{\circ}\text{C}$ and holding at this temperature for 20 minutes, and then a final $70\text{ }^{\circ}\text{C}$ per minute to $240\text{ }^{\circ}\text{C}$ and holding the final temperature for 10 minutes. Fig. 6 provides a representative chromatogram.

Analysis of standard solutions containing known amounts of reactants and products provided calibration curves, which were used to determine the amount of each component in the reaction samples. Molar yields were calculated as the moles of product formed per mole of benzil loaded into the reactor. Selectivities were calculated as the moles of product formed per mole of benzil converted.

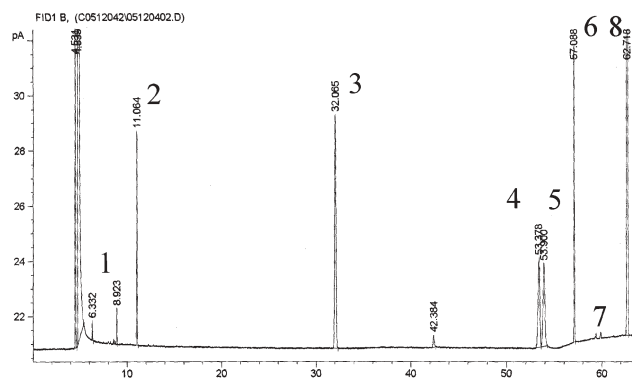


Fig. 6 Effective resolution of products on a HP-5 column. 1. Benzenes 2. benzaldehyde 3. diphenylmethane 4. benzophenone 5. benzhydrol 6. 2-phenylmethylphenol 7. phenylacetophenone 8. benzil.

Conclusions

The benzil–benzilic acid rearrangement, a base-catalyzed reaction at conventional conditions, proceeds in neutral high-temperature water with no catalyst added. Thus, this reaction is one more example of catalytic chemistry in HTW with no supplemental addition of catalyst. The benzilic acid further reacts to form benzhydrol, diphenylmethane, and benzophenone. Benzhydrol is also reactive, and it forms nearly equal yields of diphenylmethane and benzophenone.

The yield of rearrangement products shows little variation with pH at near neutral conditions, but it increases greatly at more strongly acidic or basic conditions. This behavior suggests that the rearrangement in HTW is not exclusively catalyzed by OH^- , as is the case at conventional conditions. Rather, rearrangement in HTW is also catalyzed by H^+ and by water itself. We posit potential catalytic cycles for these mechanisms. It appears that the higher temperature makes the rates of the acid- and water-catalyzed routes competitive when the OH^- concentration is low. Thus, mechanisms that are unimportant under conventional conditions may become important in HTW.

The selectivities to rearrangement products and decomposition products are both pH dependent. The former shows a minimum around pH 3 but then increases with pH whereas the latter is low at the pH extremes and a maximum at near-neutral conditions. These results show that pH can be used to control the selectivities of competing pathways for some reactions in HTW.

Acknowledgements

We thank Professor Edwin Verdej for helpful discussions regarding the reaction mechanisms. This work was supported in part by the American Chemical Society Petroleum Research Fund (37603-AC9) and by the US National Science Foundation (CTS0218772).

References

- 1 J. Liebig, *Ann.*, 1838, **25**, 27.
- 2 A. Lachman, *J. Am. Chem. Soc.*, 1923, **45**, 1529.
- 3 J. Hine and H. W. Haworth, *J. Am. Chem. Soc.*, 1958, **80**, 2274–5.

- 4 K. Unverferth and C. Rundfeldt, Antiepileptics, in *Ullmann's Encyclopedia of Industrial Chemistry*, Wiley, Hoboken, NJ, 2000, http://www.mrw.interscience.wiley.com/ueic/articles/a03_013/frame.html.
- 5 Y. Ikushima, K. Hatakeda, O. Sato, T. Yokoyama and M. Arai, *Angew. Chem., Int. Ed.*, 2001, **40**, 1, 210.
- 6 A. R. Katritzky, E. S. Ignatchenko, S. M. Allin, R. A. Barcock, M. Siskin and C. W. Hudson, *Energy Fuels*, 1997, **11**, 160.
- 7 B. Hatano, J. Kadokawa and H. Tagaya, *Tetrahedron Lett.*, 2002, **43**, 5859.
- 8 C. Choi and L. M. Stock, *J. Org. Chem.*, 1984, **49**, 2871.
- 9 F. H. Westheimer, *J. Am. Chem. Soc.*, 1936, **58**, 2209.
- 10 I. Roberts and H. Urey, *J. Am. Chem. Soc.*, 1938, **60**, 880.
- 11 Y. Cengal and M. A. Boles, *Thermodynamics an Engineering Approach*, McGraw-Hill, Boston, MA, 3rd edn, 1998, p. 905.
- 12 J. R. Lawson and M. T. Klein, *Ind. Eng. Chem. Fundam.*, 1985, **24**, 203.

RSC Journals Super Archive



18070531

Now with additional content from all of the RSC journals

from 1841 to 2004 including:

238,236 articles

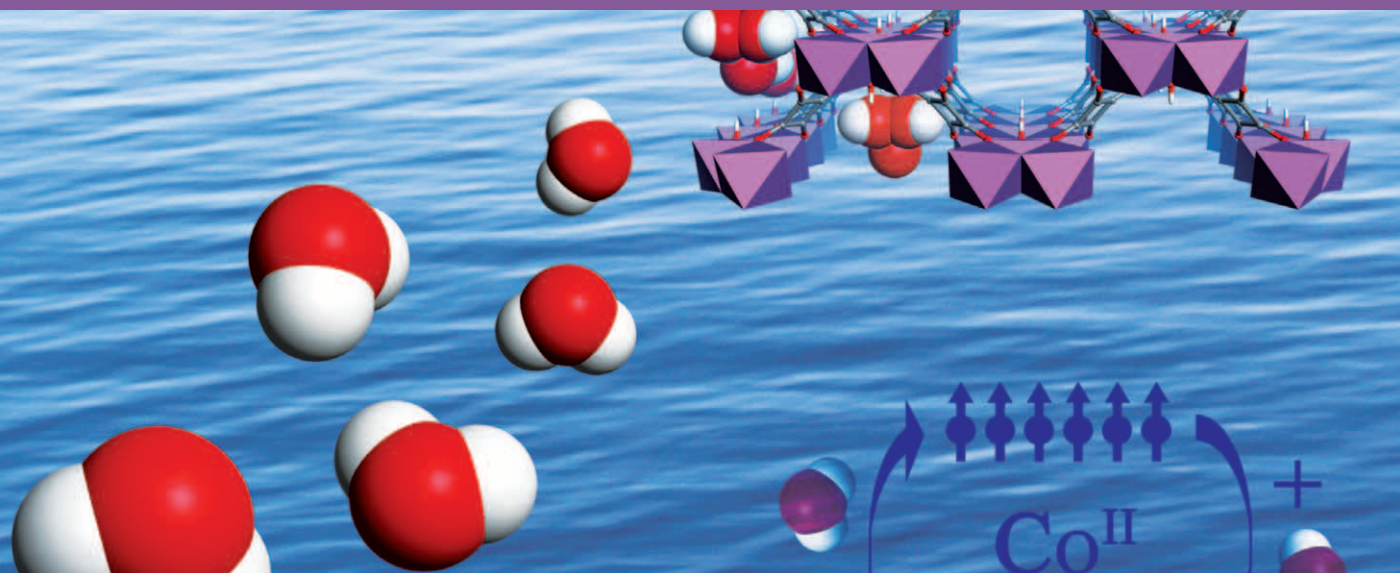
1,433,188 pages

Contact the RSC for more information at sales@rsc.org



RSC Publishing

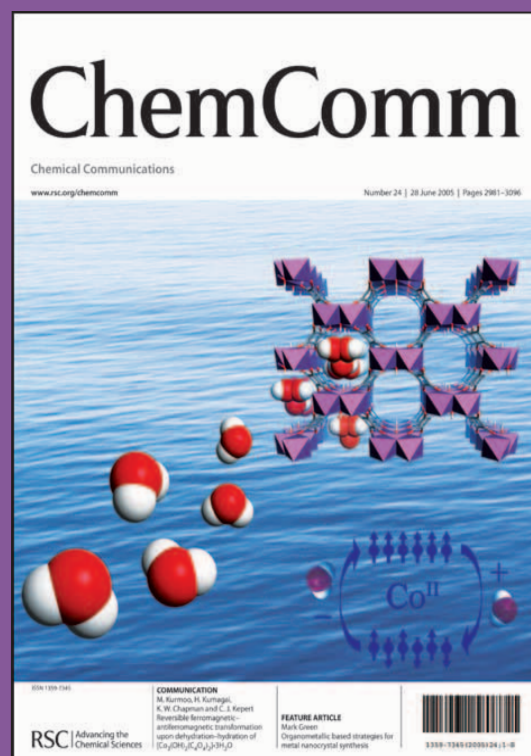
www.rsc.org



ChemComm

The leading international journal for the publication of communications on important new developments in the chemical sciences.

- Weekly publication
- Impact factor: 3.997
- Rapid publication – typically 60 days
- 3 page communications – providing authors with the flexibility to develop their results and discussion
- 40 years publishing excellent research
- High visibility – indexed in MEDLINE
- Host of the RSC's new journal, *Molecular BioSystems*



RSC Publishing

www.rsc.org/chemcomm